CHALMERS


# Improvement of the calibration, test and verification process of an interferometric fiber optic gyroscope

Bachelor's thesis in mechatronics engineering

JOHAN MATE

Department of Electrical Engineering
CHALMERS UNIVERSITY OF TECHNOLOGY
Göteborg, Sweden 2020

BACHELOR'S THESIS

# Improvement of the calibration, test and verification process of an interferometric fiber optic gyroscope

JOHAN MATE

Department of Electrical Engineering
CHALMERS UNIVERSITY OF TECHNOLOGY
Göteborg, Sweden 2020

**Improvement of the calibration, test and verification process of an interferometric fiber optic gyroscope**
JOHAN MATE



ISSN 1654-4676

Department of Electrical Engineering
Chalmers University of Technology
SE-412 96 Göteborg
Sweden
Telephone: +46 (0)31-772 1000



Cover:
Image from Saab: https://www.saab.com/products/fiber-optic-gyro-products
Image explanation: Fiber optic gyro from Saab

Chalmers Reproservice
Göteborg, Sweden 2020

# Improvement of the calibration, test and verification process of an interferometric fiber optic gyroscope

JOHAN MATE
*Department of Electrical Engineering, Chalmers University of Technology*

Bachelor's thesis

## Abstract

The purpose of this project was to investigate if the calibration, testing and verification process of fiber optic gyros from Saab Avionics Husqvarna can be improved upon and to to develop a program in LabWindows based on existing ones that will be able to perform these new processes in a better and more efficient way.

After defining important terms and objects relevant to the rest of the investigation, the current calibration process is observed. From this the potential improvements are formulated in a step by step process. An area of improvement that was formulated is building a model of the thermal process for the calibration process. This will enable the ability to better predict qualities such as the temperature stabilization time. The second improvement which was formulated is the way the gyros are calibrated which may be improved by using other data collection, calibration, calculation and regression processes.

Several different calibration, calculation and regression processes are hypothesised and implemented in a LabWindows program. These different processes form several combinations of ways to calibrate the gyros. These are then simulated into the aforementioned LabWindows program. From these two new processes which are predicted to be the best are investigated further. These new processes both have changes to the process that are used to collect the calibration data and to the calculation. One uses an interval gaussian fitting of the data and the other surface fitting of the multidimensional output data from the gyro instead of the current process which uses polynomial regression.

The two best processes are tested on a gyro using the Labwindows program that were implemented and are compared to the current process. The result from this does not give any major conclusion of a better calibration process but it shows the potential of the improvements which may then lead to further optimized calibration processes if time is invested into further tests.

The LabWindows program that was used does itself provide value and improvement to the calibration, testing and verification process by making it simpler and more efficient.

**Keywords:** Fiber optic gyro, thermal simulation, calibration , LabWindows, gaussian regression, surface regression, software

# Sammanfattning

Syftet med detta projekt var att undersöka om kalibrerings-, test- och verifieringsprocessen för fiberoptiska gyron med serienummer 8088 000-4xx från Saab Avionics Husqvarna kan förbättras samt att utveckla ett program i LabWindows som är baserat på befintliga program och kan utföra dessa nya processer på ett bättre och mer effektivt sätt.

Efter att ha definierat viktiga termer och objekt som är relevanta för resten av undersökningen så observeras den nuvarande kalibrerings processen. Utifrån detta formuleras de potentiella förbättringarna i en steg för steg-process undersökning av den nuvarande kalibrerings processen. Ett stort förbättringsområde är att formulera en modell av det termiska förloppet hos kalibrering processen. Detta gör det möjligt att bättre kunna förutsäga egenskaper såsom temperaturstabilisering tiden. Den andra förbättringen som formulerades är hur gyrona kalibreras, vilket kan förbättras med hjälp av andra datainsamling-, kalibrerings-, beräknings- och regressions processer.

Flera olika kalibrerings-, beräknings- och regressions processer formuleras och implementeras i ett LabWindows-program. Dessa olika processer bildar flera kombinationer av sätt att kalibrera gyros. Dessa simuleras sedan i det ovannämnda LabWindows-programmet. Från dessa finnes två nya processer som förutses vara de bästa undersöks vidare. Dessa nya processer har båda ändringar i testet som används för att samla in kalibreringsdata och i själva beräkningen. Intervall gaussisk regression av data används i den ena och i den andra används yt-regression av den flerdimensionella datan från utgången av gyrot till skillnad från den nuvarande processen som använder polynom regression.

De två bästa processerna testas på ett gyro med Labwindows-programmet som implementerades och jämförs med den nuvarande processen. Resultatet av detta ger ingen större slutsats av en bättre kalibreringsprocess men det visar potentialen för förbättringarna som sedan kan leda till ytterligare optimerade kalibrerings processer om man investerar tid i ytterligare tester.

LabWindows-programmet som använts i sig ger värde och förbättringar av kalibrerings-, test- och verifieringsprocessen genom att göra den enklare och mer effektiv.

# Acknowledgements

This is a bachelor's thesis done for chalmers university of technology, the mechatronics program. It was done at Saab Avionics Husqvarna, Sweden. I would like to thank everyone at Saab for enabling me to meet and learn from them. I would especially like to thank my supervisors Karl-Johan and Daniel for their support and guidance during the process. It has been a very challenging and interesting time in which I learned much new knowledge and skills, these I will definitely find use during the remainder of my life.

*Johan Mate, 2020*

# Terminology & Abbreviations

*FOG* – Fiber Optic Gyro

*BIT(unit)* – a digital integer number between $[-2^{23}, 2^{23}-1]$

*Gyro Output* – The output of gyro given in BIT or volts

*SF(Scale Factor)* – the relation between the output of the fiber optic sensor and the rotation rate

*Bias Offset error* – A stationary gyro that outputs a rotation rate

*Bias instability* – Instability of bias offset at any constant temperature

*FS* – Full scale $\iff$ range of gyro

*RS422* – A standardised digital data transmission protocol

*ARW (Angle Random Walk)* – the noise of the output modeled as a gaussian random walk.

*ADC* – Analog to Digital Conversion

*DAC* – Digital to Analog Conversion

*PDE* – Partial Derivative equation

*FDM* – Finite Difference Method

*IDE* – Integrated Development Environment

$\phi$ – Angle of gyro/rotation table

$\theta$ – Rotation speed of gyro

$\omega$ – Gyro output(dependent upon $\theta$ ), in BIT or volt

*Rate* – synonyms with $\theta$

***L*** – Image/table made/plotted in LabWindows

***M*** – Image/table made/plotted in Matlab

***E*** – Image/table made/plotted in Excel

# Contents

# 1 Introduction

## 1.1 Background

Measuring the rotational speed of an object is something a gyroscope is used for. Many applications depend on it, and for Saab Avionics and their FOG system (Fiber Optic Gyroscope) these applications are mainly for stabilized platforms both for civil and military use. Many of these applications require a high performance FOG which in turn requires that the gyro is calibrated. This leads to the task formulated by Saab regarding their new generation of FOG. This version has a built in processor which will automatically correct inaccuracies of the fiber optic sensor element. However as this new FOG is under development the calibration process is not finalized. There are currently a few software programs and procedures that do exist but these require some manual handling. Much improvement can be made on the calibration, test and verification processes for these gyros.

## 1.2 Purpose

The purpose is to first conduct an investigation on what is being done now and how it can be improved. The result of this investigation will then be implemented in a software program that can automatically calibrate, test and then verify that these gyros are to specification. The existing systems and procedures set some demands on what the program at least needs to do. Even though the end goal of this thesis is to produce a software which fulfills the purpose of automating the calibration procedure the focus of the thesis lies on the investigation of the calibration procedure itself. In explicit terms, the purpose of this thesis is to find areas where the calibration process can be improved upon and the software that is produced in the end implements this new knowledge for the user.

## 1.3 Delimitations

There are a few areas which are not within the scope. These are the software of the processor within the FOG and the calibration equipment. The software of the processor is out of the scope of this thesis since digging into it is not something the company really needs from this thesis. However this doesn't mean that theoretical findings that might improve the product could be recommended for implementation by this thesis. It simply means that the code part of the processor in the FOG is not something that will be accounted for by this thesis. The calibration equipment is fixed and nothing can be done on this front. The Hardware that is available is the one this thesis will be using.

Furthermore it is not necessary for the result of this investigation to conclude in a fully functional program as this does take time to fully test and verify the functionalities. From the results Saab will have to decide whether they want to continue forward with it, regardless where it concludes.

## 1.4 Specification

The following questions are to be investigated such that an answer can be found:

- Are there ways in which the current process could be improved such as to reduce the time taken, increase accuracy after calibration or increase reliability of the process?
- Can a program be implemented in Labwindows which contains the found improvements to the calibration, test and verification process?
- Does this program offer any other benefits in accessibility, efficiency or Ease of use over the currently used one?

# 2 Theory/ Background material

## 2.1 Sagnac effect

A laser Gyroscope is a device which uses the sagnac effect of two beams of light travelling in the opposite direction to measure the rotation speed. The sagnac effect is the result of special relativity. The two light beams travel in opposite directions with the reference frame rotating with an angular speed of $\theta$. The rotation results in a difference in the effective path of the two light beams which in turn (due to relativistic effects) results in a phase difference. The phase difference is given by the sagnac formula:

$$\Delta\varphi = \frac{8\pi A\theta}{\lambda c} \tag{2.1}$$

Where $A = area$, $c$ =speed of light, $\lambda$=wavelength of light

## 2.2 The fiber optic gyroscope

There are two primary types of laser gyroscopes. The Ring Laser Gyroscope (RLG) and Fiber Optic Gyroscope(FOG). Both use the sagnac effect to measure the rotation speed, the difference between the function of the two is quite significant. In the RLG a laser cavity is used to both generate the lasers and measure the difference of their frequencies (as a result of the sagnac effect), the cavity often take the form of a triangle as shown in image 2.1:A or a square. The FOG on the other hand uses a fiber optic coil to construct the path[5]. There are two different types of FOG: the Interferometric fiber optic gyros (IFOG) and the resonator fiber optic gyros (RFOG). The RFOG has a similar operation to the RLG in that it uses the sagnac effect to generate two light beams with different frequencies and measure the interference of these beams. A IFOG on the other hand measures the phase using fringe patterns (light intensity patterns due to different phases)[5]. The FOG produced by Saab are of the IFOG type.

A principal depiction of a typical IFOG is seen in figure 2.1:B. The light beams are generated in the SLD (SuperLuminescent Diode). The purpose of the first coupler (used to connect fiber optic cables) is to allow the returning light from the fiber coil to enter the detector. The light from the SLD is then polarized and split between the two ends of the fiber coil by a second coupler. The phase modulator consists of a piezoelectric crystal that is used to measure the rotation direction by stretching the fiber optic wire with a frequency resulting in an output intensity that oscillates. The addition of rotation to this oscillation results in a wave that is shifted up or down by: $shift = amplitude \times sine(frequency of phase modulator) + shift due to rotation$

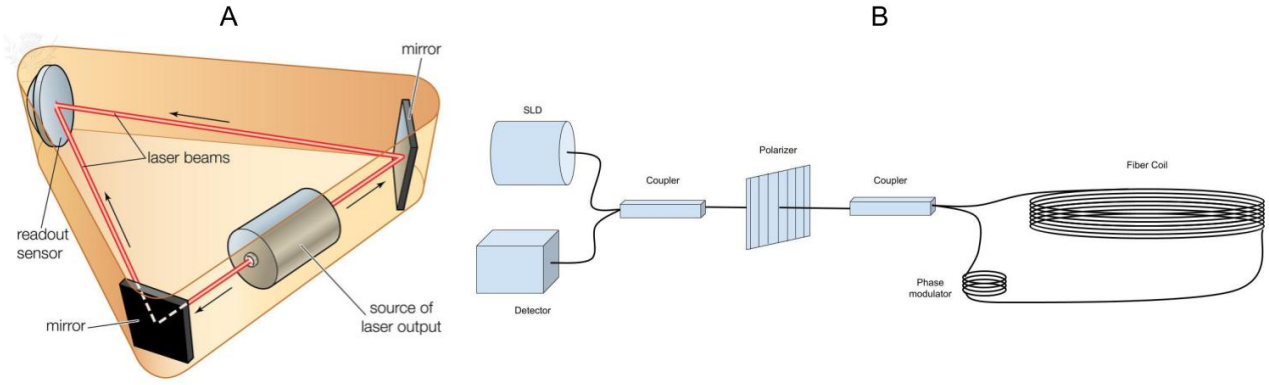


*Figure 2.1: A: Example of RLG[1], B: Example of IFOG*

[1]Source: Encyclopaedia Britannica, Inc. Rights Managed / For Education Use Only acquired using Britannica ImageQuest

## 2.3 Importance of calibration of FOG

Due to the inherent properties of the fiber coil, coupler and polarizer elements the FOG are highly dependent upon temperature. The main contributor to the error of the output of the coil is known as the shupe effect [1]. The temperature impacts the output of the gyro in the following ways.

- The Scale Factor(SF) of the gyro changes over temperature
- The Bias Offset changes over temperature[1]
- The Bias Offset changes over temperature change rate[6]

The Scale Factor is defined as the relation between the rotation and the output of the fiber optic sensors. Since this value is pre-calibration not constant over temperature the relation between the gyros output and the actual rotation will be wrong. Thus this has to be modified internally to assure a linear relation of the SF.

The Bias offset can be viewed as the occurrence of a value when the gyro is stationary, this value changes with temperature and thus it as well needs to be calibrated away. The bias can be seen as the base noise of the gyro output, often white noise is used as a model for this. However according to [2] this is better approximated using a gaussian random walk (ARW).

Besides the bias and SF error there is also a linear error over the defined rotation range. This error takes the form of a third degree polynomial that is compensated by an internal polynomial function calculator. This function calculator needs its polynomial coefficients calibrated in order to match the linear error.

Both the scaling factor error and the bias error of these sensors generally take the relation of a second degree polynomial and these are compensated by using an internal array of compensation values. This can be used as a quick and simple way to determine if the calibration process was successful, however for an actual determination of the accuracy a verification procedure is needed. A verification process is the same process as a calibration process but instead of uploading the compensation values to the gyro the values are compared to the specified values of the product. Only when the gyro is well calibrated can it achieve the high requirements for precision measuring of the rotation speed.

## 2.4 Saab FOG general characteristics overview

General characteristics of Saab 8088 000-4xx gyros are specified in the appendix B. Values of the most relevant characteristics for calibration of the 8088 000-4xx gyros that were used for testing in table 2.1, these values are taken from internal technical documents.

| Name | Characteristics | Unit |
|---|---|---|
| Range | $\pm 150$ | $\frac{deg}{s}$ |
| Operating temperature range | $[-40, 75]$ | $^{\circ}C$ |
| Analog SF | 26 | $\frac{mV}{\frac{deg}{s}}$ |
| Digital SF | 0.00001825 | $\frac{\frac{deg}{s}}{BIT}$ |
| Bias error OTR | $\pm 40$ | $\frac{deg}{hour}$ |
| SF error OTR | $\pm 0.5$ | % |
| Non-Linearity 0-75$\frac{deg}{s}$ | $\pm 0.1$ | % of FS max |
| Non-Linearity 0-150$\frac{deg}{s}$ | $\pm 0.2$ | % of FS max |

*Table 2.1: Most relevant characteristics for the Saab 8088-00 4xx gyros used for testing*

## 2.5 Calibration and test equipment

For temperature adjustment a temperature chamber, which is a sealed and thermally isolated chamber with adjustable temperature, is used. The max temperature change speed that this device possesses is $\approx 2.5\frac{C^o}{min}$. The temperature tests will be run over the temperature range $[-40°C, 75°C\ ]$. This is due to it being the specified optimal temperature range of the gyros (OTR).

In addition to this a rotation table (precise rotation speed) will be used. The specified range of the gyros are $\pm 150\frac{deg^o}{sek}$. According to internal procedures the rate tables have the property of being momentarily inaccurate however are sufficiently accurate over full rotations.

$$In\ explicit\ terms:$$

$$\theta =: desired\ value\ of\ rotation\ speed$$

$$\phi =: angle\ of\ table$$

$$\Theta(\phi) =: value\ achieved\ at\ \phi$$

$$\theta' \neq \theta$$

$$\theta = \frac{1}{2\pi n}\int_0^{2\pi n} \Theta(\phi)\ d\phi \tag{2.2}$$

Where n=number of rotations

This means averaging over n rotations solves the issue of non momentary accuracy of the rate table. Internal practice says that n should be around 1 rotation. For times when the rotation table is operating at higher speed such as $\pm 150\frac{deg^o}{sek}$ this is simple to achieve as staying at that speed for $\approx 3sek$ fulfills the one or more rotations condition. However when the speed is close to zero for example 5 $\frac{deg^o}{sek}$ to reach one rotation it needs to stay at that speed for $\frac{360}{5} = 72\ sek$, which is over a minute. This could lead to a dilemma as to how to most time efficiently fulfill the one rotation demand using the rate table.

In order to measure the analog value from the gyro an analog measuring card is used. This measuring card takes a specified amount of measurements of the analog outputs of the gyro at a specified frequency and then stores them in an array.

## 2.6 Thermal simulation

### 2.6.1 Thermal PDE

In order to simulate the thermal process the heat equation needs to be solved. The general case is:

$$\frac{\partial T}{\partial t} = \alpha \nabla^2 T \tag{2.3}$$

Where $\alpha$ is the thermal Conduction capacity[3] which is defined as.

$$\alpha = \frac{k}{\rho c_p} \tag{2.4}$$

Where $k$ = thermal conductivity, $\rho$ = density, $c_p$ = specific heat capacity

### 2.6.2 Finite Difference Method

Solving the heat equation exactly is quite a daunting task and that level of accuracy is not necessary here, thus an approximation of the thermal equation is needed. The chosen method is the finite difference method(FDM). Other more accurate methods do exist, however this is chosen due to simplicity in its implementation.

The definition of the derivative is: $f'(x) = \lim_{h \to 0} \frac{f(x+h)-f(x)}{h}$ and one of the simplest finite difference approximations of this is setting h to a nonzero but small value. The approximation then becomes $f'(x) \approx \frac{f(x+h)-f(x)}{h}$ $(i)$ $(1D\ form)$. Since the approximation of the heat equation uses a finite amount of data points, which is generated as a data grid. Therefore (i) in an equispaced finite form is: $f'[n] \approx \frac{f[n+h]-f[n]}{h}$. However in the heat equation there are only partial derivatives. Thus a FDM approximation is needed. From [8] we get the FDM approximation for partial derivatives:

$$\frac{\partial f}{\partial x} \approx \frac{f[i+1,j] - f[i-1,j]}{2\Delta x}\ (first\ order) \tag{2.5}$$

$$\frac{\partial f}{\partial y} \approx \frac{f[i,j+1] - f[i,j-1]}{2\Delta y}\ (first\ order) \tag{2.6}$$

$$\frac{\partial^2 f}{\partial x^2} \approx \frac{f[i+1,j] - 2f[i,j] + f[i-1,j]}{\Delta x^2}\ (second\ order) \tag{2.7}$$

$$\frac{\partial^2 f}{\partial y^2} \approx \frac{f[i,j+1] - 2f[i,j] + f[i,j-1]}{\Delta y^2}\ (second\ order) \tag{2.8}$$

where f[i,j] is the i:th datapoint on the x axis and the j:th datapoint on the y axis.

Since these are approximations to the derivative there is an unknown error value, however often what the error is proportional to can be known. For example the error of the FDM approximation of the second partial derivative of x is $\mathcal{O}(\Delta x^2)$. This is useful since if one were to reduce the distance between the points by some fraction (in the x distance), the error gets reduced by the square of that.

### 2.6.3 Hopscotch

In [[7] page 143] a method for solving the 2D heat equation using FDM is examined. The method is called the Hopscotch method. The method is a two step calculation method where the first step is calculated on every point on the thermal grid where i+j+n=even. Where n is the iteration number. The second step is calculated for the points where i+j+n=odd.

$$Step\ 1:$$

$$\frac{u^{n+1}_{[i,j]} - u^n_{[i,j]}}{\Delta t} = \alpha(\delta^2_x u^n_{[i,j]} + \delta^2_y u^n_{[i,j]}) \tag{2.9}$$

$$Step\ 2:$$

$$\frac{u_{[i,j]}^{n+1} - u_{[i,j]}^{n}}{\Delta t} = \alpha(\delta_x^2 u_{[i,j]}^{n+1} + \delta_y^2 u_{[i,j]}^{n+1}) \tag{2.10}$$

Where([7]; page137):

$$\delta_x^2 u_{[i,j]}^{m} = \frac{u_{[i+1,j]}^{m} - 2u_{[i,j]}^{m} + u_{[i-1,j]}^{m}}{\Delta x^2}$$

$$\delta_y^2 u_{[i,j]}^{m} = \frac{u_{[i,j+1]}^{m} - 2u_{[i,j]}^{m} + u_{[i,j-1]}^{m}}{\Delta y^2}$$

Where: $u_{[i,j]} \coloneqq$ the temperature grid

Within [7] the terms implicit and explicit solutions to a FDM problem are discussed. The terms can be simplified to be in reference to how the future value $u_{[i,j]}^{n+1}$ is calculated. An explicit calculation uses current values [n] of u to calculate a next value [n+1]. In contrast the implicit solution uses a combination of current and future values, which results in needing it to be solved using algebraic equations. This is somewhat complicated and time consuming. The advantage of implicit is that they are more stable. The Hopscotch method uses two steps, the first step is explicit and the second is implicit. However since the future values for step 2 was calculated in step 1, no algebraic solution is needed [[7] page 144] and thus the method is still explicit but also its unconditionally stable [[7] page 143]. This is why this method was chosen over others; it's simple to implement but still stable.

Notably is also that the error of the hopscotch method is given to be $\mathcal{O}(\Delta t, \Delta x^2, \Delta y^2)$. [[7] page 144]

## 2.7 LabWindows CVI

The IDE that is used is LabWindows developed by National Instruments, which is used due to much work to control and receive data to hardware and the gyro is already implemented. LabWindows is a C based IDE and much is the same as many similar softwares. However LabWindows has a library called advanced analysis library. Some functions in this library will be relevant for the calibration process, these are briefly explained here in no particular order.

- PolyFitX : Fits data using polynomial fitting where the used algorithm can be chosen.
- GaussFit : Fits data using a gaussian model
- CubicSplineFit : Fits data using a cubic spline fit
- SolveEqs : Solves real linear equation $\mathbf{A} \cdot \mathbf{x} = \mathbf{B}$
- GoodnessOfFit : Calculates how good the fitted data fits the original data
- DifferenceEx : A difference calculator that approximates the derivative

## 2.8 Plotting images & presenting data

Three different softwares are used to present data. LabWindows, Matlab and Microsoft Excel. figures/tables where these programs were used are indicated by (**L**),(**M**) and (**E**) respectively. Labwindows indicate images that use builtin functions to generate a graph object and then save the graph as an image. The different plotting tools are used for different purposes. LabWindows are used whenever data that is internal to a LabWindows program needs to be displayed. LabWindows has limited ability to plot data effectively thus this method is not preferable to the others and is only used whenever the others are not available. Matlab has the best ability to plot good figures, especially in 3D. However it is somewhat time consuming to import the data to the environment and program the plot parameters. Excel is a middle between the two programs.

# 3 Method

## 3.1 Investigation/observation

During the investigative phase the primary objective is to identify the areas where the calibration procedure can be improved upon. To achieve this the current calibration process is step by step observed to get a clear picture of what is being done and how. In order to arrive at areas in the current process which could be improved upon, explicit syllogistic arguments for what the further investigation of that area should produce are useful.
The first arguments can be stated before starting the investigation (note: P=premise, C=conclusion, D=definition of words used in argument).

Argument 1:

P1: Undefined or poorly defined object/s could lead to confusion now or in the future

P2: Confusion should be avoided

P3: A undefined or poorly defined object/s is found by the investigation

C: Define the object to avoid confusion

Argument 1 becomes most relevant at the start of the investigation process as many things will be undefined. The following chapters (3.1.1 - 3.1.4) will therefore be employing argument 1.

### 3.1.1 Defining the gyro outputs and the relation between analog and digital in calibration

The gyro consists of an IFOG sensor that outputs rate value. This value is read by a microcontroller which converts the value into a digital bit value which is used for two outputs one digital and one analog. These have their own compensation values. The digital is compensated and then outputted using RS422, the analog is instead converted from a digital value to an analog via an DAC. This introduces a problem. Since the calibration process collects data on the analog, after the digital to analog conversion, but the error compensation occurs within the microcontroller such that it needs to take the DAC into account. For this a relation between the analog and digital signal is required. For SF this is trivial. Since it is a unitless multiplication of the signal the analog to digital conversion gets included in the calibration of this, or in other words $DAC_{SF}(T)$ becomes included in $A_{SF\_comp}(T)$.

For the linearisation it's slightly different, however still relatively simple. The linear function adds a value onto the existing signal that depends on the value of the existing signal. This means that the linear function needs the units BIT to BIT since the analog output has the units volts a conversion between the two is needed. The DAC runs with $V_{ref}$ volts as its analog reference and the digital signal output is a 3 byte integer which has the max value $2^{23}$. this results in:

$$\beta = \frac{V_{ref}}{2^{23}} \frac{[V]}{[BIT]} \tag{3.1}$$

$\beta$ is needed in general conversion between analog [V] and digital[BIT].

The bias compensation value becomes harder to calculate and a relation between the analog output and the analog bias compensation is needed. Starting with:

$$Analog_{val}(\theta, T) = ((SENSOR_{val}(\theta, T) - A_{bias\_comp}(T)) \times A_{SF\_comp}(T) + A_{lin\_comp}(\omega)) \times \beta \times DAC_{SF}(T) + DAC_{bias}(T) \tag{3.2}$$

where $SENSOR_{val}(\theta, T)$ is the rate output from the fiber optic sensor. When3.2 is used for calculating the bias the following conditions are true:

- $SENSOR_{val}(0, T) = SENSOR_{bias\_error}(T)$ (see definition of Bias Offset error)
- $A_{lin\_comp}(\omega) = 0$ (linear compensation is defined as zero at zero rate)
- $A_{bias\_comp}(T) = 0$ (Since when calibrating the bias error values the bias compensation is turned off).
- $A_{SF\_comp}(T) = 1$ (Since when calibrating the bias error values the SF compensation is turned off)
- $DAC_{SF}(T) = 1$ ( since $A_{SF\_comp}(T)$ includes this)

$$Analog_{val\_bias}(T) = \beta \times SENSOR_{bias\_error}(T) + DAC_{bias}(T) \tag{3.3}$$

$Analog_{val\_bias}(T)$ is the bias error on the analog output, which should be zero. This value should be calibrated away using $A_{bias\_comp}(T)$, using 3.2 when $\theta = 0$ after calibration the result is:

$$Analog_{val} = ((SENSOR_{bias\_error}(T) - A_{bias\_comp}(T)) \times A_{SF\_comp}(T)) \times \beta + DAC_{bias}(T) \tag{3.4}$$

However since the analog port is now calibrated $Analog_{val}$ should be zero and, which results in:

$$0 = (SENSOR_{bias\_error}(T) - A_{bias\_comp}(T)) \times A_{SF\_comp}(T) \times \beta + DAC_{bias}(T) \tag{3.5}$$

$$A_{bias\_comp}(T) = \frac{DAC_{bias}(T)}{A_{SF\_comp}(T) \times \beta} + SENSOR_{bias\_error}(T) \tag{3.6}$$

inserting 3.3 gives the final result:

$$A_{bias\_comp}(T) = \frac{Analog_{val\_bias} - \beta \times SENSOR_{bias\_error}(T)}{A_{SF\_comp}(T) \times \beta} + SENSOR_{bias\_error}(T) \tag{3.7}$$

These relations are used whenever the analog compensation values are calculated.

### 3.1.2 Defining general program function and purpose

Since a program needs to be programmed in the end, it is a good practice to try to in advance describe the functionality of the program. In figure 3.1 the black box model is used in order to try to describe the inputs and outputs of the program. The black box model itself is a good tool within the design process in order to avoid problems down the line.

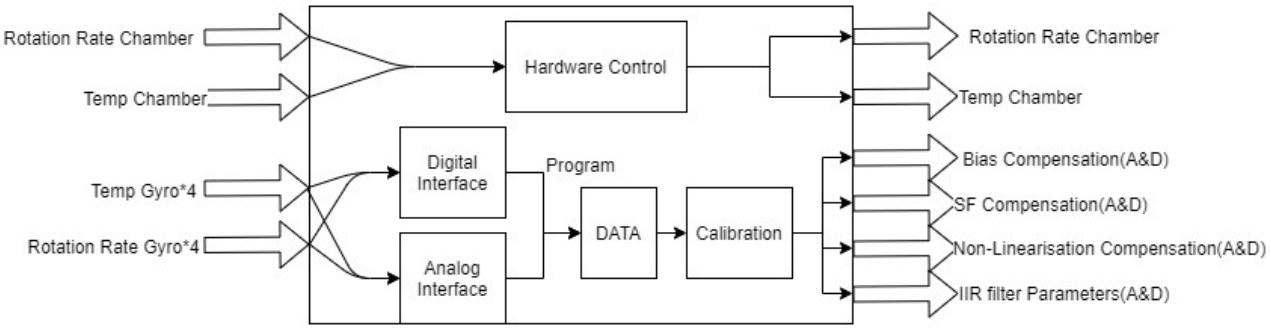


*Figure 3.1: Description of the inputs and outputs of the program using the black box model*

Another way to help the design of the program in order to make sure that it is useful for the end user is to set up a requirements list with the different categories of requirements, necessities and desirables. The contents of the list was added by using input from Saab.

Requirements (needed for the program to be useful):

1 Read data from gyro

2 Calculate SF, bias and linearity for analog and digital compensation values

3 Upload calibrated compensation values automatically

4 Control test machine

Necessities (would definitely be useful):

5 Implement auto-baudrate scanning

6 Choose calibration process

7 Manually set SF for the first calibration

8 Read the type and serial number of the gyro

Desirables (would most likely be useful):

9 Automatically tests the scale factor at the first calibration run and changes depending on the result

10 Different calibration routines

11 Calibrating more than one gyro at the time

12 Automatic COM port searching for the gyro

13 Better average forming of data

At the end in order to verify how good the program itself is, compare the results to this list by checking how many of these were fulfilled. If one of the requirements are not met the program would be considered to not be useful at the current state. A third way in the design process is to describe the intended functions of the program in a flow chart, this can be found in appendix D.

### 3.1.3 Defining product and profile

There are two definitions that when defining will include a lot of objects relating to the calibration, test and verification process and will be very useful down the line. These are the terms product and profile, these will primarily be defined in relation to the program that will be implemented later. But the definition profile will be very useful for other purposes as well. Starting with the product, in figure 3.2 the flowchart of the contents of the product are shown. The product is defined as containing a profile and settings. The profile will be defined later, settings however containing all relevant information to run the program and the specification of what gyro is run. The purpose of the definition product is to be related to a specific product of FOG from Saab that has specs and optimal settings to calibrate it.

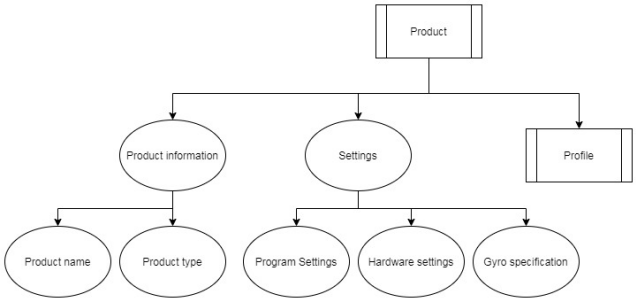


*Figure 3.2: Tree of the product*

The term profile is defined as a package of instructions for what and how the computer produces the desired result. This includes three different types of subprofiles, where a subprofile is a specific instruction for the computer relating to data collection. It also includes a calibration profile which details what calculations are to be done to get the error compensation values. In figure 3.2, the tree of the definition of the profile is shown. In this the typical subprofiles of the Temperature, rate and data are shown. Temperature subprofiles controls the temperature in the temperature chamber, this is alway given as two points which forms the function $T(t) = K \times t + T_0$ where $K$ is in the unit $\frac{^\circ C}{min}$ ($K$ can be zero). Rate subprofiles control the rotation of the rate table. These subprofiles are always the step function $\theta(t) = \theta_2 \times H(t - t_0) + \theta_1$. The data subprofiles are instructions of what specific action to do when. These takes the form:

Wait: Do not collect data from gyros

Collect Data: Collect data from gyro

Bookmark: A stamp of the data that is used to differentiate between what to do with it during the calibration functions

Calibrate: A command to start a calibrate process, can be used to calibrate in the middle of a profile

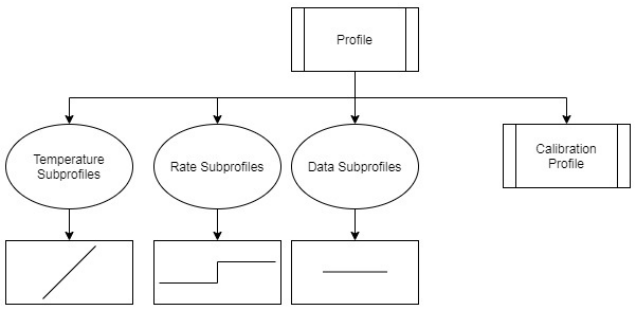


*Figure 3.3: Tree of the profile*

The Calibration profile is divided into three parts: filter, compensation calculation model and statistical model. The filter function is a way to filter the data before the calibration. The compensation calculation model is the type of calculation to be done(what mathematical method is used to derive the compensation values) and

the statistical model is what type of regression is used to find the best model who fits those data points. This relation is shown in figure 3.4.

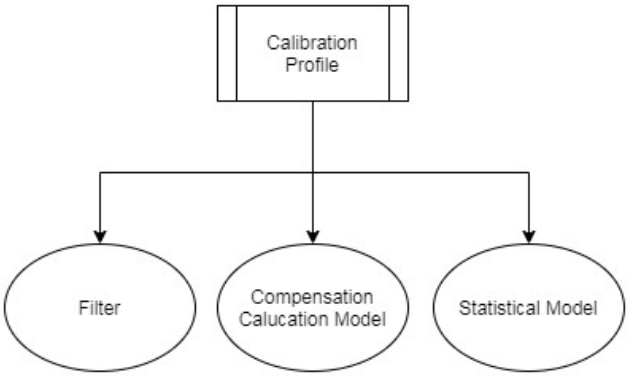


*Figure 3.4: Tree of the calibration profile*

### 3.1.4 Observing the current profile

In order to improve a process it is necessary to define and understand the previous process. To achieve this the currently used process is observed. The current process consists of the following profile:

1: Collect linear relation data at room temperature using 10 steps over the range $\theta(n) = \pm 15 \times n \, where \{n \in \mathbb{W}, 0 \leq n \leq 10\}$ for a total time of $\approx 10 \, min$.

2: Go down to -40 $°C$

3: Wait for the temperature of the gyro to stabilize

4: Run an OTR data collection over the range $[-40°C, +75°C]$

6: Calculate SF error

7: Calculate linearization error by first bias and SF compensation of the linearisation data.

8: Use polynomial fitting of bias, SF and linearisation error values in steps 5-7.

The data collection and controlling of hardware is done by a previously existing program. In figure 3.5 to 3.7 the temperature and rate for this profile leading up to step 5 in the process is shown. The data subprofiles are:

- Bookmark 1 (linear data)
- Collect Data for step 1
- Wait for step 2
- Wait for step 3
- Bookmark 4 (bias & SF data)
- Collect Data for step 4
- Calibrate for 5+

Step 5-7 is the compensation calculation model for this calculation profile, step 8 is the statistical model and no filter was used. During the times when data is collected there is an averaging over some seconds such that the end result is $\approx 100$ data points. This is the case since the data needs to be handled manually during the calibration and too many data points would be impractical in that case.

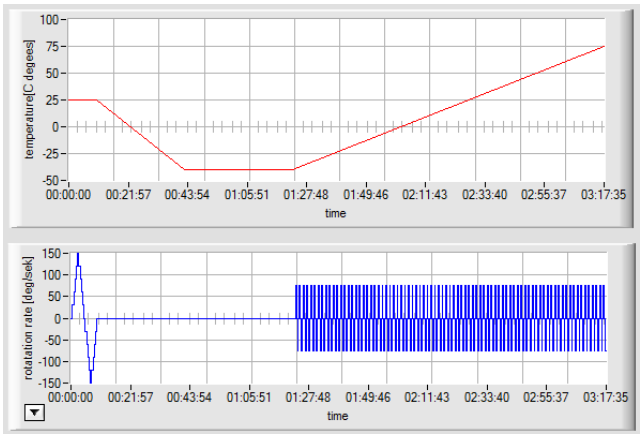


*Figure 3.5: Temperature and rate subprofiles (**L**)*

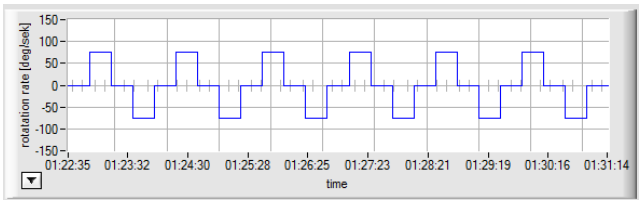


*Figure 3.6: LClose up example of rate loops (**L**)*

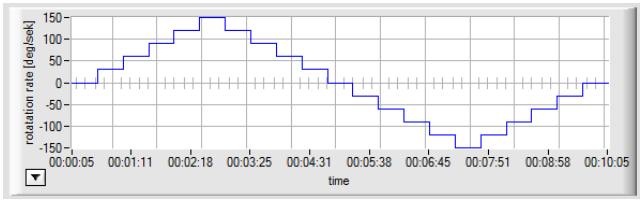


*Figure 3.7: Close up of linear loop (**L**)*

The next step is to calculate the error values of bias, SF and linearity. The error values calculated using the process described in steps 5-8 values are shown in figures 3.8, 3.9 and 3.10. In order to get the compensation values the error values need to be converted to the appropriate unit ( bias: BIT, SF: $\frac{SF_{ideal}}{SF_{err)}}$, Linear: BIT→BIT ).

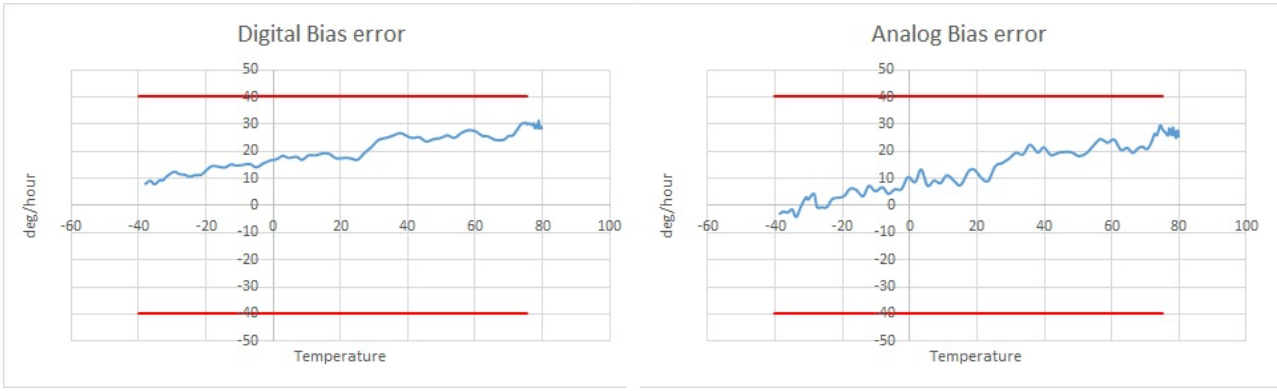


*Figure 3.8: Bias error before calibration (**E**)*

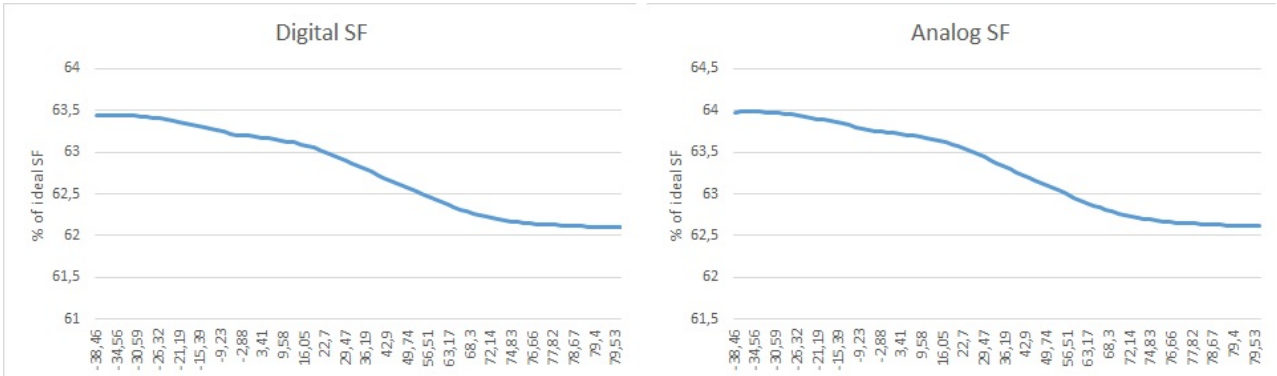


*Figure 3.9: SF error before calibration (**E**)*

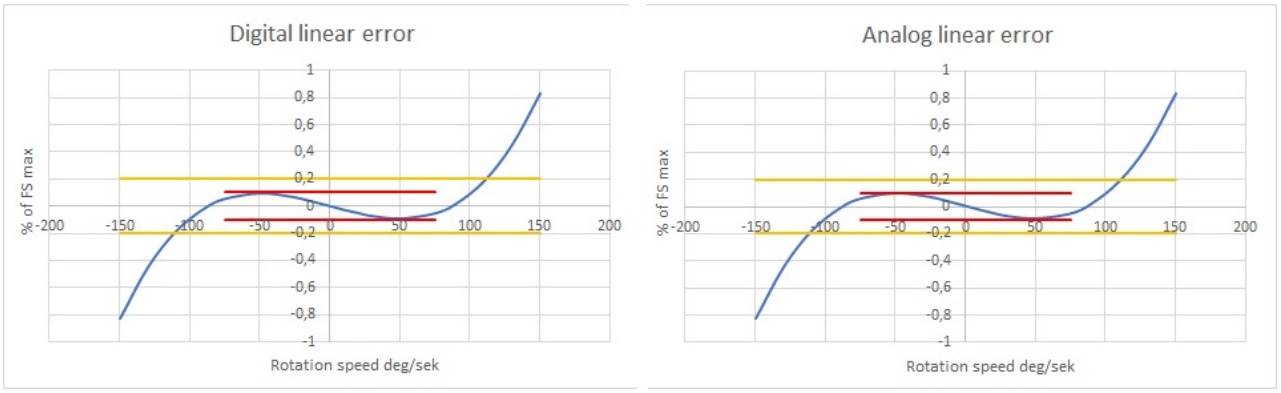


*Figure 3.10: Linearity error before calibration (**E**)*

In order to verify that the calibration was successful and result in a gyro that is within the specs of the product (table 2.1) the current profile is repeated again in the same way only now the gyro has been uploaded with the error compensation values. The resulting values for bias, SF and linearity are shown in figure 3.11, 3.12 and 3.13. In these figures the margins from table 2.1 are plotted as well.

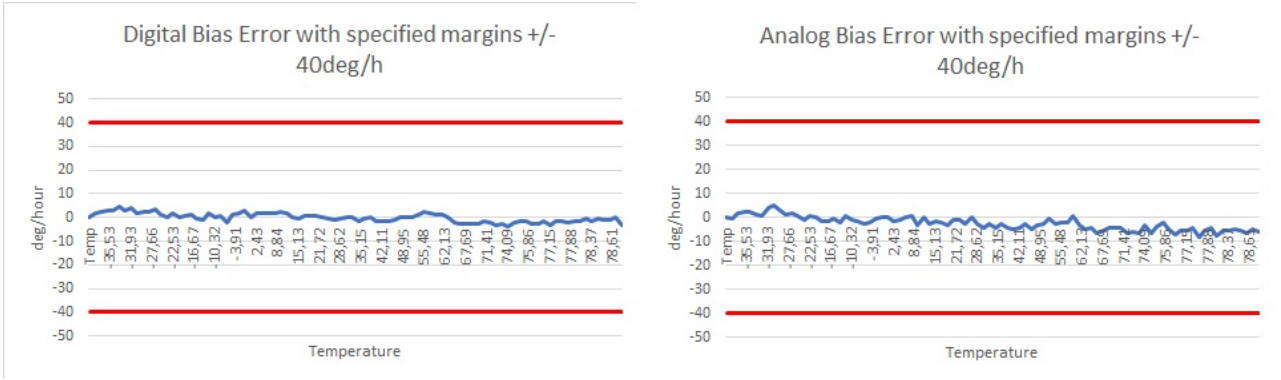


*Figure 3.11: Bias error after calibration (**E**)*

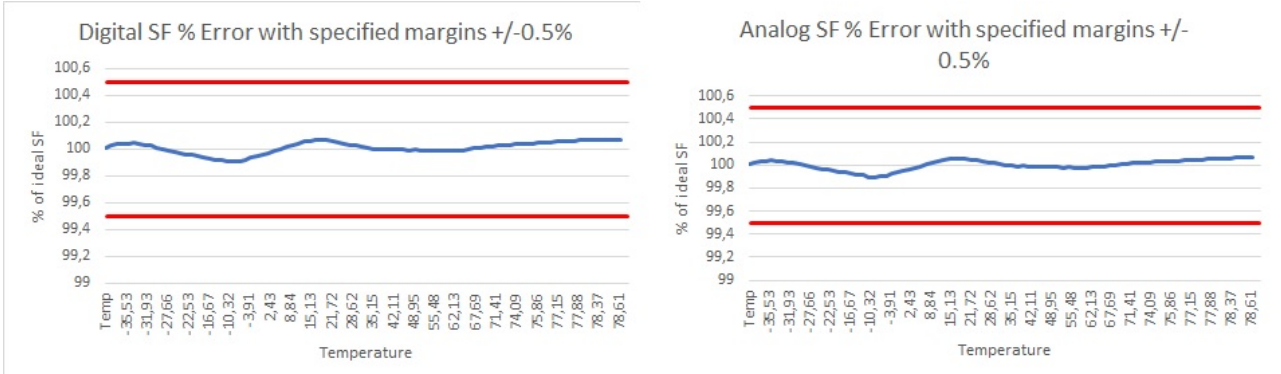


*Figure 3.12: SF error after calibration (**E**)*

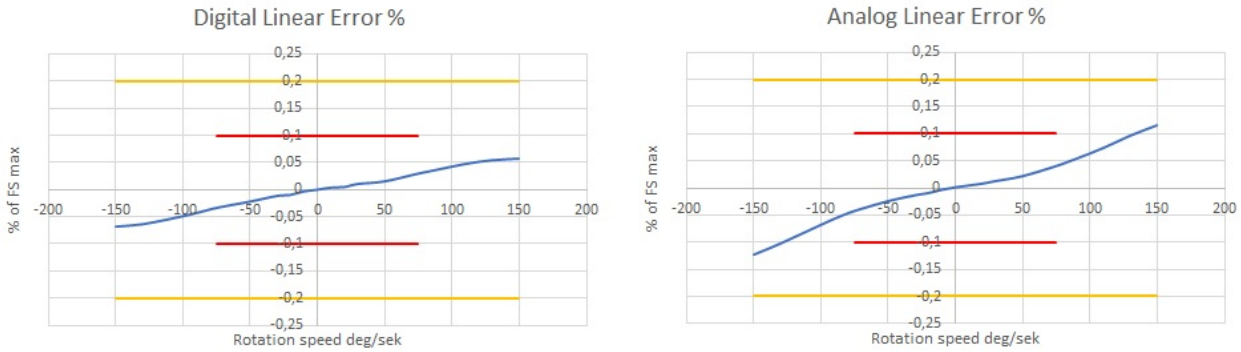


*Figure 3.13: Linearity error after calibration (**E**)*

A useful value to calculate is the reduction of the error, since this gives an idea of how good the calibration did. These reduction factors are calculated according to equation 3.8. In table 3.1 the absolute averaged values for the pre-calibration data is shown and in table 3.2 the absolute averaged values for the post calibration. in table 3.3 the reduction percentage is listed, calculated using equation 3.8.

$$f = 1 - \frac{\overline{|Error_{after}|}}{|Error_{before}|} \tag{3.8}$$

| Name | Digital | Analog | Unit |
|---|---|---|---|
| Bias | 15,49158332 | 21,30162098 | deg/hour |
| SF | 37,223651 | 36,69312882 | % of SF ideal error |
| Linear | 0,188286327 | 0,18291363 | % of FS max |

*Table 3.1: Listing of the averages of the data*

| Name | Digital | Analog | Unit |
|---|---|---|---|
| Bias | 1,661255986 | 3,378396673 | deg/hour |
| SF | 0,036743828 | 0,035844137 | % of SF ideal error |
| Linear | 0,026890181 | 0,04638709 | % of FS max |

*Table 3.2: Listing of the averages of the error compensated data*

| Name | Digital | Analog | Unit |
|---|---|---|---|
| Bias | 89,28 | 84,14 | % reduced error |
| SF | 99.901 | 99,902 | % reduced error |
| Linear | 85,72 | 74,64 | % reduced error |

*Table 3.3: Listing of the percentual reduction of the error*

### 3.1.5 Possible Improvements induced from the standard profile

In order to improve the current profile a step by step investigation process is used to figure out possible improvements using the following syllogistic arguments for that. Implementation and testing of these possibilities should reveal whether they are actual improvements (note: P=premise, C=conclusion, D=definition of words used in argument).

Argument 2 for step 1 in current profile:

P1: For max accuracy the rate table should travel $\phi \geq 2 \times \pi$ at any speed

P2: The relation $\phi = \theta \times time$ applies

P3: The rotation speed varies

C: In order to keep the values accurate the time on each step should change

Argument 2 leads to the possible improvement of changing how long the rate table stays on one level depending on how fast the table rotates.

Argument 3 for step 1 in current profile:

P1: The chosen linearisation temperature results in an optimal linear relation at or around that temperature

P2: The average ambient temperature changes depending on where the gyro is used

C: Adapting the linearity of the sold gyros to the customer using different linearity temperature

Argument 4 for step 3 in current profile:

P1: The actual stabilization time is unknown

P2: The wati time is set with a large tolerance using temperature stabilization standards

P3: There are methods to approximate the actual stabilization time

C: Finding a stabilization time using an appropriate method could lead to shorter profile

Argument 5 for step 4 in current profile:

P1: Gyro output error is partially dependent upon temperature change rate

P2: The current profile does not take temperature change rate into account

C: Gyro output compensation could be improved if profiles takes temperature change rate into account

Argument 6 for step 5-8:

D: *More advanced* = more steps and/or more complicated math that results in some advantages

D: *Manual calculation* = A manual operator who handles the data and decides which calculations to be done and how, though actual calculations are done in a computer.

P1: A computer gives access to more advanced calculation methods using more data points than manual calculation

P2: Something is calculated manually with few data points

C: There could exist a calculation method that is more advanced when it's done inside a computer

Argument 6 leads to the following new arguments.

Argument 7 for step 5-7:

P1: The output from gyro = $\omega(\theta, T)$

P2: $\omega(\theta, T)$ forms a surface

C: Surface fitting of $\omega(\theta, T)$ could be a new compensation calculation model

Argument 8 for step 5-7:

P1: The output from gyro = $\omega(\theta, T)$

P2: The SF is the constant of the relation between $\omega$ and $\theta$ which should have the ideal property $\omega = F(\theta, T) = SF \times \theta$

P2: $\frac{\partial F(\theta,T)}{\partial \theta} = SF$

C: The partial derivative could be used as new compensation calculation model

Argument 7-8 are new possible ways to calculate step 5-7. To simplify the new methods are named Surface Partial derivative for argument 7 and 8 respectively. For simplified language step 5-7 are named the independent compensation calculation method. The independent name is chosen due to the other methods using the function $\omega(\theta, T)$ whereas the error values in step 5-7 are calculated without the necessity of using information from the other steps.

## 3.2 Simulation and implementation in LabWindows program

The program that the end user will utilize is the platform where the possible improvements derived from argument 2-8 are implemented. The program is implemented partially from scratch, functions relating to the digital connection of the gyro and controlling of the hardware are taken from pre existing programs. Since multiple possible improvements have been presented which have different combinations of them, the time that it would take to perform all these would not be practical. This since the time of one full test takes around several hours. A solution to this is simulation of the test and calibration. This is also done by implementation in the program.

Since the values collected from rate and temperature are significantly fewer than that of the digital and analog signal. The values for rate and temperature are interpolated. Four interpolation types have been implemented; linear, polynomial, rational and spline. Linear uses the line of the two closest values whilst the others use internal LabWindows functions. The result of a simple test of the different interpolation methods are shown in 3.14, 3.15, 3.16 and 3.17. Here a step function $\sigma(x)$ is tested where 20 data points 0 to 20 are interpolated to 50 data points over 0 to 20 as well. This is done to see what the interpolation functions result in. From these results the polynomial and rational interpolation seems unfit for this case as they frequently result in unstable and odd results. This leaves linear and spline, spline is chosen for these as it is the fastest of the two and it seems to improve the more data points are used. This is tested on real world rate data shown in 3.18 and the result of the interpolation in 3.19.

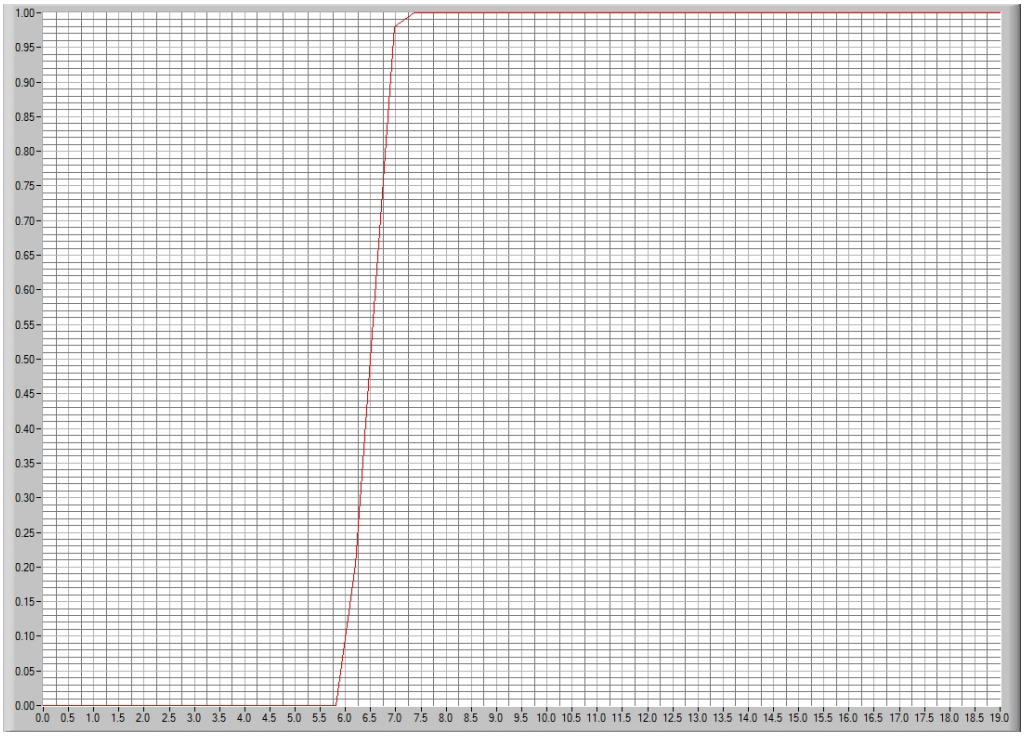


*Figure 3.14: Test of linear interpolation on $\sigma(x)$ ($\boldsymbol{L}$)*

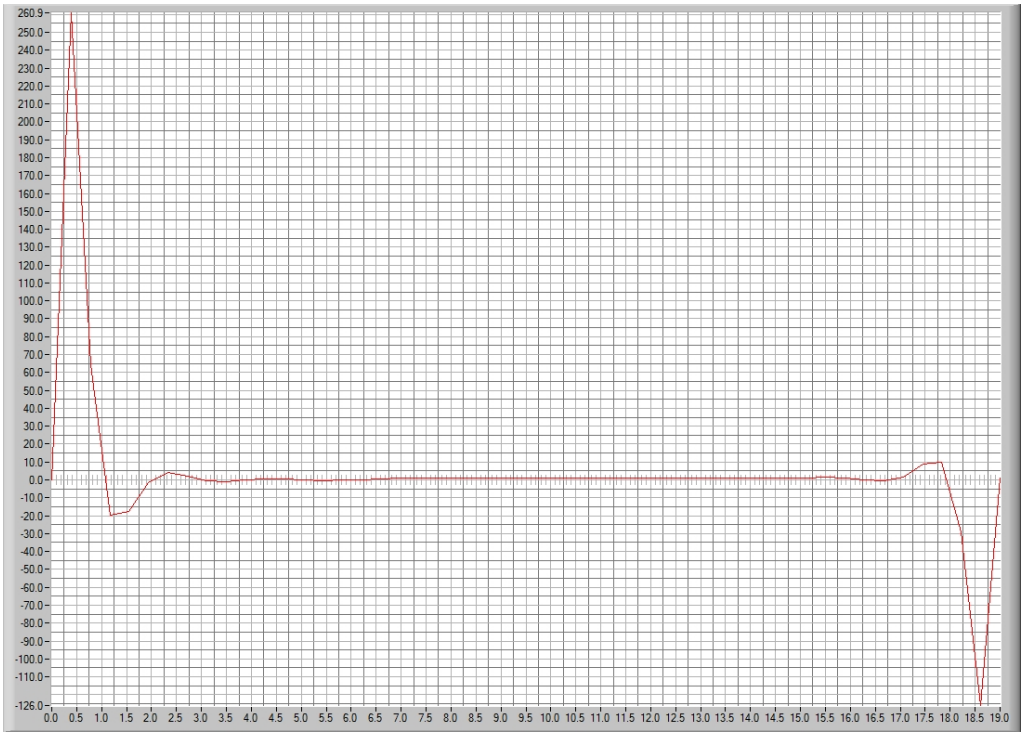


*Figure 3.15: Test of polynomial interpolation on $\sigma(x)$ ($\boldsymbol{L}$)*

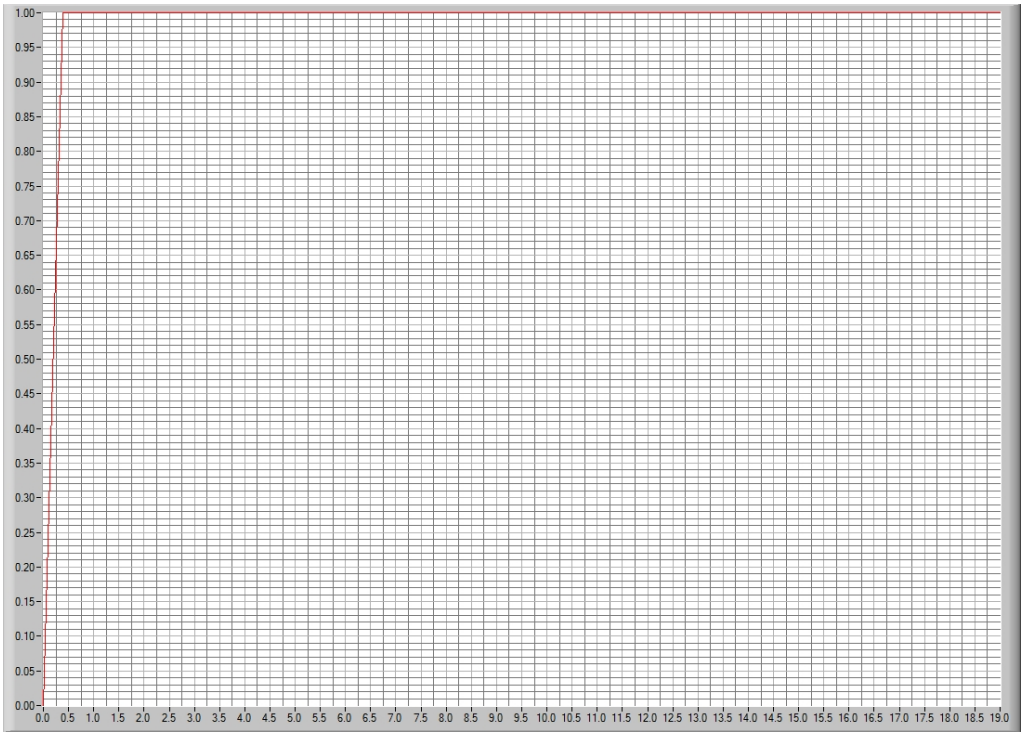


*Figure 3.16: Test of rational interpolation on $\sigma(x)$ (**L**)*


*Figure 3.17: Test of spline interpolation on $\sigma(x)$ (**L**)*

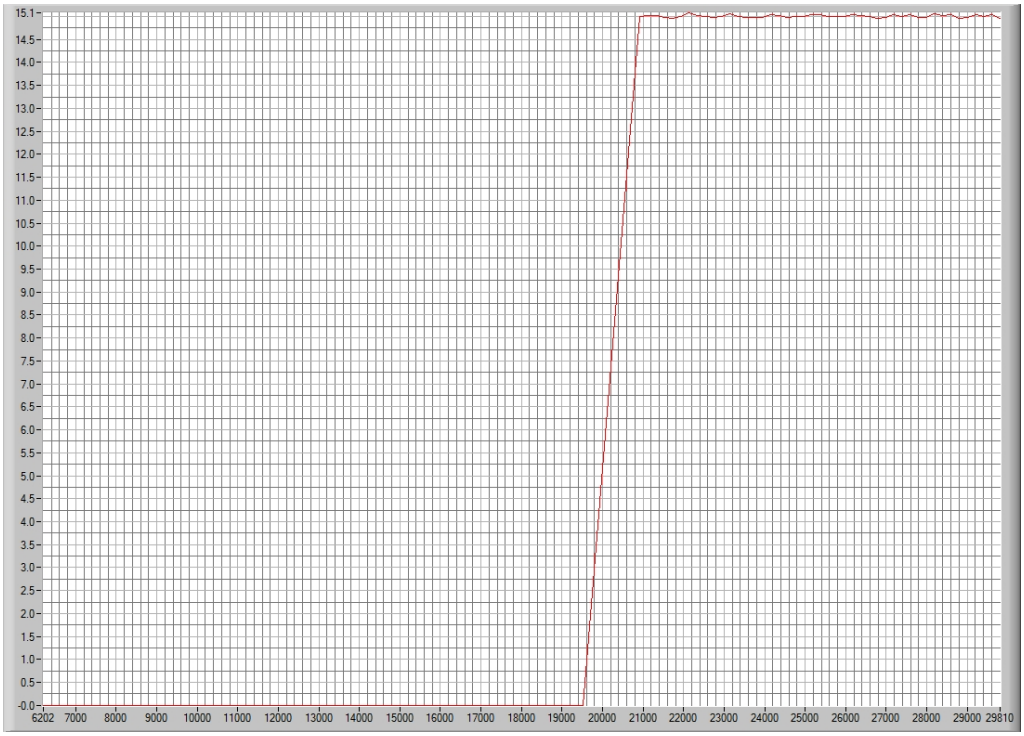


*Figure 3.18: Real world rate data 100 data points, as example of the interpolation test. (**L**)*

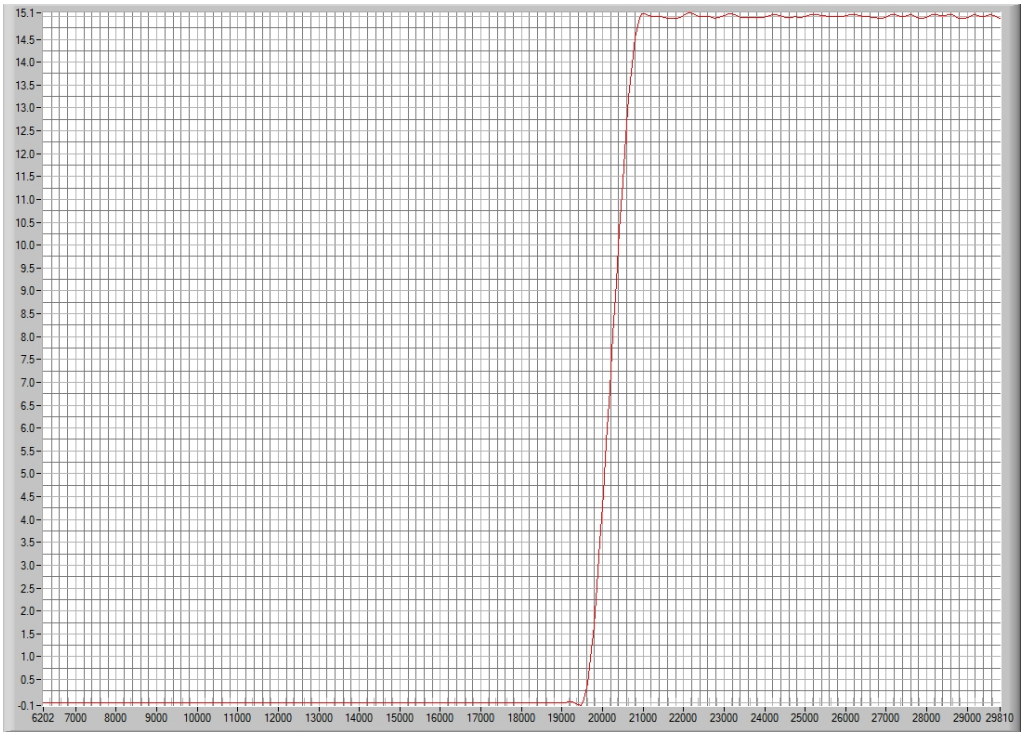


*Figure 3.19: Result of test of spline interpolation on real world rate data 100 to 300 data points. (**L**)*

### 3.2.1 Simulation of thermal stabilization process using FDM

From argument 4 the conclusion is that the thermal stabilization time needs to be calculated. To solve this thermal process it is simulated by using the FDM. Some assumptions are used during this process:

1 The gyro is symmetrical around the cylindrical Z-axis(the form of the gyro is a cylinder), which results in the thermal simulation can be approximated as a 2D- cross section of the cylinder.

2 The air convection inside the hollow cylinder is approximated as conduction. The reason for this is that convection usually has higher heat transfer than pure conduction of the same elements. This results in that the actual stabilization time should be faster than the one resulting from pure conduction.

3 The boundary layer of the thermal grid is the temperature of the temperature chamber.

Since these 3 assumptions lead to 2D heat conduction using the FDM method hopscotch is now possible. The setup for the simulation of the is displayed in figure 3.20. For this simulation the number of points are chosen to be 40 points in x direction and 20 in the z direction. The thermal conduction capacity of the material A is $\alpha_A$ and material B is $\alpha_B$ which are chosen to be two constants. These values are highly approximative constants which in reality depend upon temperature and pressure. The time step is chosen to be 0.01 sek. Since the error of the hopscotch method is $\mathcal{O}(\Delta t, \Delta x^2, \Delta y^2)$ the values $\Delta x = \frac{X_0}{40}$, $\Delta z = \frac{Z_0}{20}$ and 0.01 is what the error is dependent upon and decreasing these would lead to better accuracy of the model. However increasing the amount of points in the grid or decreasing the time steps would lead to the method taking much longer times. These values seem to be a good compromise between these two factors and sufficient for the accuracy needed here. Although further optimization of those parameters and all parameters involved within the method is possible.

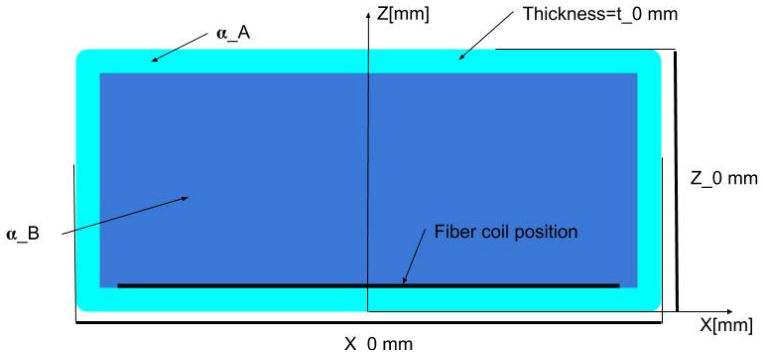


*Figure 3.20: Image of thermal simulation setup showing a crosssection*

From shupe's general theory of fiber optic sensors dependence on temperature it is stated that the temperature and the temperature change rate impact the error [1]. The temperature errors itself is what will be calibrated away at a later stage. But the temperature change rate error needs to stabilize so that it doesn't get included too much into the temperature error calibration or that the temperature of the coil is not correct when the test starts. Instead of using shupe's equation to find error values the standard deviation of the temperature of the coil surface is used. This is used since after a certain amount of time the temperature of the gyros sensor should be sufficiently stable that a test can be conducted. For this test the trigger value of the standard deviation is 0.001 $^\circ C$. In order to estimate how much the error will be the temperature of the coil surface is taken (coil surface shown in figure 3.20). The values of this coil surface is shown in figure 3.22. In figure 3.23 the average, derivative of the average, standard deviation and the derivative of the standard deviation of the coil surface are shown and in figure 3.21 four results of the thermal simulation process are shown.

The stabilization time is the difference between the time where the temperature chamber reaches the desired temperature and the time when the coil surface has achieved the desired standard deviation. In the current test this is $t_{stable} = 276.29sek$. As a last precaution the stabilization time is increased by a safety factor, this is done due to a lot of the parameters and assumptions could have led to inaccuracies in the final result. With a safety factor of 50% the total wait time of the profile at step 4 is now $414.435sek$. Which is significantly less than the current profile which has $40min = 2400sek$ as its wait time.

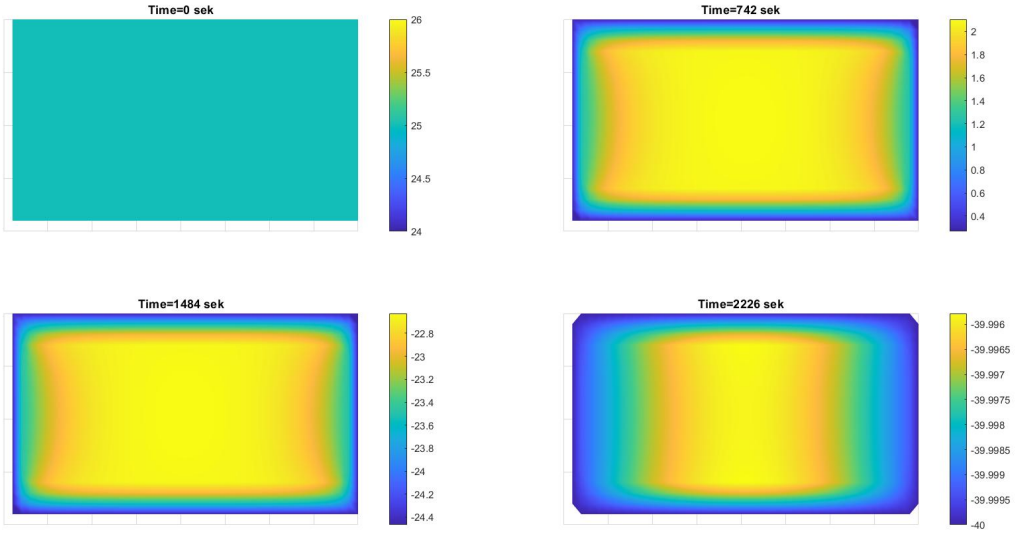


*Figure 3.21: Plot of the thermal simulation at different times (**M**)*

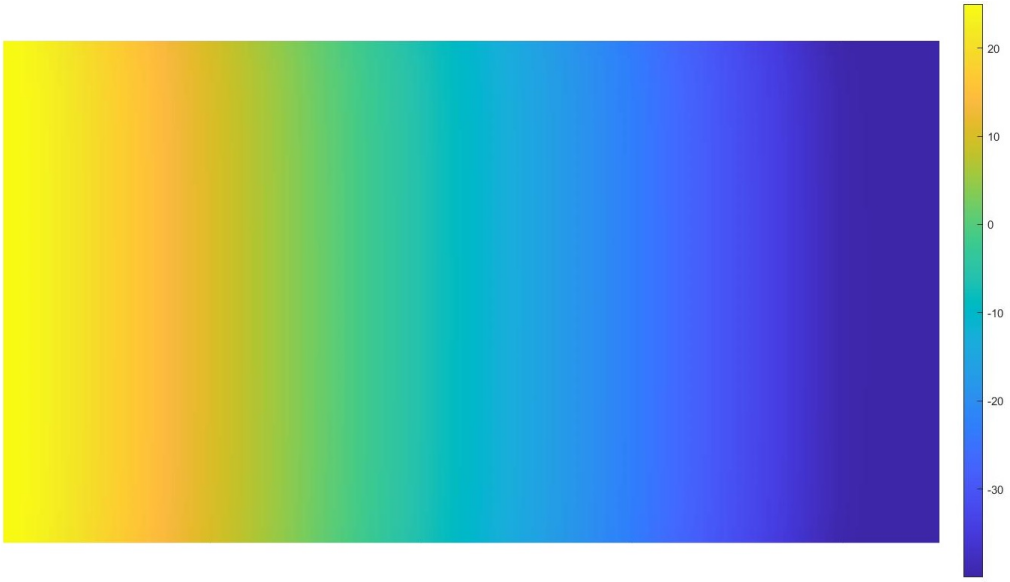


*Figure 3.22: Plot of the values of the coil surface; at leftmost column the temperature is $25°C$ and the rightmost is $-40°C$. (**M**)*

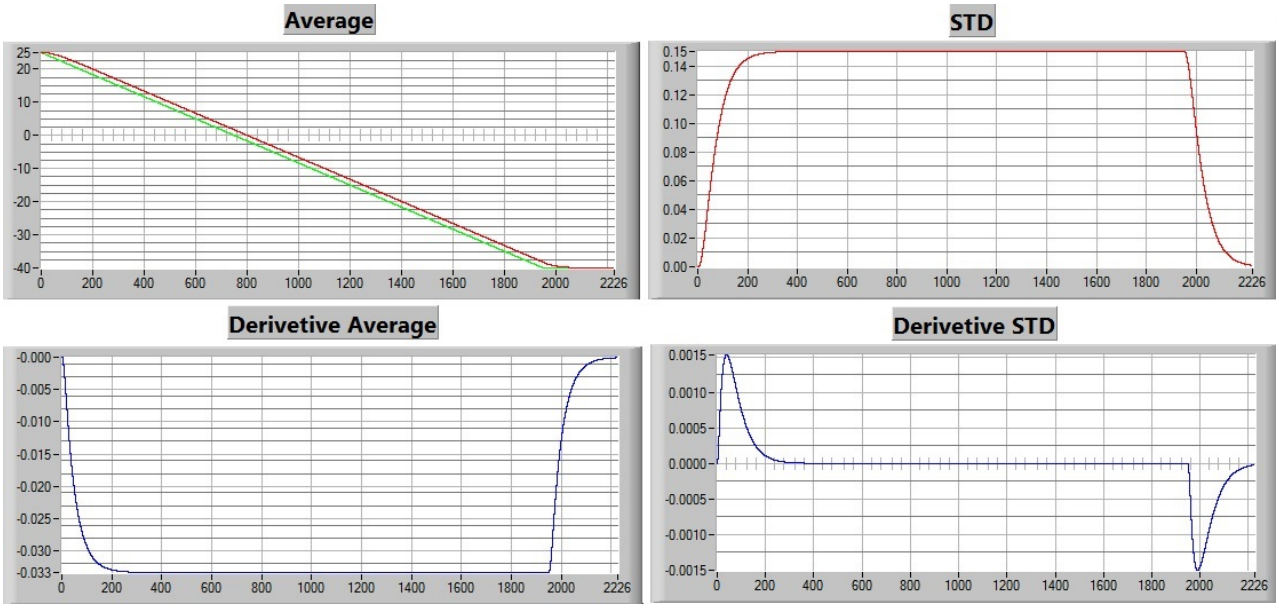


*Figure 3.23: Plot of the average, standard deviation(STD), derivative of the average and the derivative of the STD of the coil surface (**L**)*

### 3.2.2 Implementation of new profiles

Arguments 2 to 5 is to be implemented programmatically. This is done inside the aforementioned program. The program generates a profile using predefined profile templates that the user can modify with chosen parameters ( figure 4.3). Whenever there is a temperature step where the temperature needs to stabilize for some wait time, the thermal simulation process in 3.2.1 is used to calculate this when generating the profile. The current one that is used (step 1-4) can be easily generated by selecting the parameters of it such as steps in linear rate, rate OTR loops, temperature max and min. In figure 3.24 the template for the current profile with thermal simulation enabled is shown.

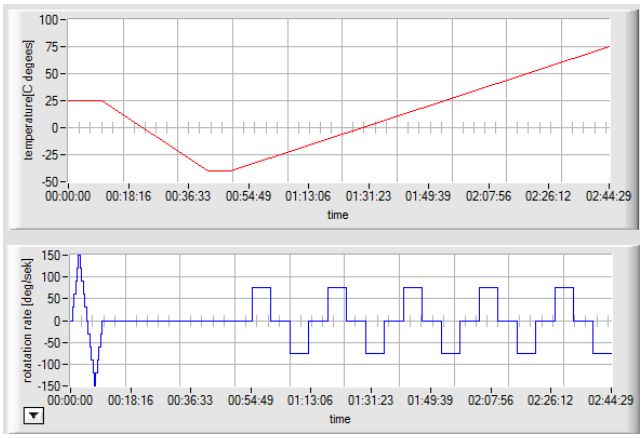


*Figure 3.24: Plot of the template of the current profile but with temperature simulation enabled (**L**)*

Using the possible improvements derived from the arguments the currently used profile can be improved using new templates. Argument 2 presents the possible improvement of constant number of rotations at different speeds. In figure 3.25 the implementation of this template is displayed, here the times of 11 steps are calculated by setting 2 rotations as the constant.

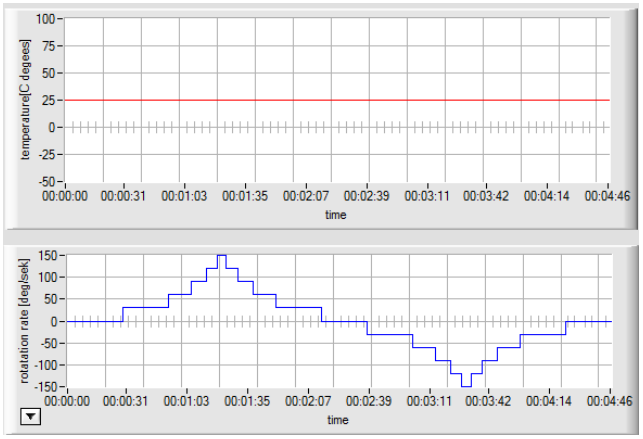


*Figure 3.25: Plot of constant rotation template for linear part of profile (**L**)*

Argument 3 is now implemented, this is shown in figure 3.26. The linearization starts at $25°C$ (which represents room temperature) and goes to $20°C$, then waits for the temperature to stabilize. In figure 3.27 the thermal simulation result of the step is shown.

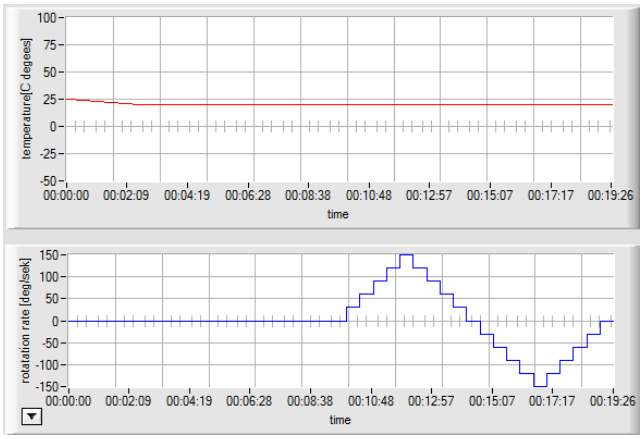


*Figure 3.26: Plot of linear temperature profile which has been temperature adjusted (**L**)*

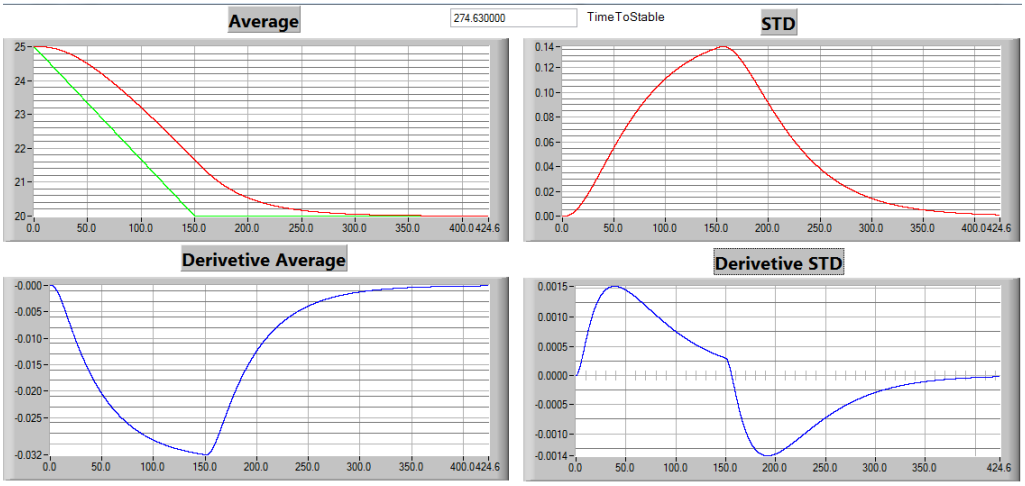


*Figure 3.27: Plot of the average, standard deviation(STD), derivative of the average and the derivative of the STD of the coil surface (**L**)*

Argument 5 leads to 2 main ways of attempting to construct a profile template that takes temperature change rate when collecting the calibration data. The first profile template removes it altogether by implementing a step process in the temperature. The template uses the thermal simulation to wait until the temperature has stabilized to the desired value. In figure 3.28 the step template is shown.

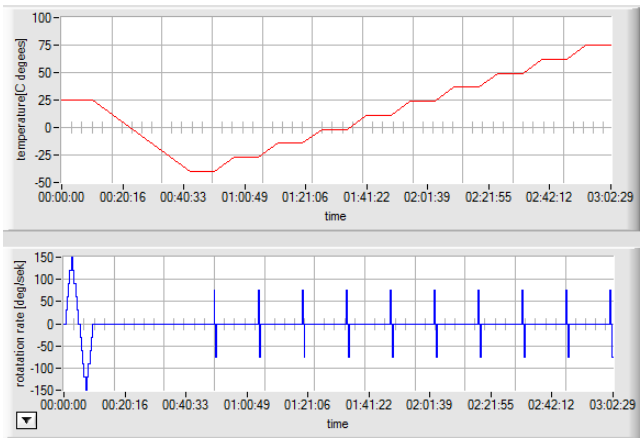


*Figure 3.28: Plot of step templatefor profile (**L**)*

The second template uses a cyclical format on the temperature. This should lead to the error that results from the temperature change rate cancels eachother out in the calibration process since the error is symmetric [6]. This template first goes to the middle of the temperature interval and waits for the temperature to stabilize. This template is shown in figure 3.29.

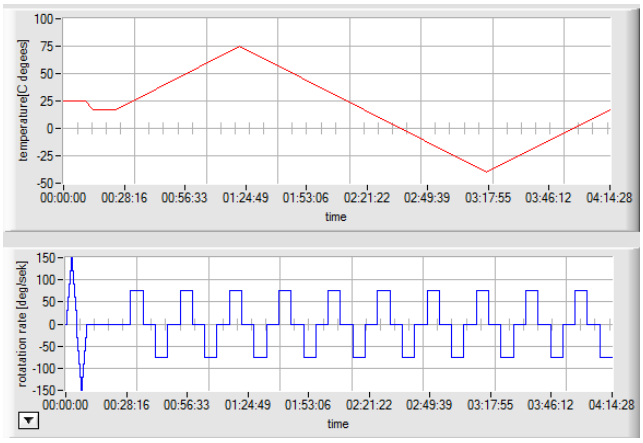


*Figure 3.29: Plot of cyclic template for profile (**L**)*

A final template relating to argument 5 is to combine the previous two templates to form a cyclic stepped template. This is shown in figure 3.30.

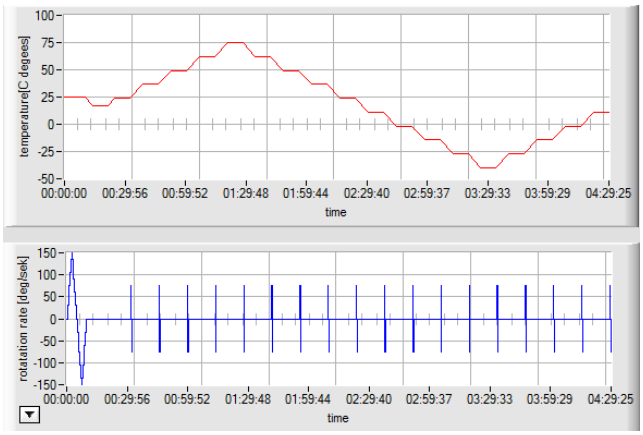


*Figure 3.30: Plot of cyclic step template for profile (**L**)*

For the compensation calibration methods that use the function $\omega(\theta, T)$ (partial derivative and surface) the profiles need their linear profile inside the rate loops. This is because of how they are calculated (by the $\omega(\theta, T)$ function). The template for these calibration methods are the same as before except the linear part is removed from the start and is embedded inside the OTR run. This is shown in figure 3.31 by modifying the current profile template.

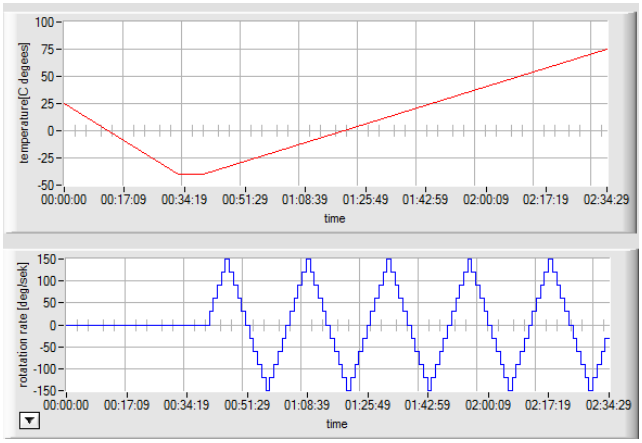


*Figure 3.31: Plot of a modification to the current profile template with thermal simulation for the surface and partial derivative compensation calculation methods (**L**)*

| | Profile Template | [h:m:s] | Image |
|---|---|---|---|
| 1 | Current (Acyclic) | 3:17:35 | 3.5 |
| 2 | Acyclic w Therm Sim | 2:44:29 | 3.24 |
| 3 | Acyclic w Linear in OTR | 2:34:29 | 3.31 |
| 4 | AcyclicStep@10*steps* | 3:02:29 | 3.28 |
| 5 | Cyclic@1$\frac{^\circ C}{s}$ | 4:14:28 | 3.29 |
| 6 | Cyclic@1.3$\frac{^\circ C}{s}$ | 3:14:30 | 3.29 |
| 7 | Cyclic@1.5$\frac{^\circ C}{s}$ | 2:43:25 | 3.29 |
| 8 | Cyclic@2$\frac{^\circ C}{s}$ | 2:05:05 | 3.29 |
| 9 | CyclicStep@5*steps* | 3:15:32 | 3.30 |
| 10 | CyclicStep@10*steps* | 4:29:25 | 3.30 |
| 11 | CyclicStep@15*steps* | 5:47:11 | 3.30 |

*Table 3.4: Total time taken for each profile*

The cyclic templates show the trend of being more time consuming, however table 3.4 row 6-8 shows that since they may calibrate away the temperature change rate. The temperature change rate may justifiably be increased which has a large result on the total time of the profile.

### 3.2.3 Implementation of new calibration processes

Argument 6-8 is to be implemented into the program. In appendix C the flowchart of the independent calibration process is shown as implemented into the program. The two new compensation calibration methods are described.

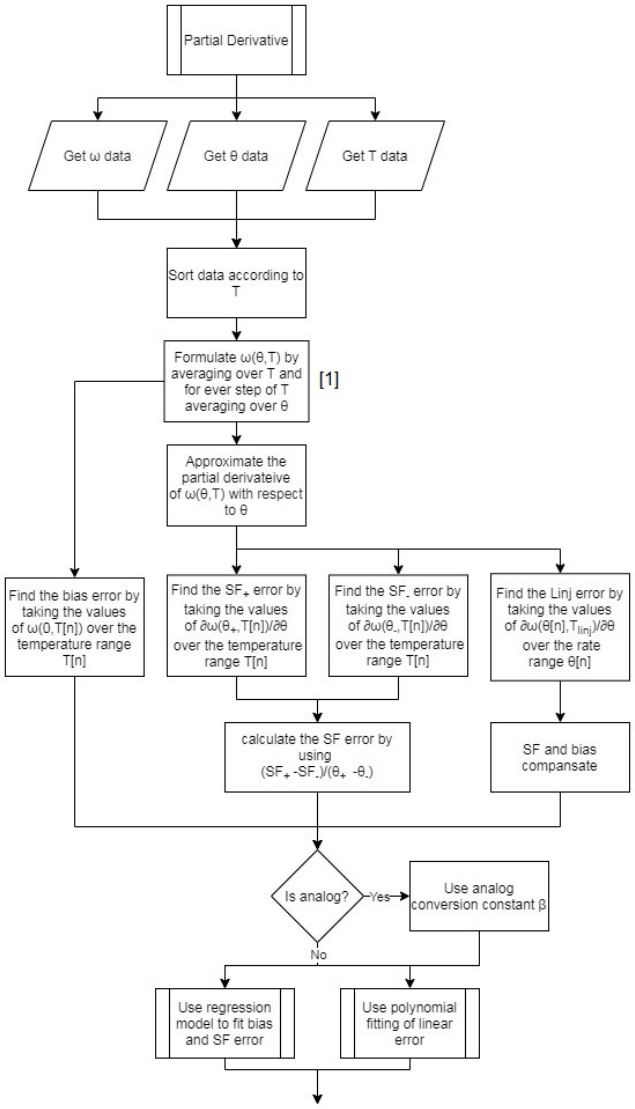


*Figure 3.32: Flowchart of the partial derivative compensation calibration process that is implemented in the end program (**L**)*

In step [1] in figure 3.32 the function $\omega(\theta, T)$ is calculated by an averaging process. The $\omega(\theta, T)$ function in the partial derivative process will form a finite matrix where the size is going to be dependent upon the steps of the linear steps and number of rate loops in OTR. For example if steps in linear = 11 and rate loops is 100, this will result in:

$$\omega(\theta, T) \Rightarrow \omega[n][m] \; where \; \{n \in \mathbb{W}, 0 < n < 100\} \; and \; \{m \in \mathbb{W}, 0 < m < 11\}$$

Here the rows represent the temperature $T[n]$ and columns represent $\theta[m]$. $\omega[n][m]$ is formed by for every step in $n$, average omega over all steps in $m$. Due to that the $\omega[n][m]$ function is discrete the partial derivative needs to be approximated. This is done by the DifferenceEx function.

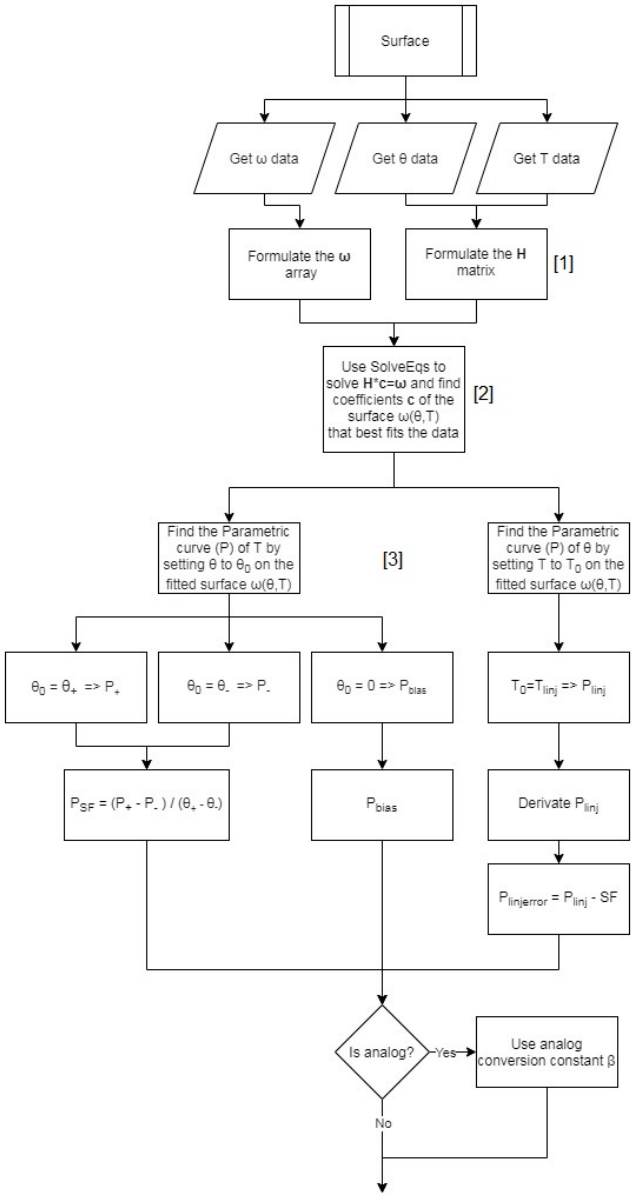


*Figure 3.33: Flowchart of the surface compensation calibration process that is implemented in the end program (**L**)*

In step [1] in figure 3.33 the H matrix refers to a matrix where the values of $\theta$ and temperature are put in a surface function of the form:

$$F_{surf}(\theta, T) = \sum_{i=0}^{n} \sum_{j=0}^{n-i} C_{i,j} \theta^i T^j \tag{3.9}$$

This is a polynomial surface where $n$ is the maximal polynomial order within the surface function. In step [2] in figure 3.33, solving the $\mathbf{H} \cdot \mathbf{c} = \omega$ equation system will result in the coefficients $C_{i,j}$ in $F_{surf}(\theta, T)$ to be known. This is the fitted surface to the data. In step [3] in figure 3.33 to arrive at a parametric curve for the surface one variable in $F_{surf}(\theta, T)$ to a constant. When one variable is set to a constant the function becomes dependent on one variable instead which can be used to find specific relations on the surface.

Next step is to implement some filter functions. The chosen are weighted average, butterworth IIR and gaussian as a good start for some simple filters to implement. With these filters a fast fourier transform was also implemented with the intention to be able to analyse the signal so that optimal frequency parameters for the butterworth IIR can be found. If this can't be done other aspects of gyro signal properties can be

investigated for future purposes. These functionalities will not be tested further though and are explained in more detail in appendix A.

Lastly the statistical models are implemented. These are presented and shortly described in table 3.5. In table 3.6 which statistical models that work with which compensation calibration process.

| | Statistical model name | Description |
|---|---|---|
| 1 | Polynomial | Uses the builtin function PolyFitX to fit the data to the best order |
| 2 | Spline | Uses the CubicSplineFit function in labwindows to spline fit the data |
| 3 | Point | Divides the data to regress into x amount of steps and then find the best average that fits the data of these step |
| 4 | Gaussian | Divides the data to regress into x amount of steps and forms a histogram of the data then uses GaussFit to fit the probability of the data. The center of the fitted gaussian fit is the most average |
| 5 | Surface | Uses SolveEqs to find coefficients for the surface function |

*Table 3.5: The different statistical models*

| | Works with compensation model |
|---|---|
| 1 | Independant, Partial derivative |
| 2 | Independant, Partial derivative |
| 3 | Independant, Partial derivative |
| 4 | Independant |
| 5 | Surface |

*Table 3.6: table of which statistical models can be used with which compensation calculation process*

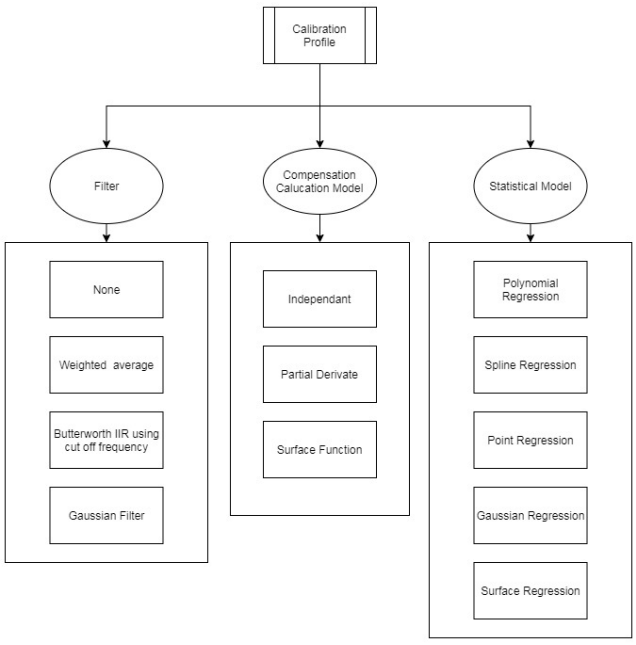


*Figure 3.34: Updated calibration profile with the possible selections that have been implemented*

### 3.2.4 Simulation of calibration process using profile simulation based on collected values

In order to figure out which combination of profile and calculation method would lead to the best accuracy and reliability. Since running multiple tests where every test takes several hours would take a very long time which would be impractical. To solve this a simulation of the calibration process is constructed. The compensation calibration process is the same as for the real case. The profile and data collection of that however needs to be simulated. This will be done by first collecting data about the properties of the different signals in the process then trying to replicate this in the program. In figure 3.35 a static data collection is done where rotation is zero and temperature is room temp. In table 3.7 the STD values of these signals are shown, these values will be important for the simulation.


*Figure 3.35: Static noise collection (**E**)*

| | Signal | STD |
|---|---|---|
| 1 | Digital | 812.718 |
| 2 | Analog | 0.000361 |
| 3 | Temperature | 0.204467 |
| 4 | Rate | 0.000736 |

*Table 3.7: Table of the STD values of the noise*

The simulation takes the current active profile and generates certain amounts of data for each signal. From the static data collection the temperature data points are $\approx 1$ sek apart and the rate is $\approx 0.2$. The Digital and analog are much faster however due to limitations the data rate is set to 0.1 in the simulation. This is still somewhat realistic as a maximum amount of data points are set in the program in order to not influence performance (time and memory) which removes some amount of data points with an even interval. Next the error values need to be simulated. Since the typical values these are known this is trivial. The values for these are shown in figure 3.36, 3.37 and 3.38 which for easy viewing are set to around 10 times larger than

the actual values of the gyro. These are applied in the reverse order of the description in chapter 3.1.1. wich is: $\omega\_Error_{Sim} = (SF \times \theta_{sim} + Linear\_Error_{Sim}(\omega))/SF\_Error_{Sim}(T) + bias\_Error_{Sim}(T)$. After this a gaussian noise is applied to all signals which uses the values collected in the static data collection. The end result of this is shown in figure 3.39 where $\omega(\theta, T)$ are simulated and plotted over $\{-150 \leq \theta \leq 150\}$ and $\{-40 \leq T \leq 75\}$.

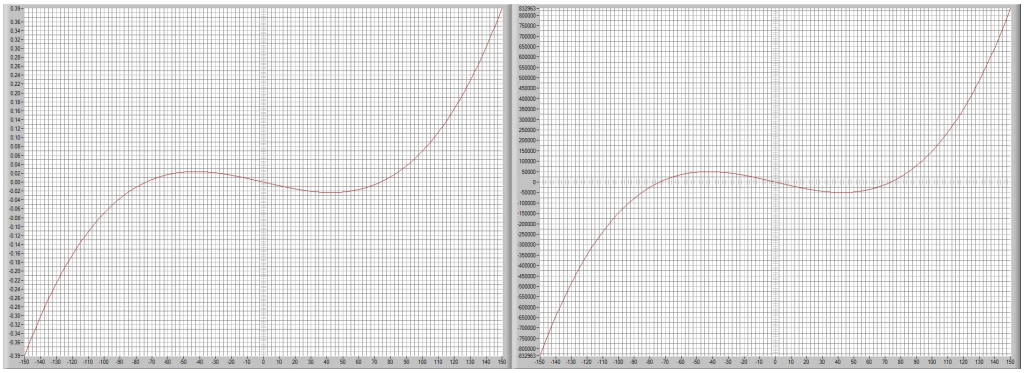

*Figure 3.36: Simulated digital and analog linear error (**L**)*

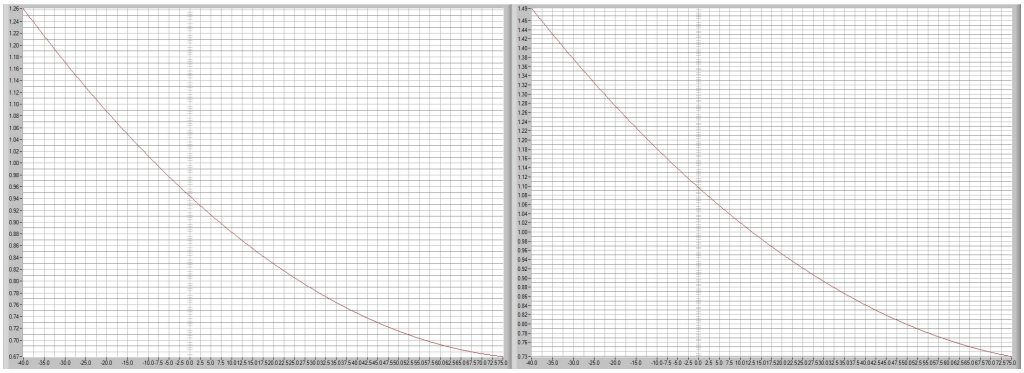

*Figure 3.37: Simulated digital and analog SF error (**L**)*

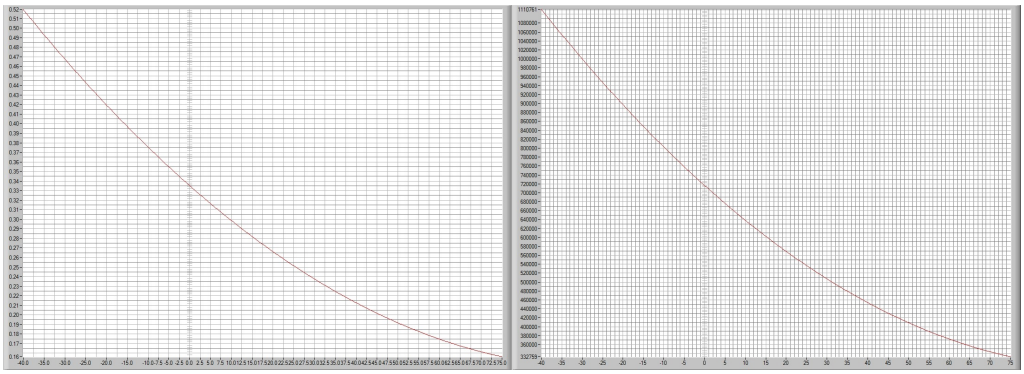

*Figure 3.38: Simulated digital and analog bias error (**L**)*

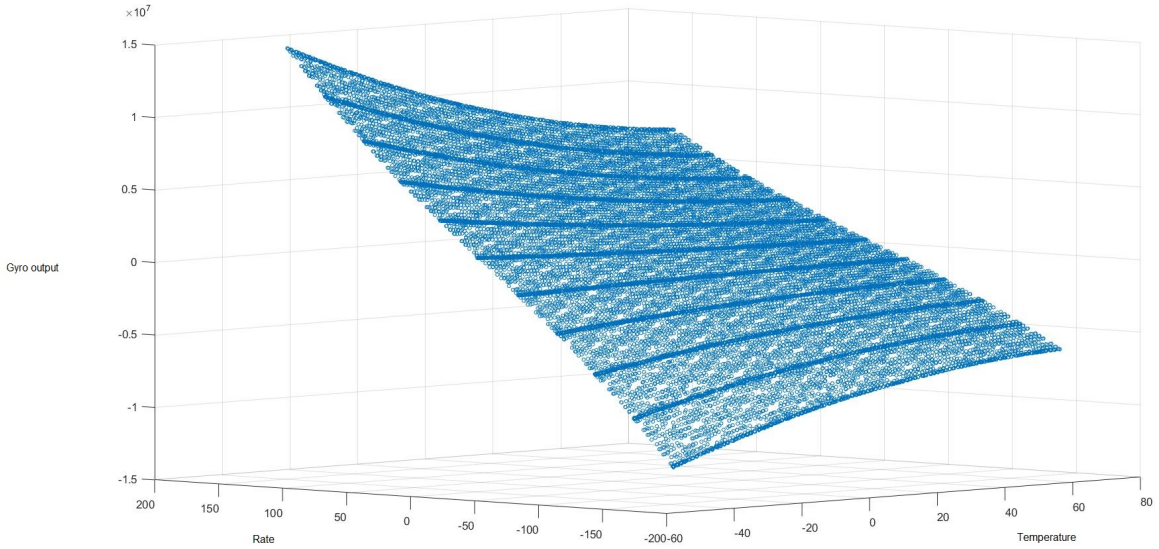


*Figure 3.39: The values of the simulated gyro using the error values in figure 3.36, 3.37 and 3.38 (**M**)*

The simulations that are to be done are of the profiles which could have a significant impact on accuracy and reliability. Things such as Argument 2-3 impact versatility when constructing the profile or when optimizing for a specific climate. Thus these should not have to be tested more than that they work as advertised. This primarily results in the temperature profile templates, the compensation calibration process and the statistical model. In table 3.8 a matrix combination shows what simulation tests are to be done. Here 0 represents the base comparison, which is the current profile.

| | Acyclic | Acyclic Step | Cyclic | Cyclic step |
|---|---|---|---|---|
| Independent_poly | 0 | 4 | 8 | 12 |
| Independent_spline | 1 | 5 | 9 | 13 |
| Independent_point | 2 | 6 | 10 | 14 |
| Independent_gauss | 3 | 7 | 11 | 15 |
| Partial deriv_poly | 16 | 19 | 22 | 25 |
| Partial deriv_spline | 17 | 20 | 23 | 26 |
| Partial deriv_point | 18 | 21 | 24 | 27 |
| Surface_surface | 28 | 29 | 30 | 31 |

*Table 3.8: Table of the STD values of the noise*

Each test is simulated with new randomized error parameters and repeated 10 times. The accuracy is determined using the GoodnessOfFit function which uses $R_{square}$ as the measurements of how good the fit is. The formula for this is:

$$R_{square} = 1 - \frac{\sum_{i=0}^{n-1}(y_i - fittedData_i)^2}{\sum_{i=0}^{n-1}(y_i - \overline{y})^2} \tag{3.10}$$

$R_{square}$ is a value which is closer to 1 the better the fit, therefore in the test the following modification is done:

$$Accuracy = \mid 1 - R_{square} \mid \times 10^6 \tag{3.11}$$

The $10^6$ is to remove several zeros that would otherwise occupy space. The reliability is determined by STD of these 10 simulation tests. In Figure 3.40 the results of the simulation tests are shown. The accuracy and stability are normalized by dividing by test number 0. This is done to represent an improvement or deterioration

in accuracy or stability with respect to the current profile. The column most to the right displays the tests results as the average of the normalized accuracy and normalized stability.

| Number | MeanError | MeanSTD | MeanError % | MeanSTD % | Result |
|---|---|---|---|---|---|
| 0 | 96492,83683 | 26269,3985 | 1 | 1 | 1 |
| 1 | 90915,92535 | 43082,22282 | 0,942203881 | 1,64001558 | 1,29111 |
| 2 | 31171,65161 | 40249,56713 | 0,323046276 | 1,532184573 | 0,927615 |
| 3 | 22379,25698 | 21579,41272 | 0,231926615 | 0,82146581 | 0,526696 |
| 4 | 30353,10907 | 39115,8024 | 0,31456334 | 1,48902543 | 0,901794 |
| 5 | 28783,85894 | 20297,57748 | 0,298300474 | 0,772670051 | 0,535485 |
| 6 | 17514,51505 | 27763,61534 | 0,181511039 | 1,056880512 | 0,619196 |
| 7 | 33718,41676 | 21717,41772 | 0,349439584 | 0,826719261 | 0,588079 |
| 8 | 28305,84516 | 52265,78517 | 0,293346595 | 1,98960723 | 1,141477 |
| 9 | 14991,73272 | 16141,45247 | 0,155366276 | 0,614458396 | 0,384912 |
| 10 | 33683,55648 | 27072,61577 | 0,349078311 | 1,030576158 | 0,689827 |
| 11 | 11182,78161 | 11366,88311 | 0,11589235 | 0,432704354 | 0,274298 |
| 12 | 55296,21718 | 59168,63834 | 0,573060333 | 2,252378879 | 1,41272 |
| 13 | 56003,69044 | 40611,37162 | 0,580392206 | 1,545957423 | 1,063175 |
| 14 | 43299,89522 | 35553,63691 | 0,448736887 | 1,353424096 | 0,90108 |
| 15 | 952451,6701 | 1251884,402 | 9,870698193 | 47,65561733 | 28,76316 |
| 16 | 1286003,173 | 706755,0946 | 13,32744704 | 26,90412172 | 20,11578 |
| 17 | 1861879,489 | 1152016,512 | 19,29552028 | 43,85393568 | 31,57473 |
| 18 | 1783591,945 | 872135,981 | 18,48419016 | 33,19969359 | 25,84194 |
| 19 | 1165569,617 | 529765,5028 | 12,07933827 | 20,16664001 | 16,12299 |
| 20 | 1441549,453 | 1026582,945 | 14,93944525 | 39,07904269 | 27,00924 |
| 21 | 2463791,981 | 2172915,564 | 25,53341846 | 82,71660899 | 54,12501 |
| 22 | 2266333,941 | 1017445,801 | 23,48706925 | 38,73121803 | 31,10914 |
| 23 | 2956655,113 | 484416,0912 | 30,64118757 | 18,44031911 | 24,54075 |
| 24 | 3276434,838 | 550468,0922 | 33,95521311 | 20,95472769 | 27,45497 |
| 25 | 8452047,02 | 7637851,675 | 87,59248145 | 290,7509159 | 189,1717 |
| 26 | 5614139,187 | 4499435,495 | 58,18192698 | 171,2804918 | 114,7312 |
| 27 | 11079004,41 | 6600944,076 | 114,8168587 | 251,2788436 | 183,0479 |
| 28 | 16047,30305 | 25279,7964 | 0,166305641 | 0,962328711 | 0,564317 |
| 29 | 25673,40861 | 30497,6674 | 0,266065435 | 1,160957964 | 0,713512 |
| 30 | 12930,45065 | 12075,37843 | 0,134004254 | 0,459674721 | 0,296839 |
| 31 | 20801,55569 | 28702,96683 | 0,215576165 | 1,092638906 | 0,654108 |

*Figure 3.40: The results from the simulations, displayed as accuracy, stability, normalized accuracy, normalized stability and result where the 2 best are green, worst is red and best ot the worst are blue (**E**)*

From the table in figure 3.40 the best performing simulation results are displayed in green. The best is the independent compensation calibration with a gaussian statistical method using a cyclic temperature template. The second best is the Surface compensation calibration with a cyclic temperature template. The worst performing over all are the partial derivative compensation calibration method with a worst result of 189.17 to a best of 16.12. In order to investigate this the results from the individual tests for 19 are shown in figure 3.41 taken out from appendix G. From this it seems that the partial derivative function is as expected from the very high stability value, very unstable and doesn't seem very reliable. However some iterations

result in good accuracy when compared to 0.

| | TotAccuracy | linjAccuracy_D | linjAccuracy_A | SFAccuracy_D | SFAccuracy_A | biasAccuracy_D | biasAccuracy_A |
|---|---|---|---|---|---|---|---|
| 1 | 978371,4865 | 387544,7155 | 387224,3082 | 101291,2769 | 101299,9849 | 505,559133 | 505,641812 |
| 2 | 1646929,471 | 725789,0077 | 725852,365 | 97220,56247 | 97220,17103 | 423,387277 | 423,977178 |
| 3 | 495032,6293 | 142522,8563 | 142585,345 | 104722,8355 | 104707,6836 | 246,75462 | 247,154281 |
| 4 | 1985726,787 | 885114,1244 | 885149,4913 | 104359,8039 | 104366,5079 | 3368,19132 | 3368,668625 |
| 5 | 860002,7553 | 327164,0108 | 326909,683 | 102099,6546 | 102095,6405 | 866,768245 | 866,998306 |
| 6 | 947626,9362 | 349840,7107 | 349704,9982 | 123671,268 | 123661,4712 | 374,201223 | 374,286839 |
| 7 | 987419,1386 | 394778,0907 | 395031,4899 | 97822,25563 | 97819,19168 | 983,680913 | 984,429832 |
| 8 | 512223,9144 | 143820,3657 | 143701,3559 | 112033,4524 | 112026,0807 | 321,041874 | 321,617865 |
| 9 | 1172375,298 | 493617,2471 | 493494,3956 | 91386,57912 | 91382,72147 | 1247,548371 | 1246,806189 |
| 10 | 2069987,749 | 935047,0691 | 934790,034 | 97186,39029 | 97182,71919 | 2891,63999 | 2889,896722 |

*Figure 3.41: Table of a closer examination of tests from 19 found in appendix G (**E**)*

## 3.3 Testing and verification of best simulated calibration processes on gyro

From the simulation the best methods were provided. These are now to be tested on an actual gyro in the calibration equipment, this gyro is a different 4xx gyro from the one tested in 3.1.4 which was not available for these tests. Due to the gyros having slightly different characteristics the results derived from these tests are not directly comparable to the results in chapter 3.1.4 and the noise in figure 3.35, however may still serve as guidelines. This is to be done to verify that the program and the calibration functions that have been implemented does work and how well they work. The three tests to be done is first the acyclic independant poly profile. This is done to give a benchmark on performance of the final test. The others are the two best that were derived from the simulation (Cyclic independent gaussian and cyclic surface). These tests are done by first collecting data using the program then calculating the compensation values from that data, this due to the automatic part of the program is untested at this point. The compensation values are uploaded manually and data is collected again. From these the current error values are calculated using the same calibration method. If the previous compensation values were the error value should be zero for the bias and linear and one for the SF. In table 3.9 the tests are stated with specified parameters used for the templates and some stats when calibration. In figures 3.42, 3.43 and 3.44 these profiles are shown.

| Param | Test 1 | Test 2 | Test 3 |
|---|---|---|---|
| Time [h:m:s] | 2:46:59 | 4:14:28 | 4:04:28 |
| Temperature range | [-40,+75] | [-40,+75] | [-40,+75] |
| Test Temperature change rate $\frac{^\circ C}{s}$ | 1 | 1 | 1 |
| Steps in linear | 21 | 21 | 0 |
| Steps in OTR rate | 3 | 3 | 11 |
| OTR rate loops | 100 | 200 | 100 |
| Max data points | 10k | 1M(linear 10k) | 1M |

*Table 3.9: Table of tests to be done and parameters for them*

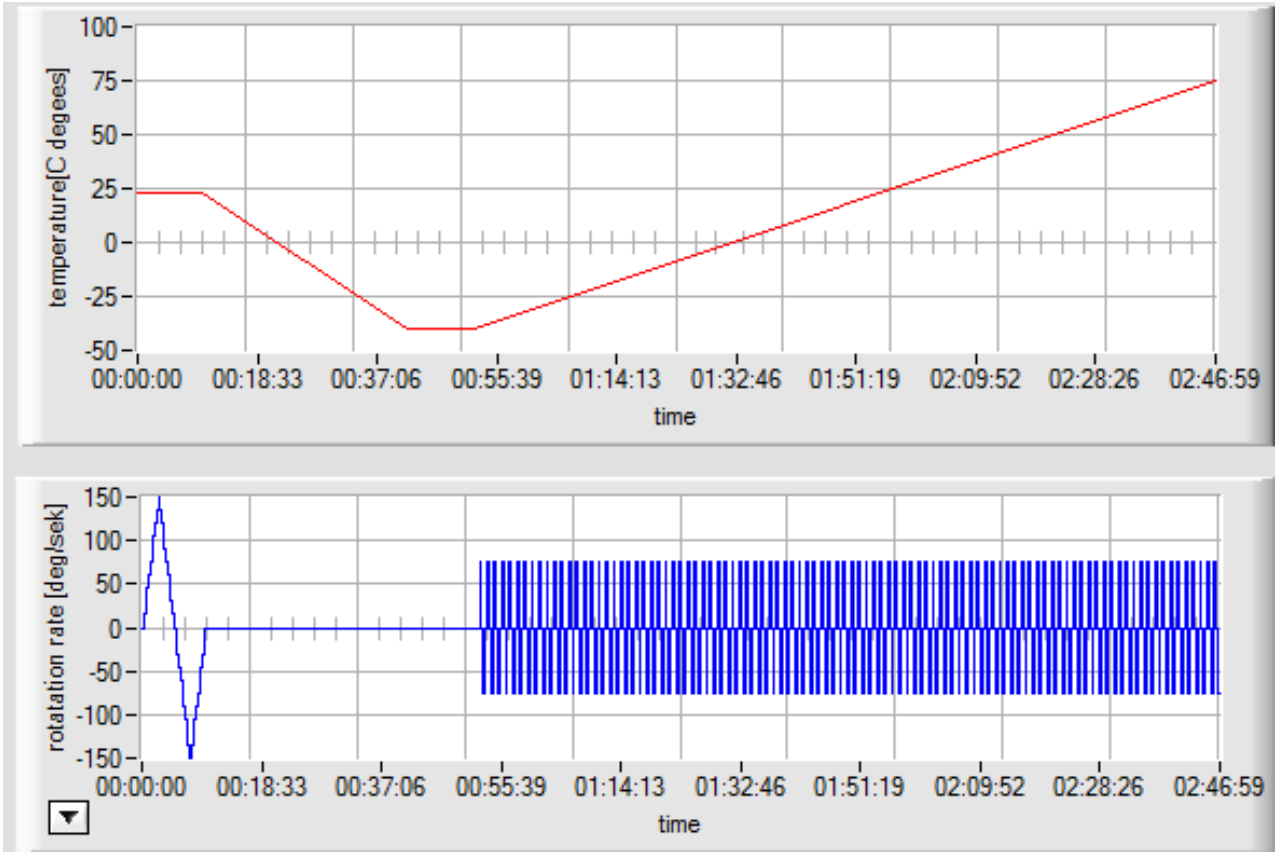


*Figure 3.42: Test number 1 (**L**)*

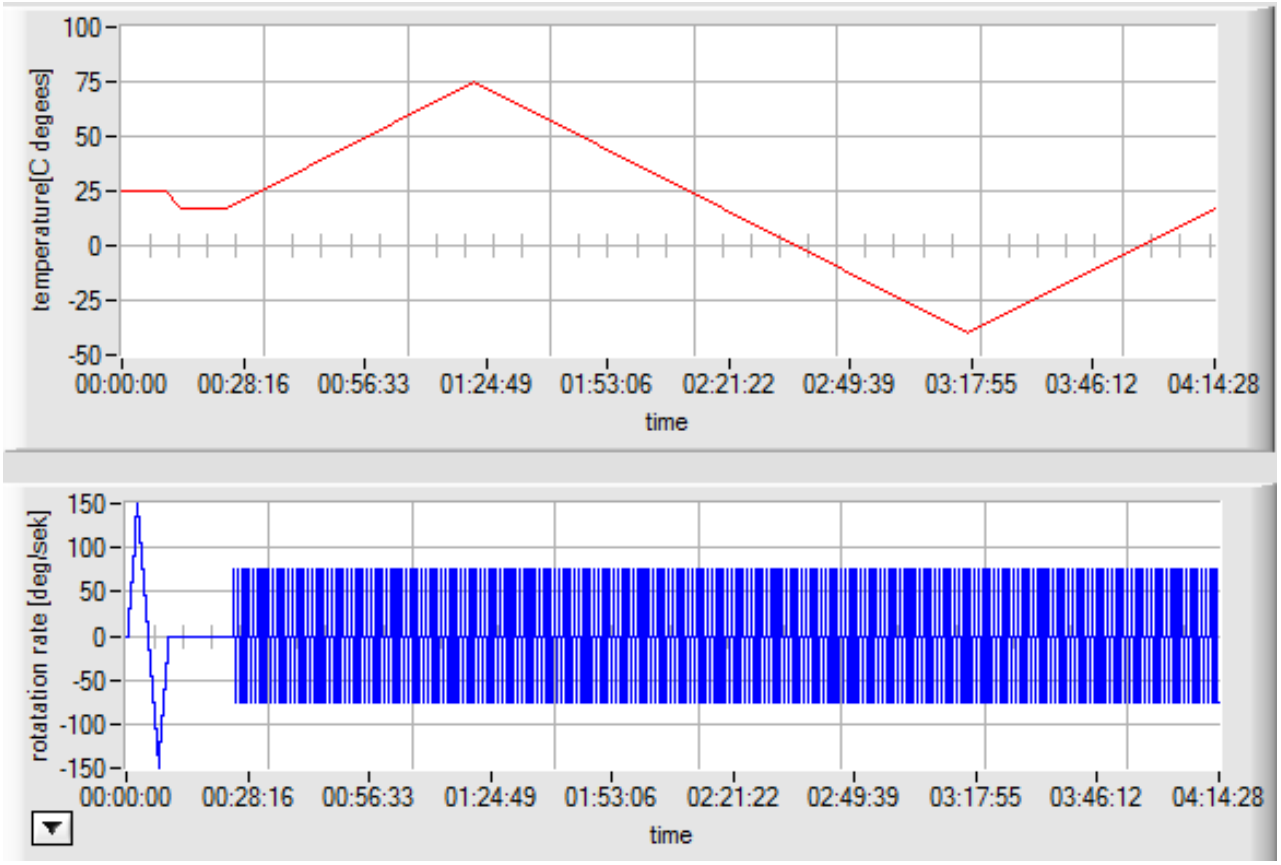


*Figure 3.43: Test number 2 (**L**)*

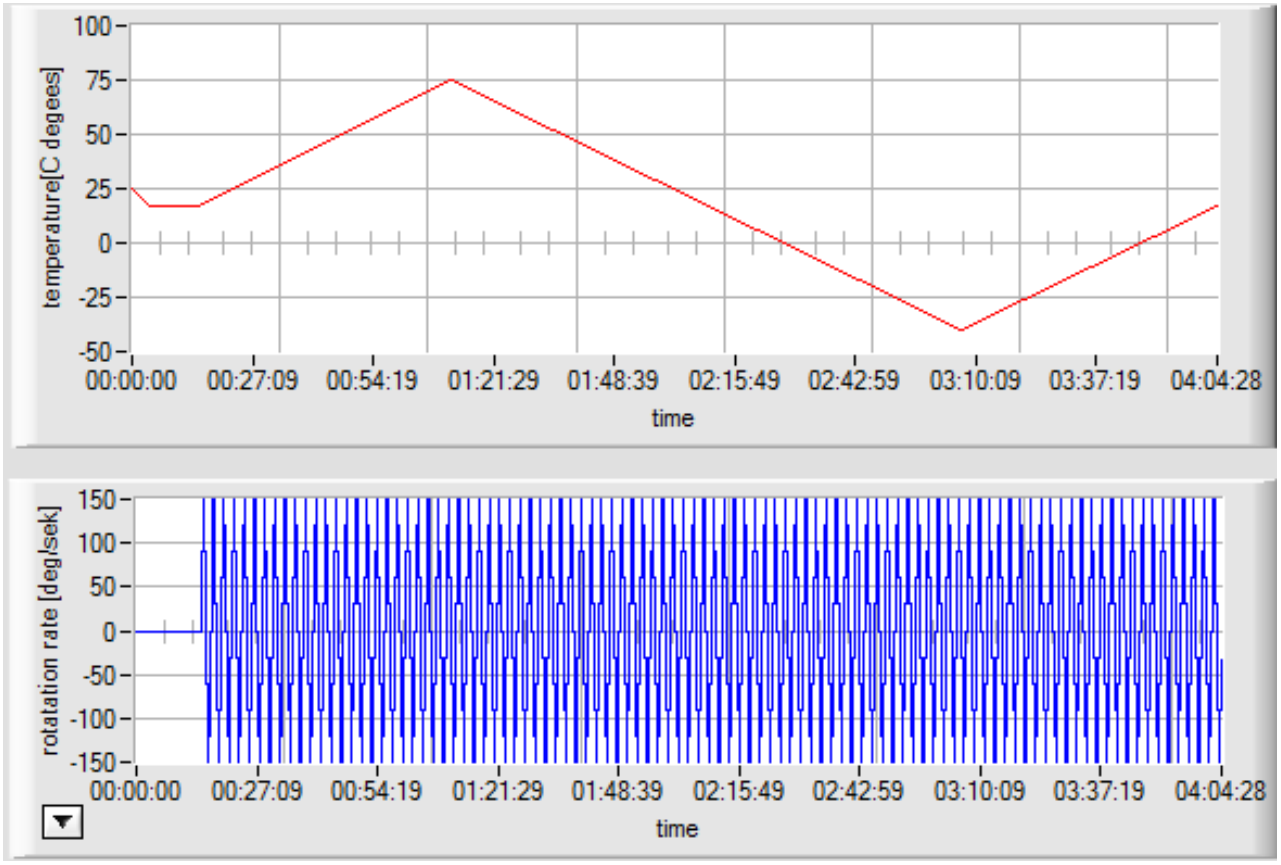


*Figure 3.44: Test number 3 (**L**)*

# 4 Results

## 4.1 CaTV program (Calibration, Test and Verification)

The result of the implementation in LabWindows is the program now named calibration, test and verification (CaTV), the main panel of this program is shown in figure 4.1, in figure 4.2 the flowchart of the various functionalities of this panel is displayed . The program is roughly 99 megabytes with ≈14 000 lines of code implemented, ≈500 of these is code that were previously developed and have been modified for use in this program. The program uses the product and profile definitions discussed in 3.1.3 and has a system which enables creation of new profiles and products and simple switching between them. multithreading was implemented in order to achieve high performance by allowing some parallelization of the data collection process, this parallelization extends to the calculation and calibration process as well. This multithreading has the tendency to lock the interface of the main program due to high priority of the additional threads, this is however probably not necessary and the priority should be lowered in order to make sure the interface does not bugg out or crash. The calculation thread is the tread that handles all calibration, testing and verification tasks. it does so by using a function stack. In this stack functions to be executed are placed depending on the type of operation and when the calculation thread starts it executes these functions one at a time.

The Program data collection process just takes the raw data from the gyros and hardwares and stores them in temporary files. These temporary files are then converted into data files where each individual data point is sorted according to bookmark. the advantage of this process is that little time is that the data can quickly be collected and the accuracy of the time that it was taken maintained more precisely, this in combination with the program utilizing the built in high precision windows timer for timing purposes results in a data collection process which most likely have a good time accuracy and large amounts of data points. Since the collected amounts of data points over a few hours at max data rate speeds for the hardware easily reaches several millions for the signals the program has a function which limits the amount of data. This is done to ensure that the calibration process can be done in reasonable time, without this and the process would take several hours with so many data points at the current iteration. However some calibration processes can handle more data points than others due to their function. The surface compensation calibration process can handle 1 million data points without problems and wears the independent polynomial approximately at the same time with one hundred thousand data points. This is due to a sorting that needs to take place before the polynomial fitting, this is however not needed in the independant gauss compensation calibration process for bias and SF. This results in the independent gauss process being able to as well handle 1 million for bias and SF calibration but since a sorting is done on the third degree linear error polynomial fitting this has to be limited to hundred thousand data points just as the independent poly process.

In order to deal with different temperature chambers, rotation tables, power sourcer and analog measuring cards a DLL(Dynamic Link Library) loader for the hardware controlling functions has been implemented. This will enable the program to much easier be able to be configured to different stations or changes in hardware. The test function enables the user to test filters and their parameters and perform fast fourier transform of the signal, these functionalities have not been tested thoroughly on the gyro though it is implemented.

In figures 4.1 to 4.7 a closer look at the resulting CaTV program itself is taken where figure caption is used to describe the various functionalities.

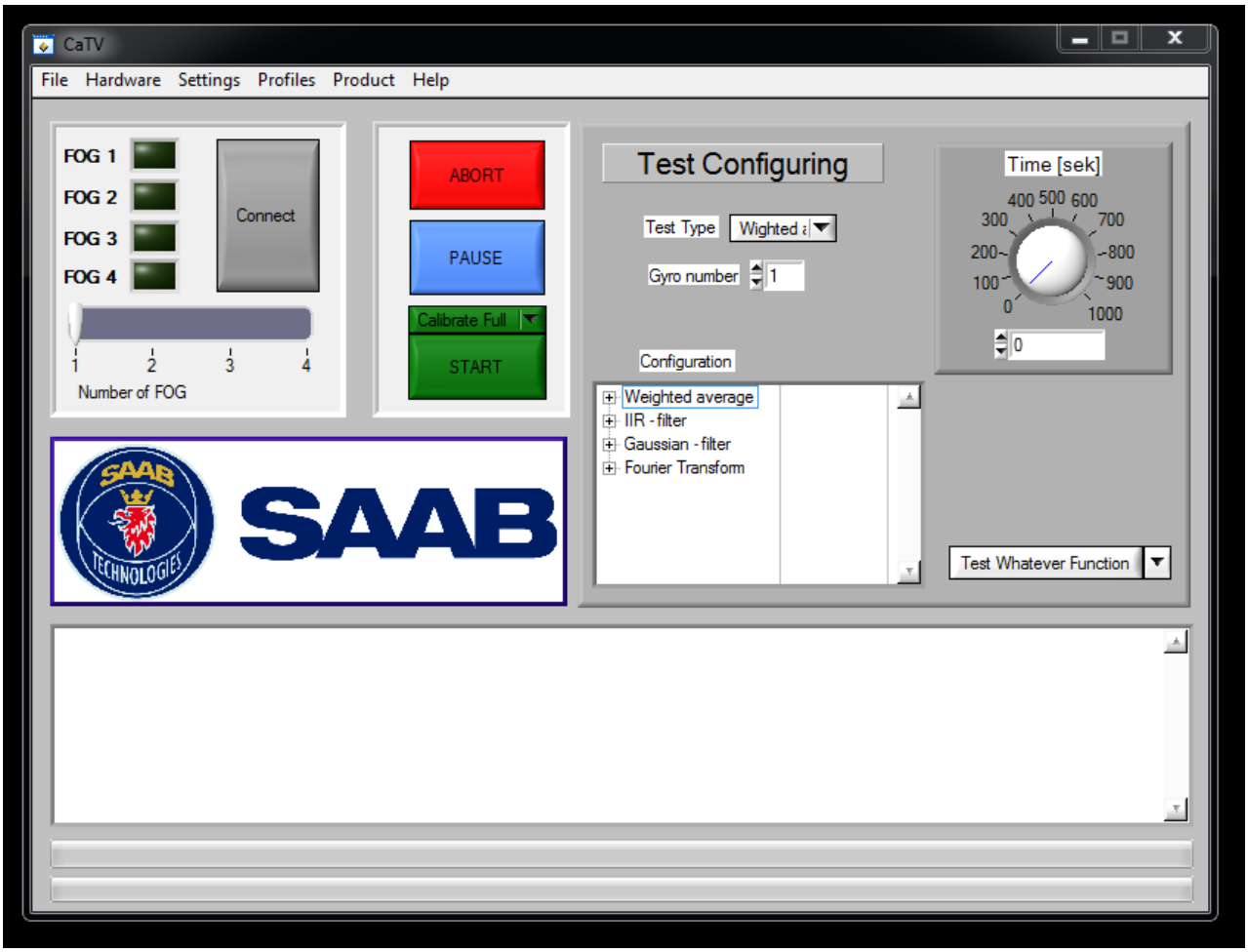


*Figure 4.1: Main panel of CaTV; number of FOG slides is used to quickly set the number of FOGs to use. When a gyro has successfully connected and its signal verified to be correct the lights FOG 1-4 light up green. The green menu ring above start is used to select the operation to be done. Abort and pause functionalities have not been sufficiently tested and although much of the implementation of them are there they are currently quite buggy. The test configuring panel is a panel used to set up a test operation where the configuration tree is used to set up parameters for the filter and FFT tests. The time knob is used to set the test length, test type selects what type of test (data collection, filter or FFT) and gyronumber set which gyro to do the test on. Test whatever is a function where various other functions can be put into and then tested to verify that the function properly. The test whatever function is not the same as a test operation. The large white box at the bottom with scroll bar to the right is a text box where the status of the program is outputted such as data found, temperature stabilization progress, image printed to which location and which stage of the calibration process is currently being worked on. Lastly there are the two progress bars at the bottom the top indicate progression of the profile data collection part and the bottom one indicate progression on the function stack.*

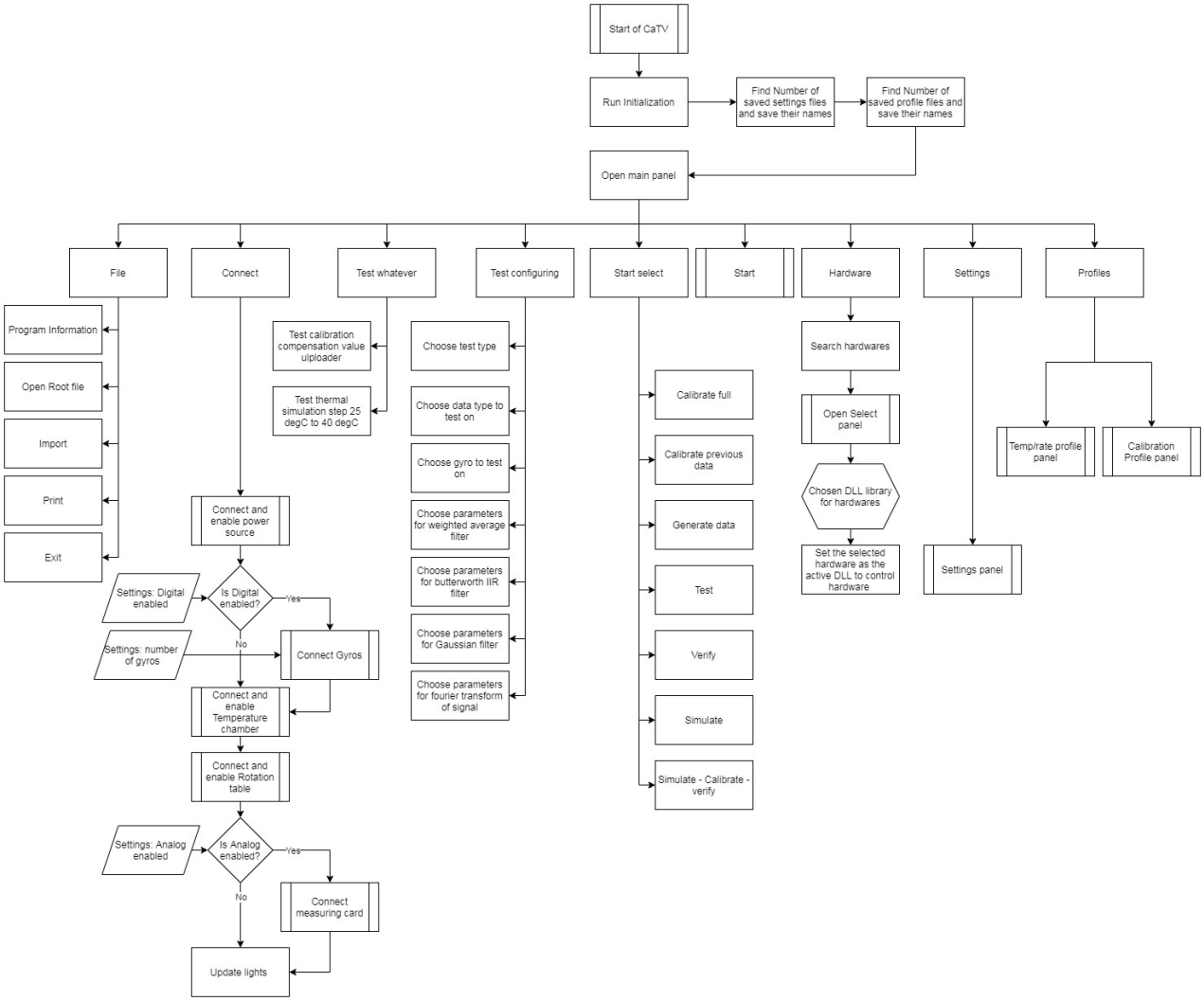


*Figure 4.2: Flow chart of main panel of CaTV, the functions of import and print does not currently do anything. Start select(green ring in 4.1) is a ring menu where the type of operation to be done is selected. The connection of the power source, digital gyro, temp chamber, rotation table and analog measuring card uses previous existing functions.*

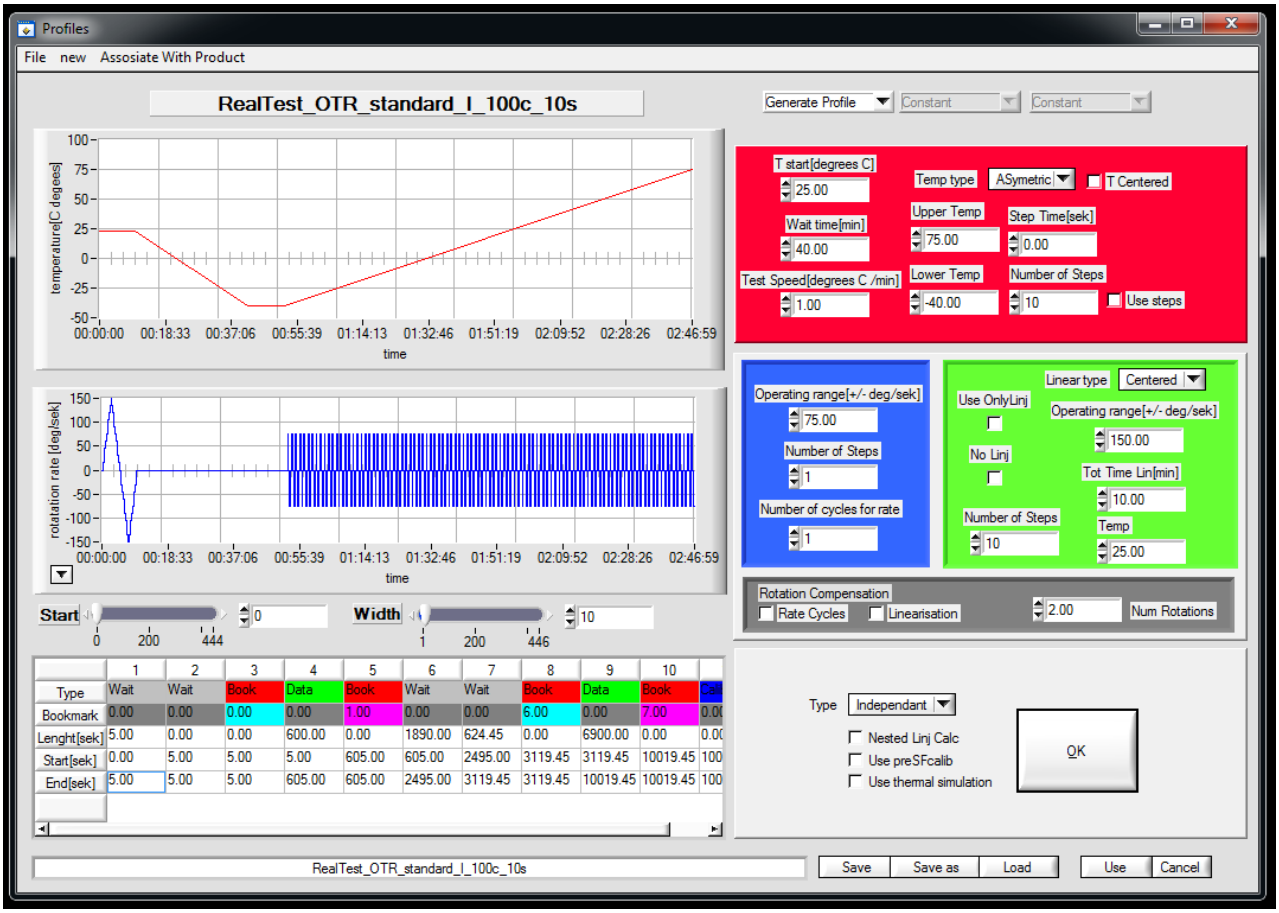


*Figure 4.3: Temp/rate profile panel where generate profile with choosable parameters for the different templates is open; The graph of rate has a function that enables the choosing of the interval to plot, to enable this the button to the left of the graph is pushed and then the plot interval can be selected by using the start and width sliders. These indicate which rate subprofile to start at and how many to plot. The different colored panels are used to adjust different parameters which when the large OK button is pressed the program generates a new profile from a template. The red indicates Temperature profile template parameters, the blue the rate loops, the green the linear template and the gray rotation compensation. The type ring is used to set which bookmarks are used on the data (Independent, Partial Derivative and Surface). the bottom colourful table is used to display Data subprofiles.*

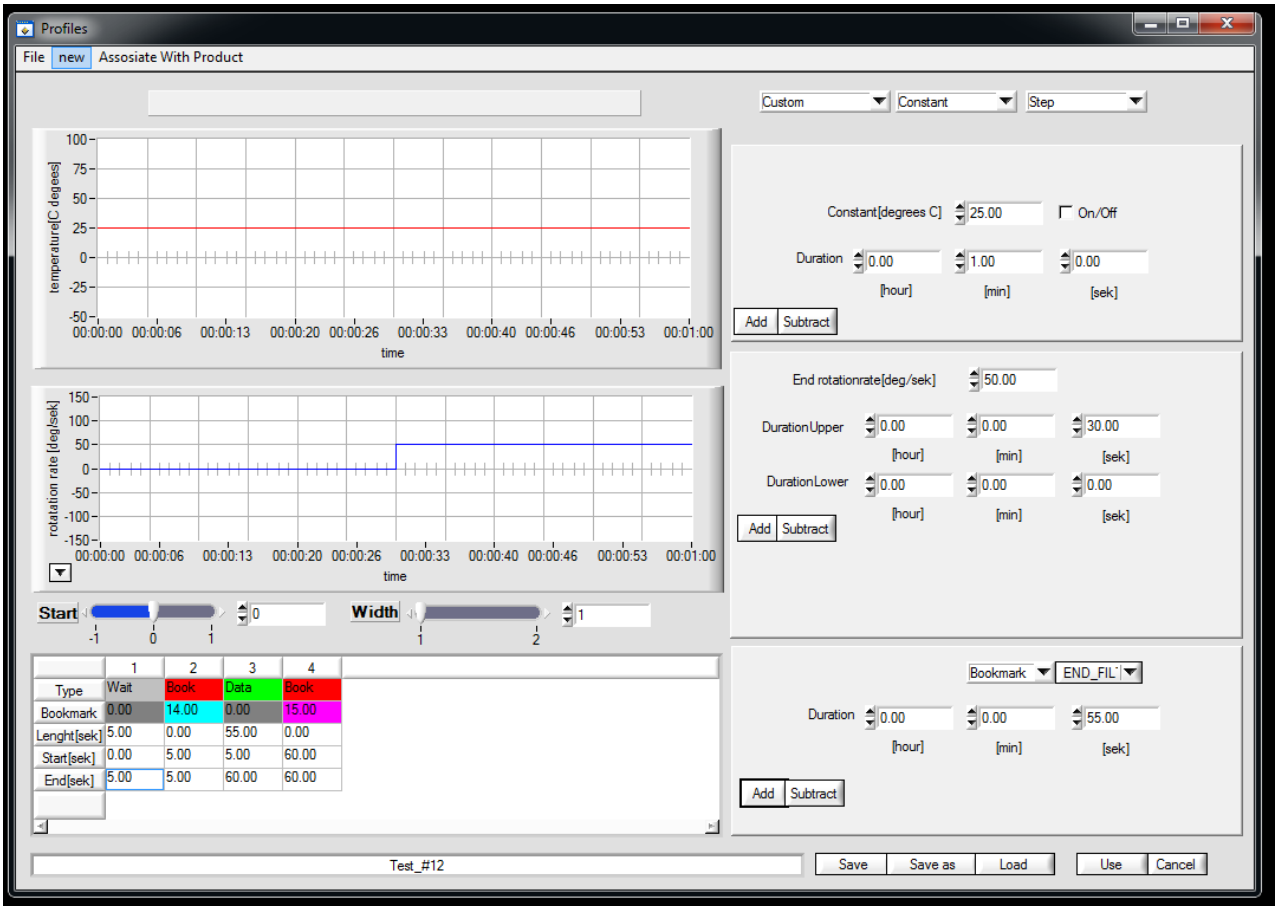


*Figure 4.4: Temp/rate profile panel where custom profile generation is open; The custom profile panel is activated by changing the selection menu to "Custom". This enables the adding and subtraction of individual subprofiles to Temperature, rate and data.*

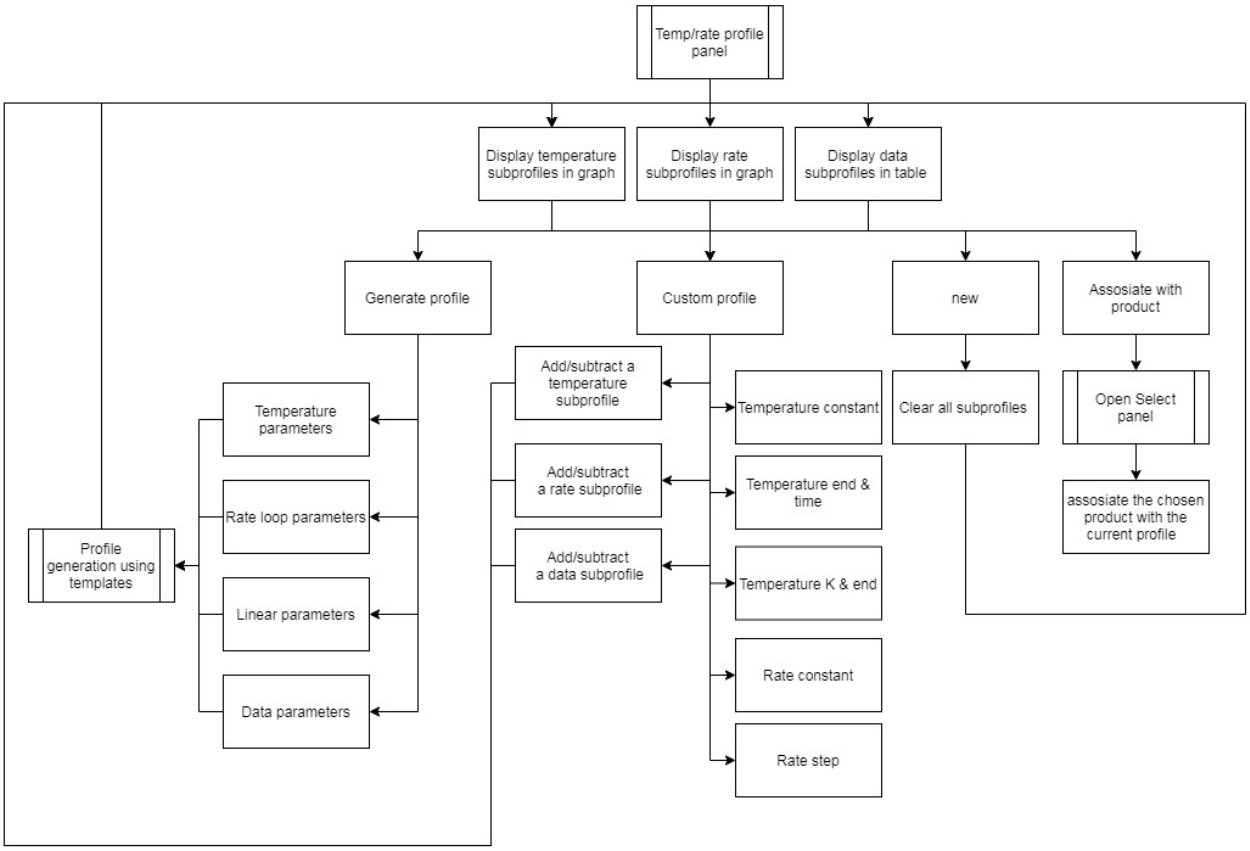


*Figure 4.5: Flow chart of temp/rate profile panel*

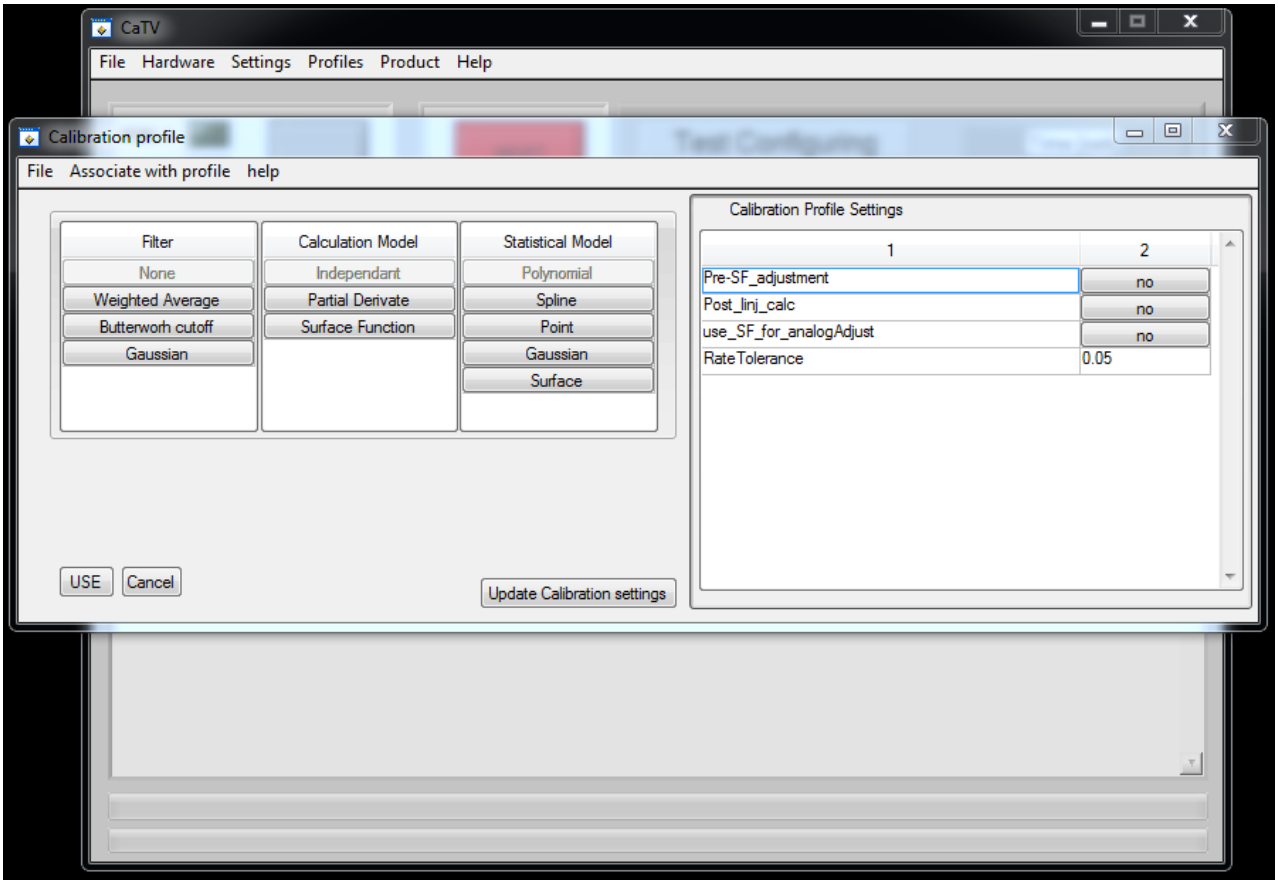


*Figure 4.6: Calibration profile panel of CaTV; The calibration profile is changed by selecting one of the filters, calculation model and statistical model. When this is done the calibration profile settings updates and shows which parameters can be changed for that calibration profile. The option to auto pre-adjust the SF is always shown here, rate tolerance refers to the functions tolerance of the values for rate $\theta$, for example when searching for values where $\theta = 0$ during bias calibration the rate tolerance determines which values fall under that.*

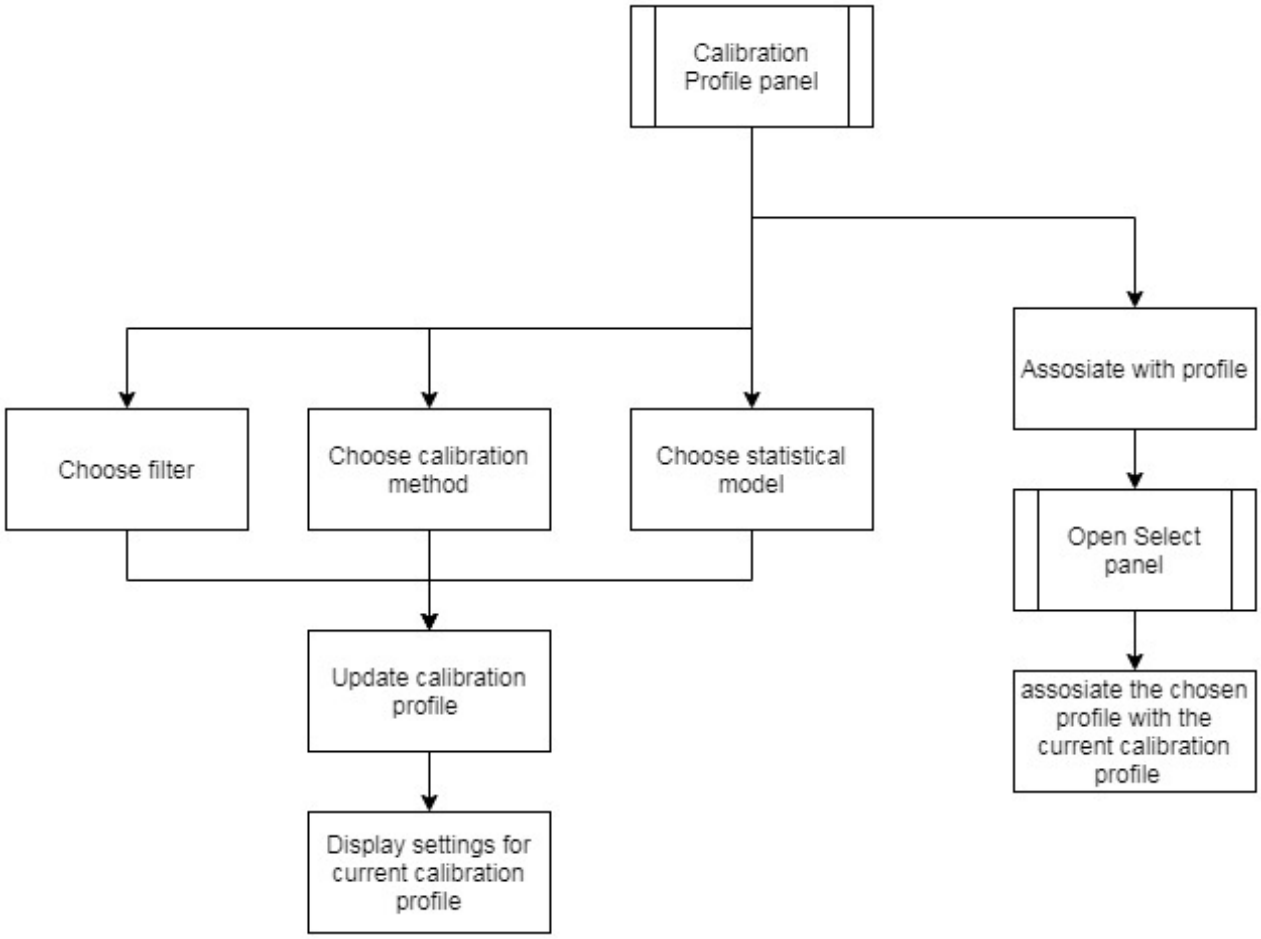


*Figure 4.7: Flowchart of the calibration profile panel*

More images and flow charts of the various panels of CaTV can be found in appendix E and F.

Returning to the demands list described in chapter3.1.2 will show how well the program fulfills the requirements, necessities and Desirables.

Requirements:

1 Can successfully read both analog and digital data from the gyro

2 Can calculate SF, bias and linearity compensation

3 Can upload compensation values automatically although full automatic procedure ($collectData \rightarrow calculateCompensationValues \rightarrow uploadCompensationValues \rightarrow verify$) has not been fully tested

4 Can fully control temperature chamber, rotation table, power source and analog card

Necessities:

5 Scan the digital ports after a gyro (found in settings under connection) and adapt the baud rate after the output of the gyro connected (this utilizes a modified previous software)

6 This is included in the profile/product and can be changed in various ways

7 Is implemented but not tested

8 no

Desirables:

9 is implemented but not tested

10 yes found in calibration profile

11 Is implemented but not tested

12 yes (found in settings under connection)

13 The calibration processes uses a method where large data sets are used to from the average, this should lead to better data average

## 4.2 Test 1: Acyclic independant poly

Figures 4.8 and 4.9 show the collected data of digital, analog and temperature, rate respectively data of this test. In figure 4.10 the bias error values are shown before the calibration as a result from the independent process finding the values are $\approx 0$ within a interval of of $[-\frac{range}{numsteps} \times 0.05, \frac{range}{numsteps} \times 0.05]$. Figure 4.11 shows the calculated SF values from the independent process.Figure 4.12 displays the linearity error as input into the third degree polynomial fitting function. Both the SF and linearity shows unusual spikes, since this is something that the gyro should not be able to do and does not show up in it is most likely something in the calculation process. What this could be caused by is most likely the interpolation in combination with too low tolerances for the values of the steps. When the function calculates the SF a deviation by the values for rate are needed and if these have some variation it can have a large effect on the en value. What this means is that the value of 0.05 that was used for the tolerance for rate was too high and needed to be tighter. How much this impacts the final results is unknown however it will most likely be a significant factor in inaccuracies. In figures 4.13,4.14 and 4.15 the calculated compensation values are shown are show polynomial fitted from the data in 4.13,4.14 and 4.15 respectively, these values are presented in the same units as the specified characteristic in 2.1 with the specified margins. from figures 4.13,4.14 and 4.15 the averages of the data are calculated, these are listed in table 4.1.

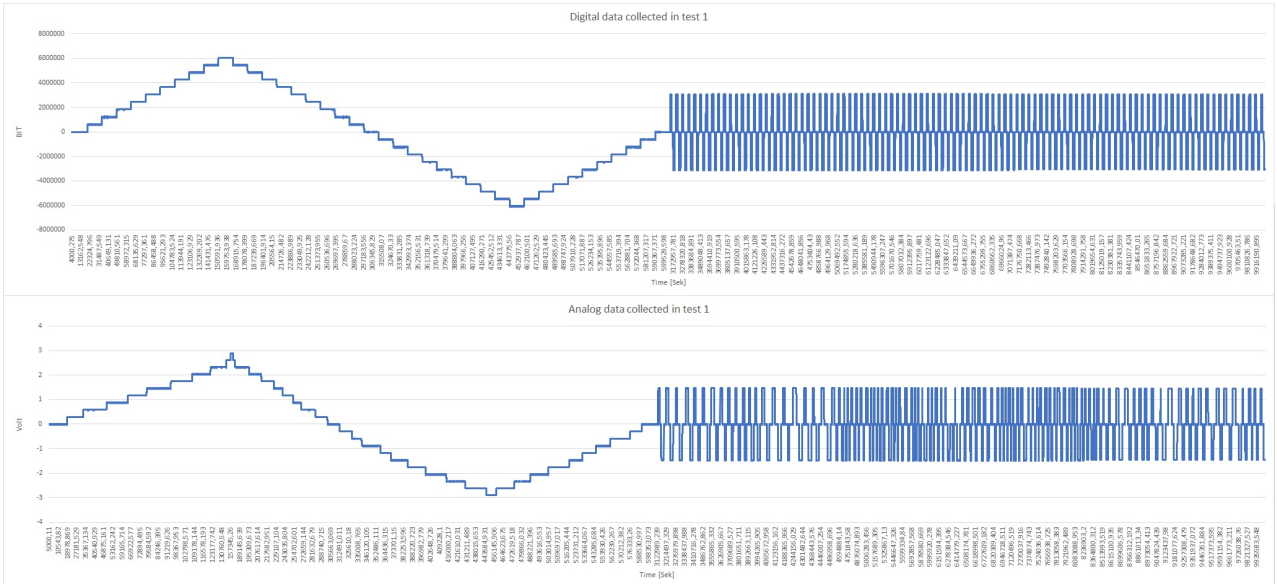


*Figure 4.8: Digital and analog collected data values (**E**)*

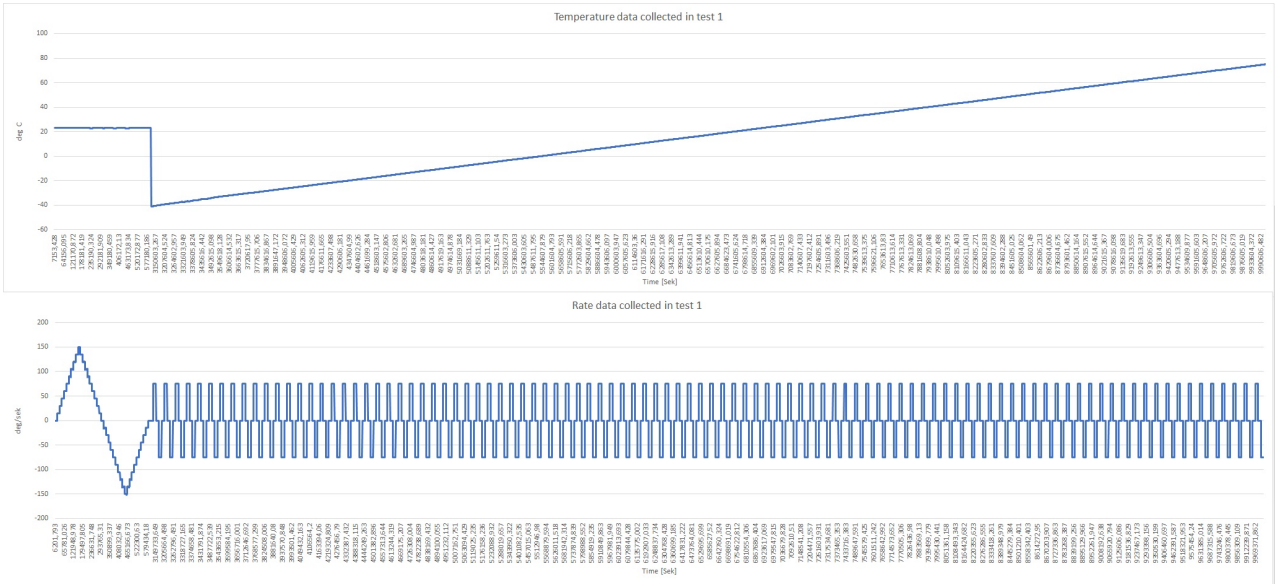


*Figure 4.9: Temperature and rate collected data values (**E**)*

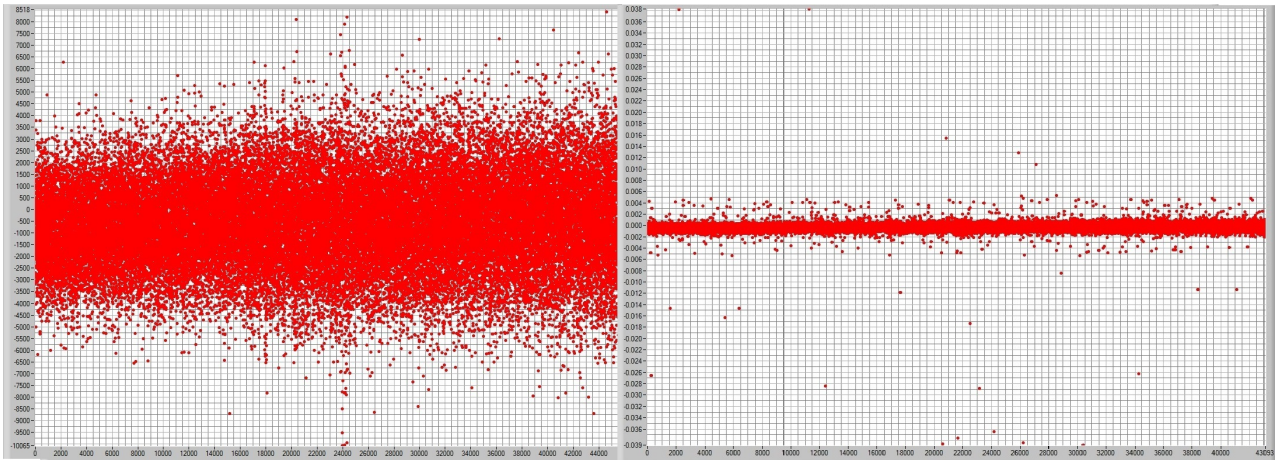

*Figure 4.10: Figure of bias error value as outputted from the independent function in CaTV (in the units BIT, volt) (left Digital, right Analog) (**L**)*

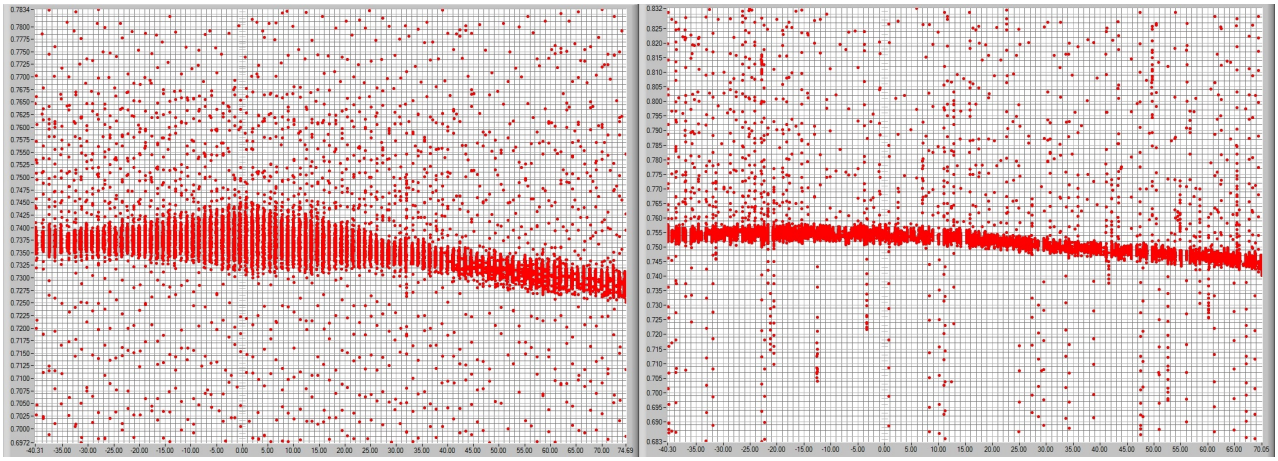

*Figure 4.11: Figure of SF error value as outputted from the independent function in CaTV (in the units $\frac{SF_{error}}{SF_{ideal}}$) (left Digital, right Analog) (**L**)*

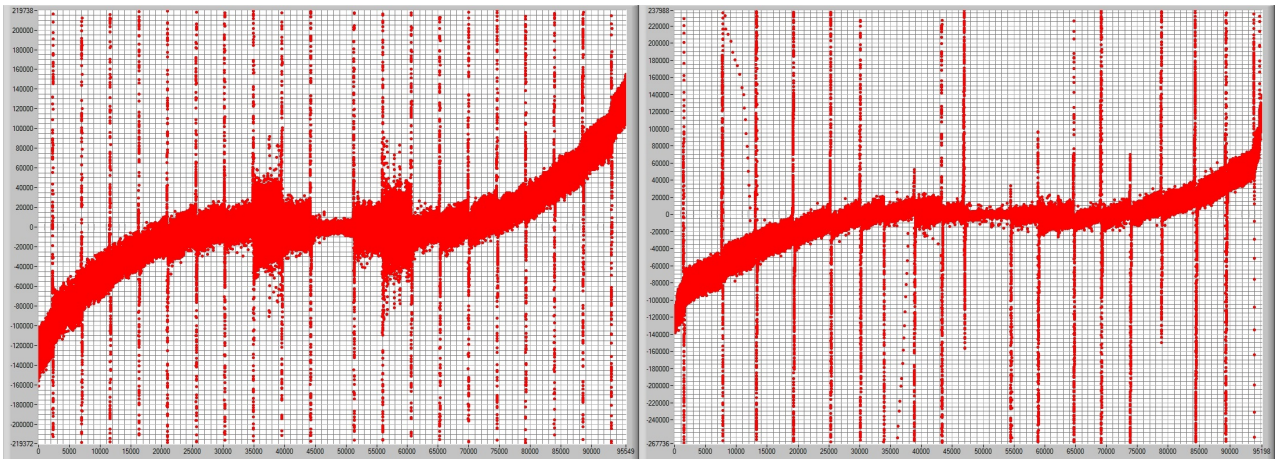

*Figure 4.12: Figure of linear error value as outputted from the independent function in CaTV (in the units BIT) (left Digital, right Analog) (**L**)*

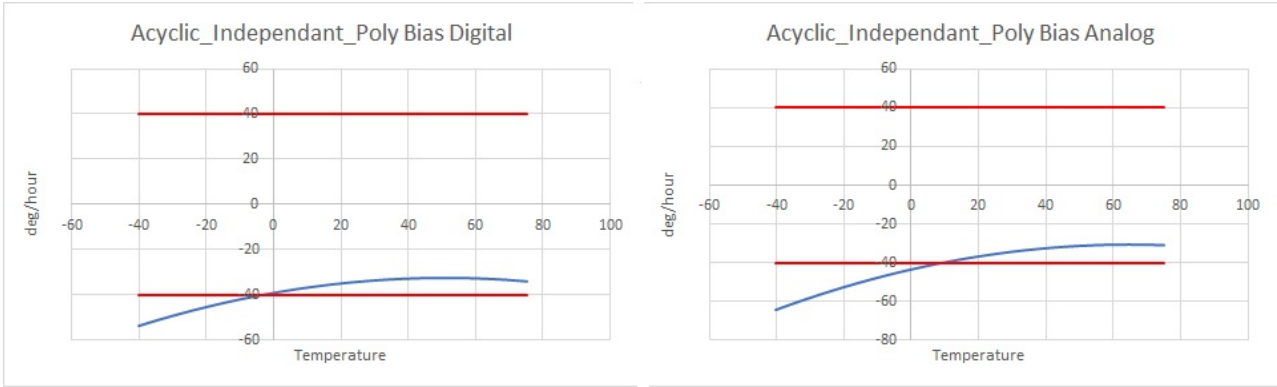


*Figure 4.13: Bias fitted value output from independant poly compensation calibration process (**E**)*

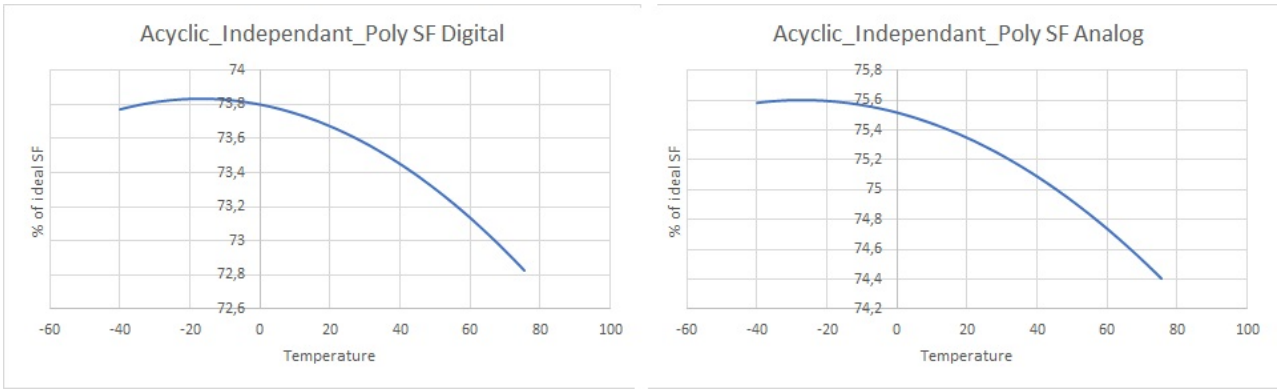


*Figure 4.14: SF fitted value output from independant poly compensation calibration process (**E**)*

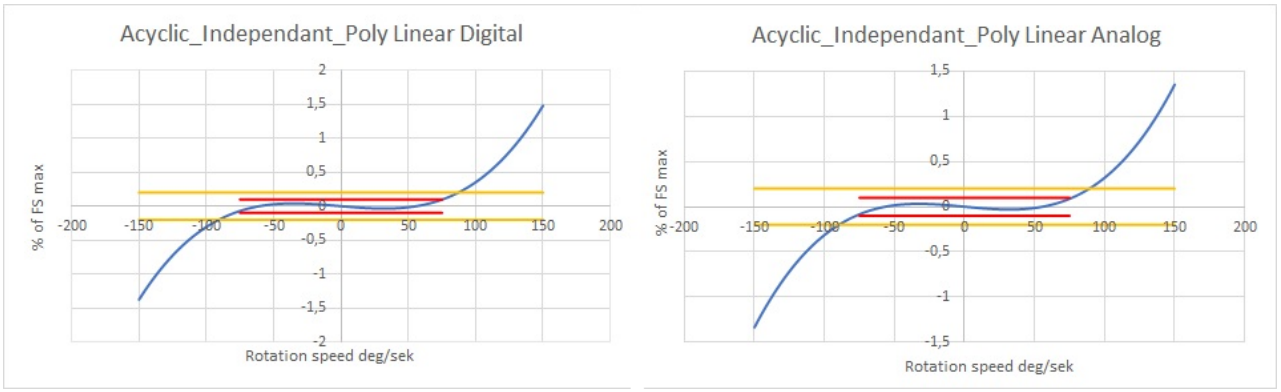


*Figure 4.15: Linear fitted value output from independant poly compensation calibration process in (**E**)*

| Name | Digital | Analog | Unit |
|---|---|---|---|
| Bias | 38,26506849 | 40,57801886 | deg/hour |
| SF | 26,43983086 | 24,75685263 | % of SF ideal error |
| Linear | 0,313453248 | 0,296280755 | % of FS max |

*Table 4.1: Listing of the averages of the fitted data*

## 4.3 Test 1: Verification

The same procedure is repeated again to give the verification values, these are shown in figures 4.16, 4.17 and 4.18. From this data the averages of the results are calculated, this is shown if table 4.2. Using the values calculated from the error values in table 4.1 a percentage reduction of the errors is calculated and this is presented in table 4.3.

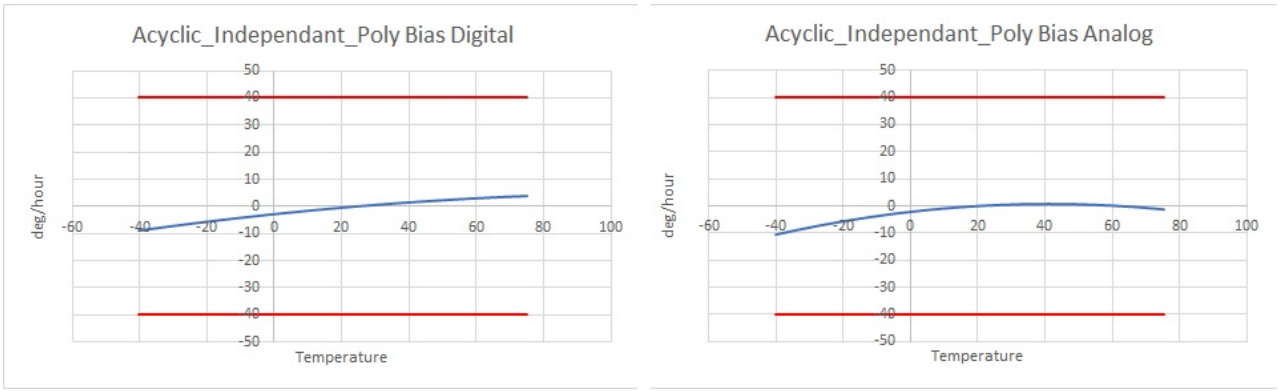


*Figure 4.16: Bias verification (**E**)*

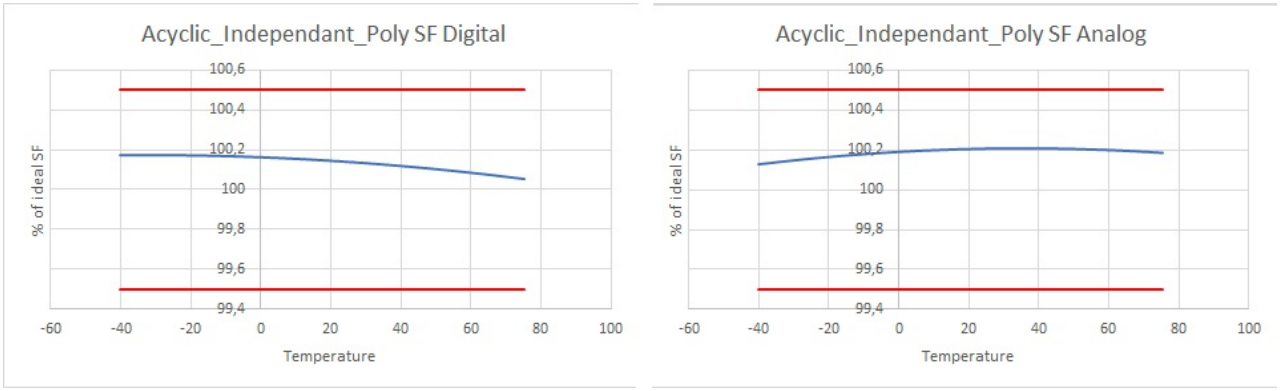


*Figure 4.17: SF verification (**E**); both of the SF values are somewhat shifted up, this could be because of the too weak tolerances*

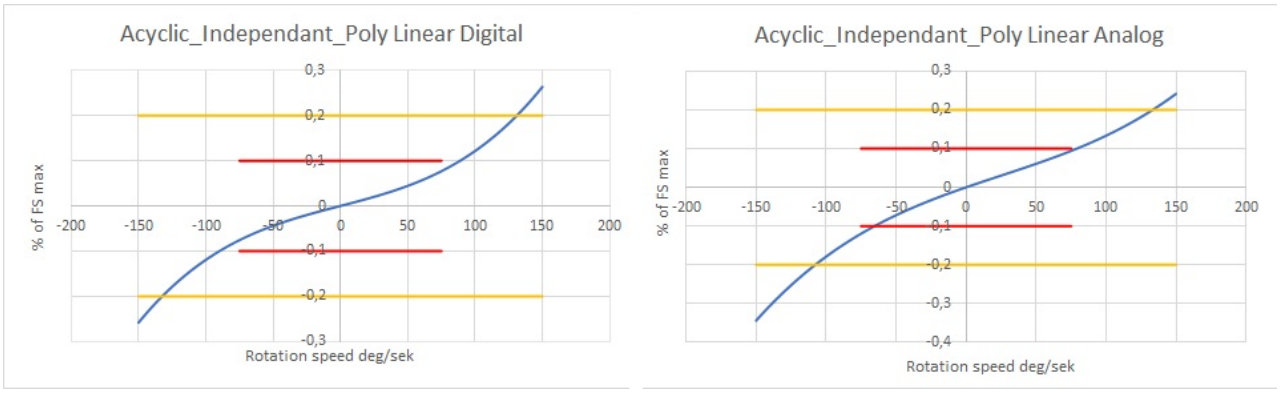


*Figure 4.18: Linear verification (**E**); poor result from linearisation, does not meet requirements in the 0-150 range*

| Name | Digital | Analog | Unit |
|---|---|---|---|
| Bias | 3,267433204 | 2,474239047 | deg/hour |
| SF | 0,1351731 | 0,1880049 | % of SF ideal error |
| Linear | 0,09435305 | 0,12013718 | % of FS max |

*Table 4.2: Listing of the averages of the compensated data*

| Name | Digital | Analog | Unit |
|---|---|---|---|
| Bias | 91,47 | 93,9 | % reduced error |
| SF | 99,49 | 99,24 | % reduced error |
| Linear | 69,9 | 59,5 | % reduced error |

*Table 4.3: Listing of the percentage reduction of the error*

## 4.4 Test 2: Cyclic independant gauss

Figures 4.19 and 4.20 show the collected data of digital, analog and temperature, rate respectively data of this test. In figure 4.21, 4.22 and 4.23 shows the bias error, SF error and linearity error of the independent process. This test uses the same rate tolerance of 0.05 for the independent process which results in these spikes in these values showing up again but now more prevalent since the increase to 1 million data points. In figures 4.24,4.25 and 4.26 the calculated compensation values are shown are show gaussian point regressed from the data in 4.24,4.25 and 4.26 respectively. The number of points that were regressed over were equal to the number of rate loops (which were 200).

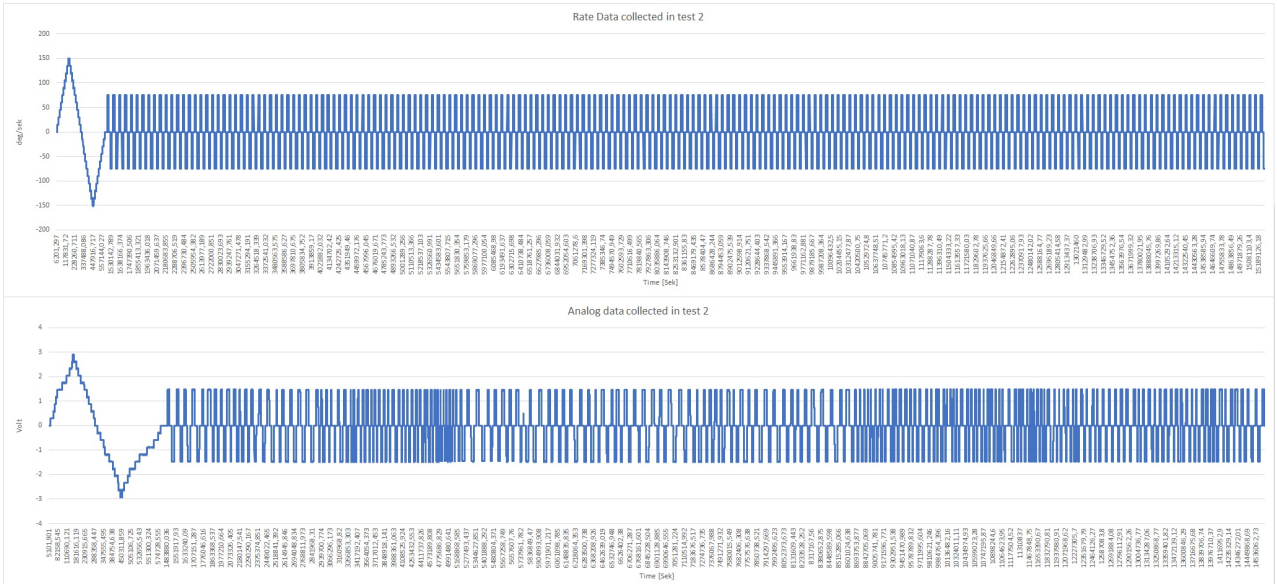


*Figure 4.19: Digital and analog collected data values (**E**); the reason for the trailing analog signal is unknown*

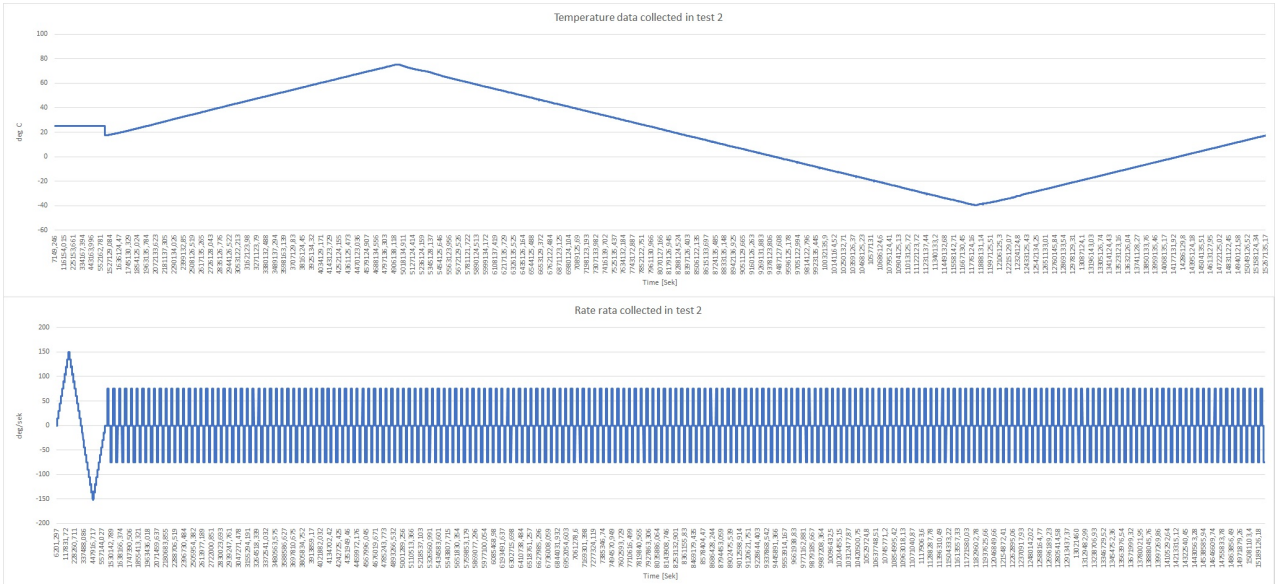


*Figure 4.20: Temperature and rate collected data values (**E**)*

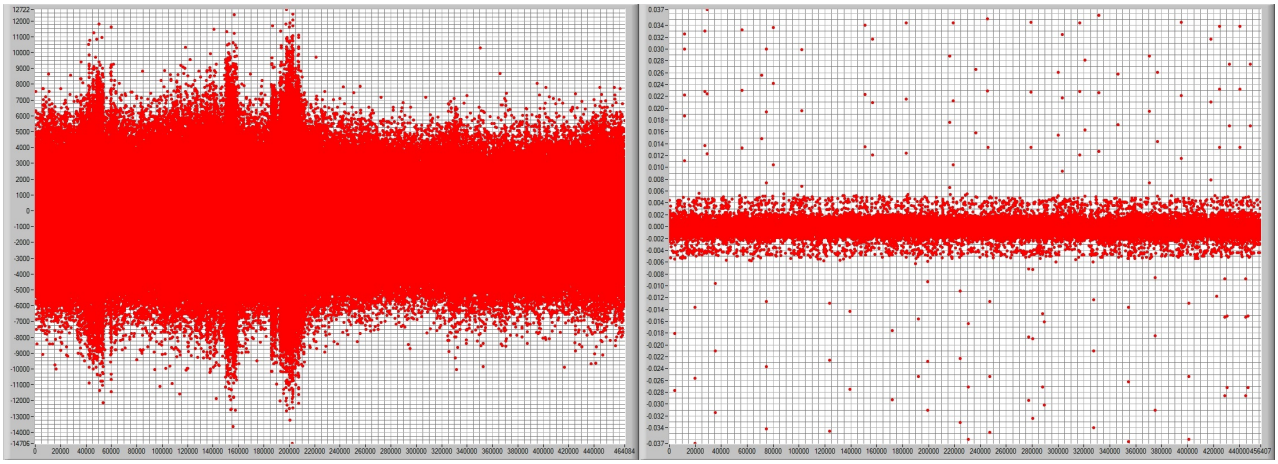

*Figure 4.21: Figure of bias error value as outputted from the independent function in CaTV (in the units BIT, volt) (left Digital, right Analog) (**L**)*

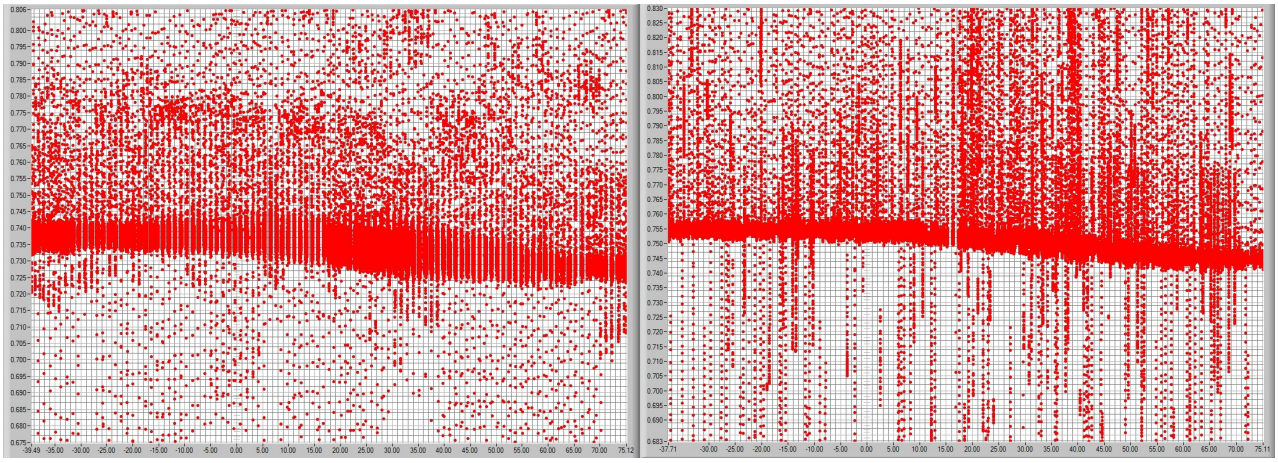

*Figure 4.22: Figure of SF error value as outputted from the independent function in CaTV (in the units $\frac{SF_{error}}{SF_{ideal}}$) ( left Digital, right Analog) (**L**)*

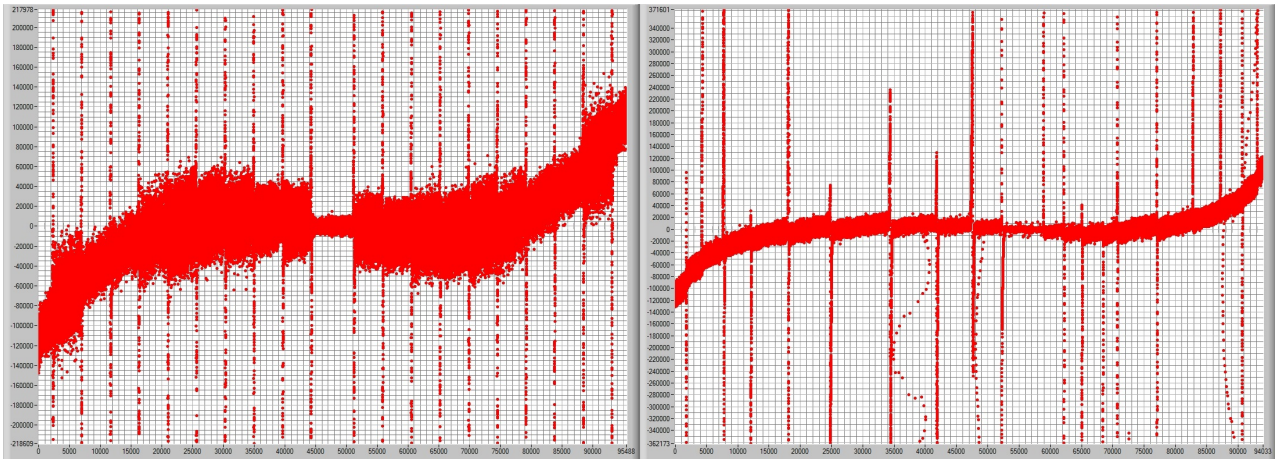

*Figure 4.23: Figure of linear error value as outputted from the independent function in CaTV (in the units BIT) (left Digital, right Analog) (**L**)*

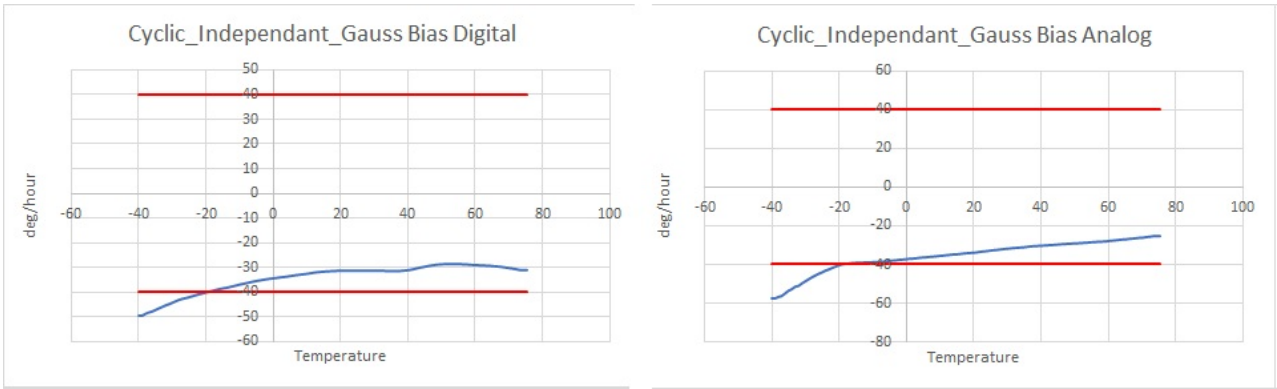


*Figure 4.24: Bias fitted value output from independant gauss compensation calibration process (**E**)*

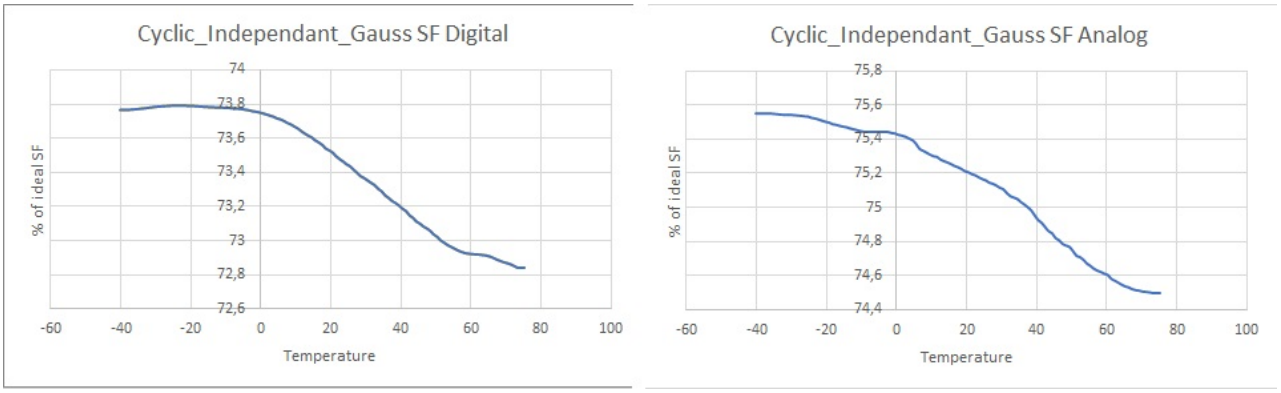


*Figure 4.25: SF fitted value output from independant gauss compensation calibration process (**E**)*

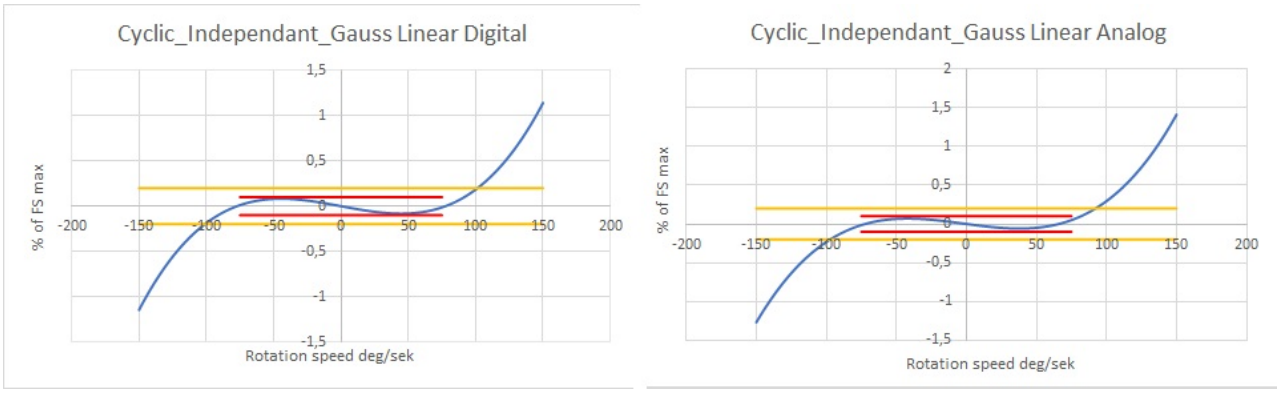


*Figure 4.26: Linear fitted value output from independant gauss compensation calibration process (**E**)*

| Name | Digital | Analog | Unit |
|---|---|---|---|
| Bias | 34,3955738 | 35,4463633 | deg/hour |
| SF | 26,56330184 | 24,85952562 | % of SF ideal error |
| Linear | 0,237658835 | 0,283517195 | % of FS max |

*Table 4.4: Listing of the averages of the fitted data*

## 4.5 Test 2: Verification

Same process as in test 1 is redone here now only using the gaussian regression instead. The results from this is shown in 4.27 ,4.28 ,4.29 and tables 4.5 and 4.6.

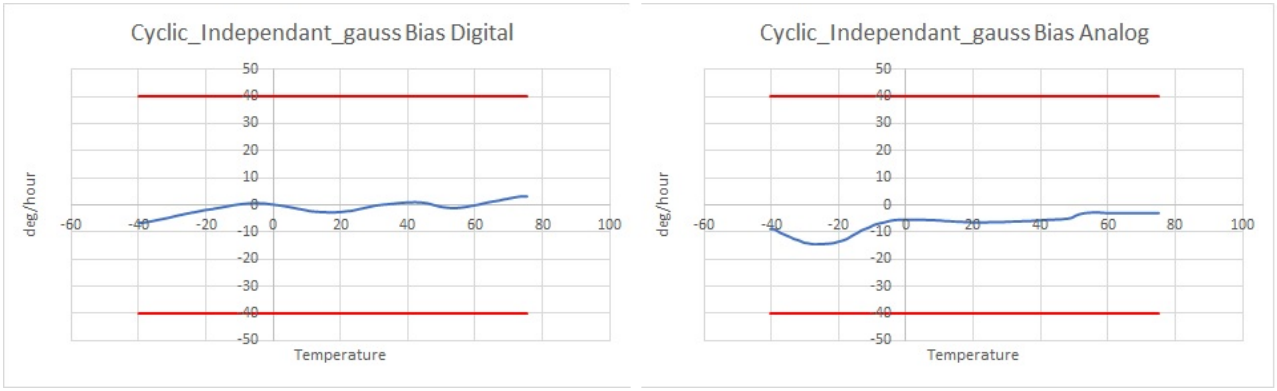


*Figure 4.27: Bias verification (**E**)*

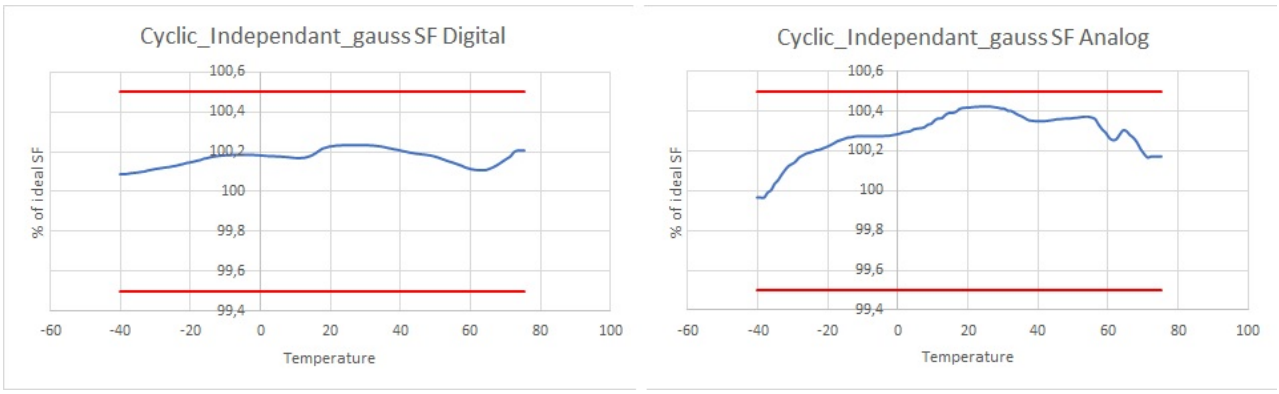


*Figure 4.28: SF verification (**E**); even more shifted upwards seems to correlate to the increased data point and the increase in noise peaks*

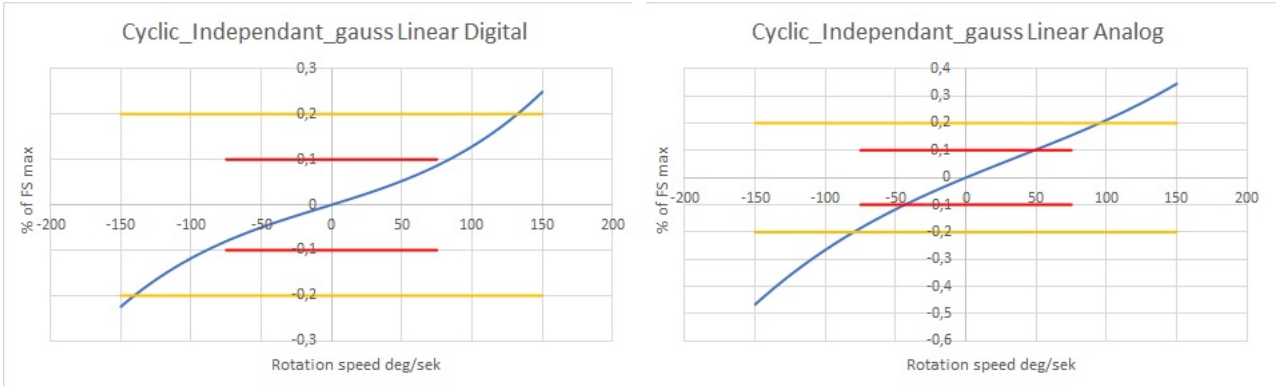


*Figure 4.29: Linear verification (**E**); very poor results from linearisation*

| Name | Digital | Analog | Unit |
|---|---|---|---|
| Bias | 1,690415552 | 6,733095445 | deg/hour |
| SF | 0,1679937 | 0,289961776 | % of SF ideal error |
| Linear | 0,094985477 | 0,181164728 | % of FS max |

*Table 4.5: Listing of the averages of the compensated data*

| Name | Digital | Analog | Unit |
|---|---|---|---|
| Bias | 95,09 | 81 | % reduced error |
| SF | 99,4 | 98,83 | % reduced error |
| Linear | 60 | 36,1 | % reduced error |

*Table 4.6: The percentage reduction of the error*

## 4.6 Test 3: Cyclic surface

The surface profile is fundamentally different to the independent profile and the figures 4.30 and 4.31 where the collected data is displayed, show this difference as the many rate loops which run OTR instead of at one temperature stand out. Since the surface function uses the $\omega(\theta, T)$ for its fitting and since $\omega$ is tridimensional it seems logical to plot the output of the gyros in 3D to better represent what the surface function will work with. This is shown in figures 4.32 and 4.33. although the bias, SF and linearization errors are too small in proportion to the range of the output to view in this image one interesting thing that can be seen is a hysteresis error that appears during the linear loops. In figure 4.34 ,4.35 ,4.36 bias, SF and linearity errors are shown as they are returned from the surface calibration process.

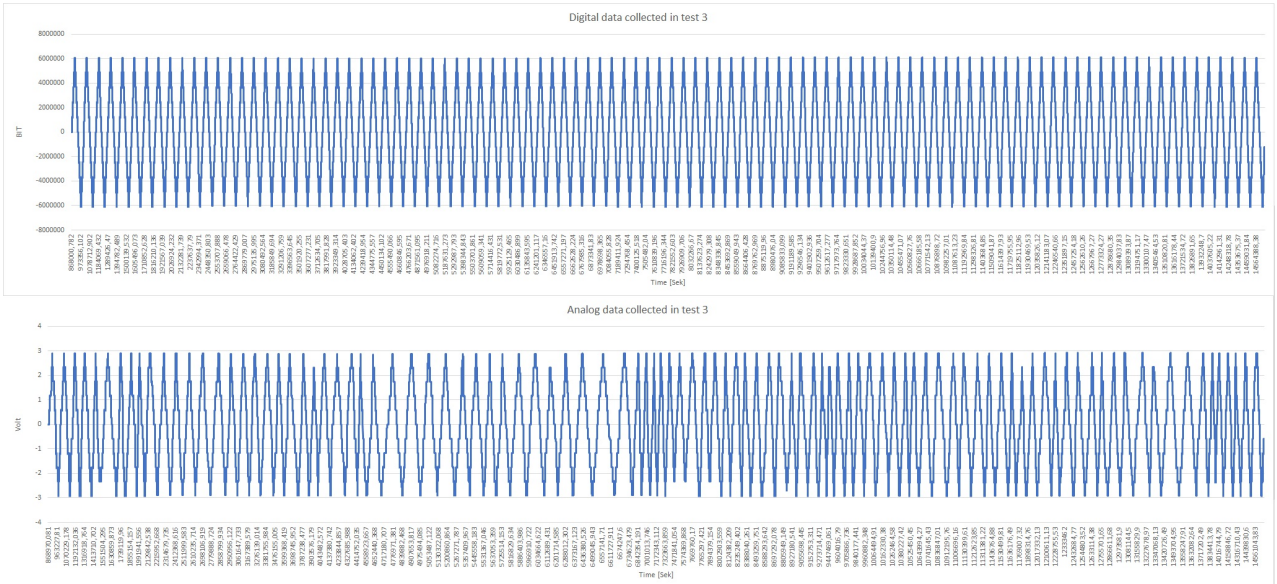


*Figure 4.30: Digital and analog collected data values (**E**)*

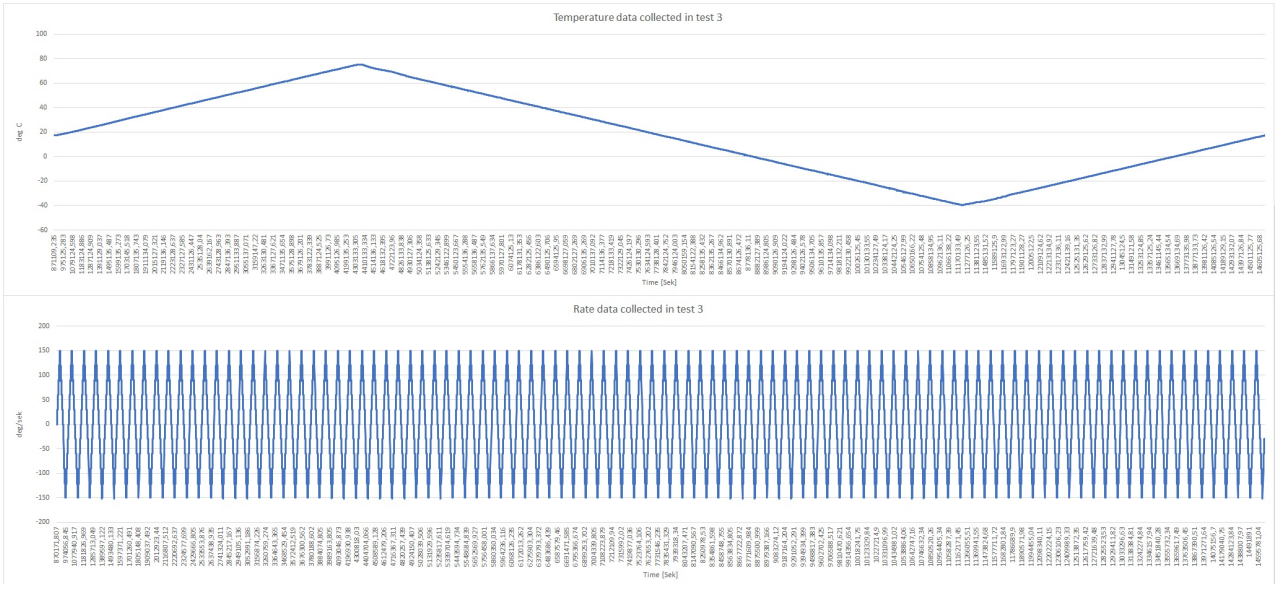


*Figure 4.31: Temperature and rate collected data values (**E**)*

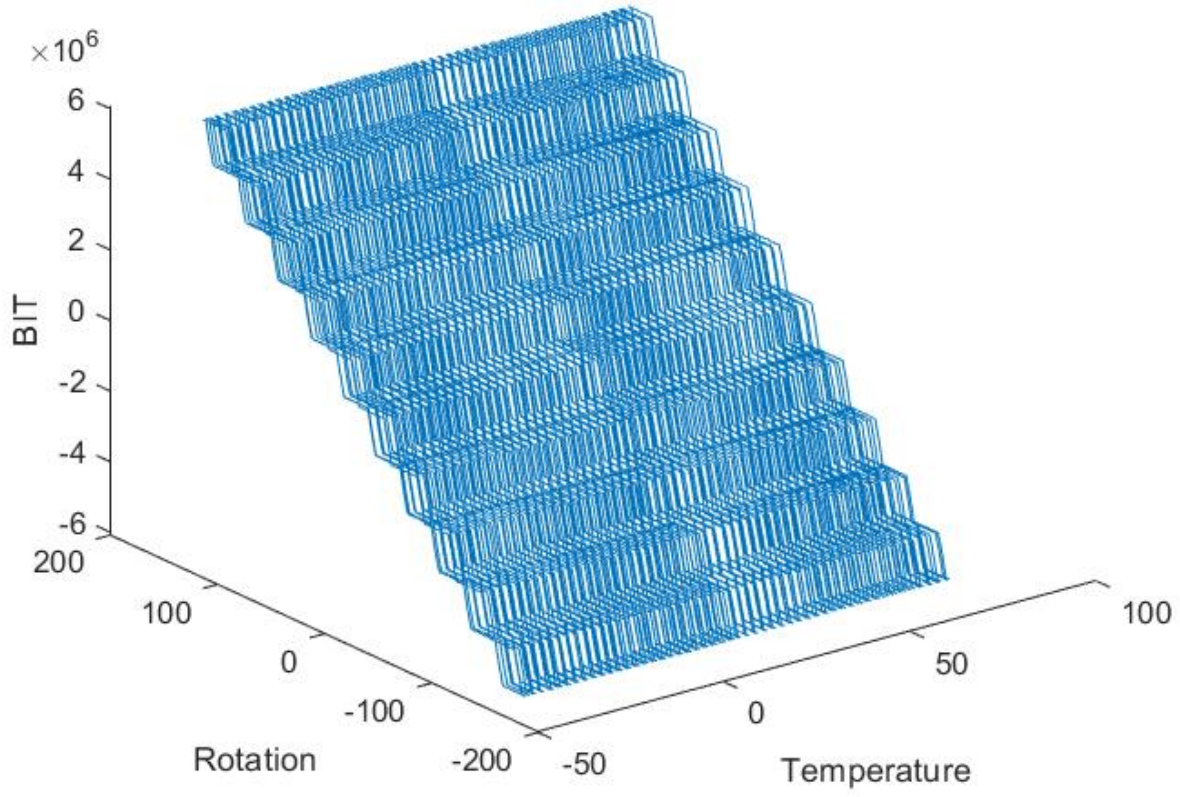


*Figure 4.32: 3D plot of data points of digital gyro output in BIT (**M**)*

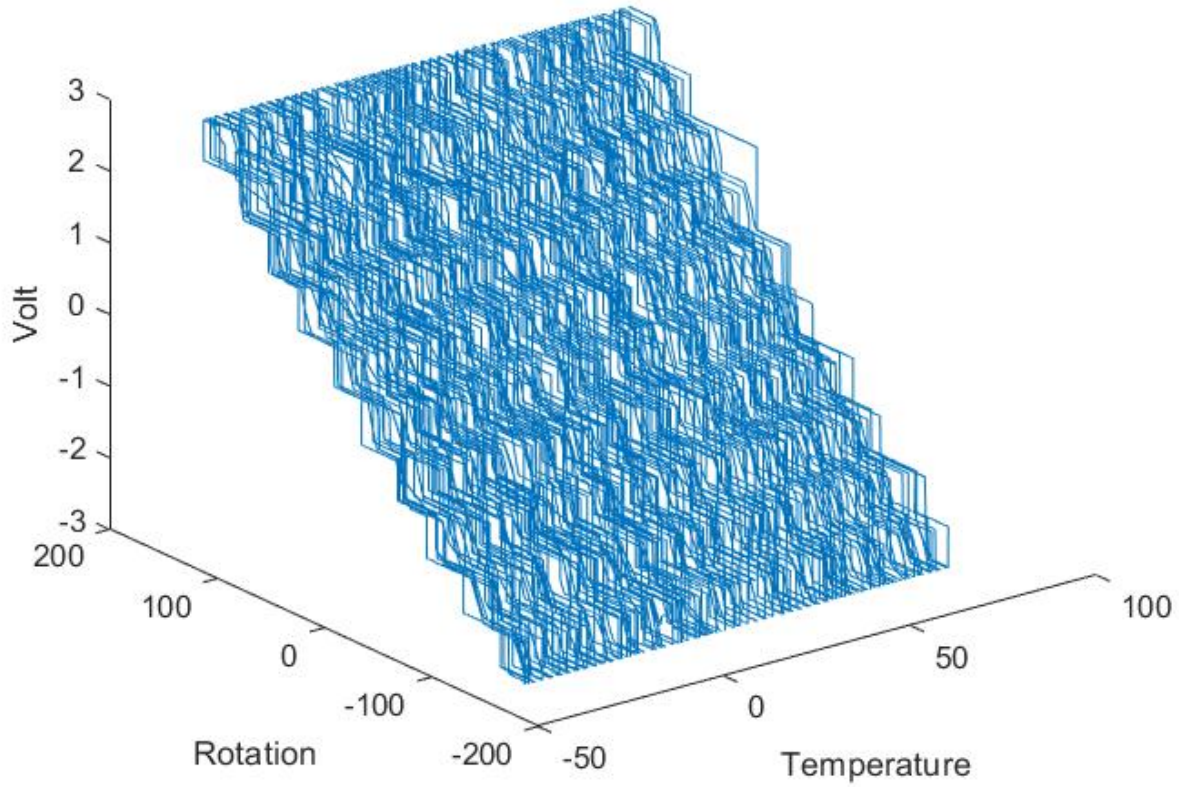


*Figure 4.33: 3D plot of data points of analog gyro output in volt (**M**)*

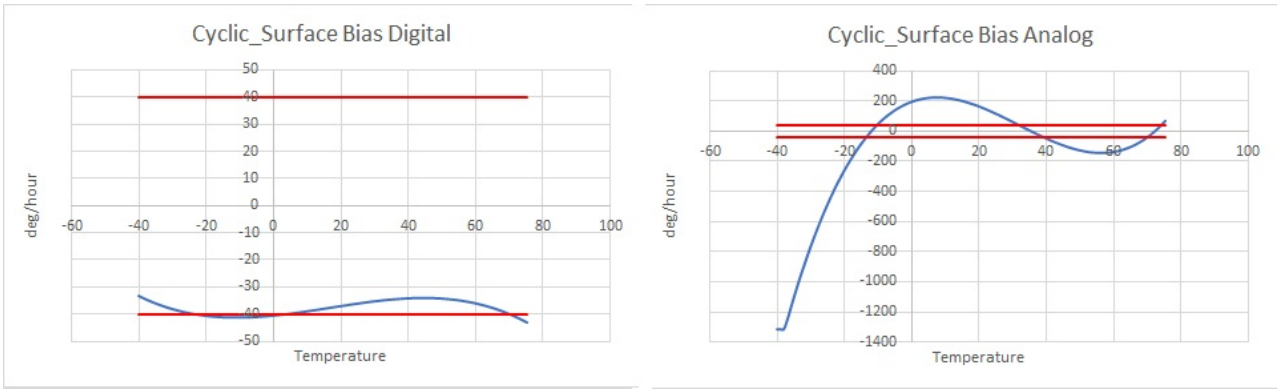


*Figure 4.34: Bias fitted value output from surface compensation calibration process (**E**); the digital and analog bias error values differs very much and one is most likely not correct, since the analog is using a values which the bias is typically not in the order of it is most likely wrong.*

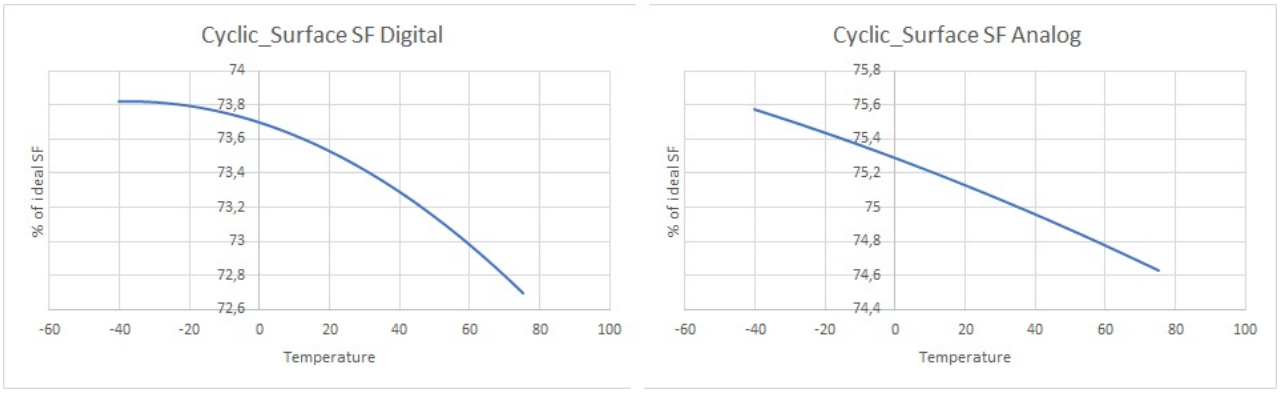


*Figure 4.35: SF fitted value output from surface compensation calibration process (**E**)*

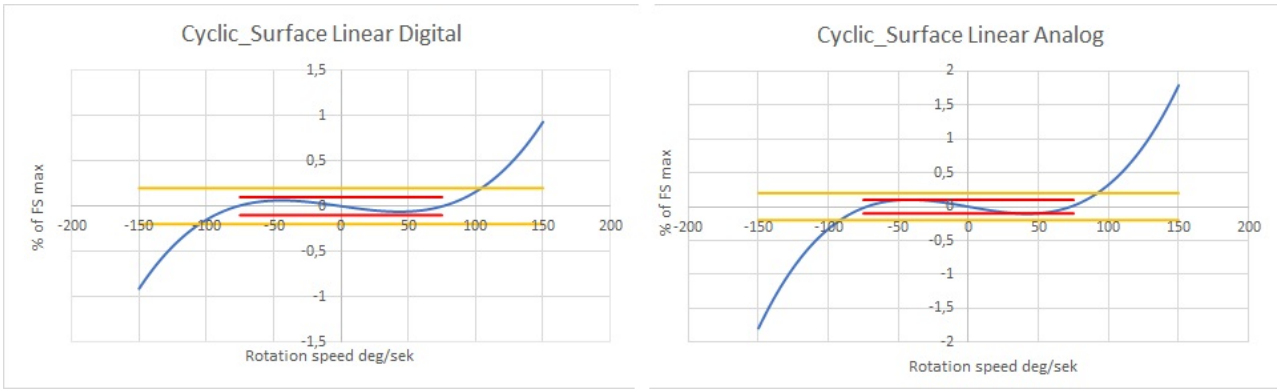


*Figure 4.36: Linear fitted value output from independant poly compensation calibration process (**E**)*

| Name | Digital | Analog | Unit |
|---|---|---|---|
| Bias | 37,5897989 | 239,8938218 | deg/hour |
| SF | 26,54566276 | 24,8654549 | % of SF ideal error |
| Linear | 0,19185623 | 0,374887409 | % of FS max |

*Table 4.7: Listing of the averages of the fitted data*

## 4.7 Test 3: Verification

Just as in previous tests the compensation data is uploaded and a new test is run and the errors are calculated using the surface function. The result of this is shown in figure 4.37 ,4.38 ,4.39.

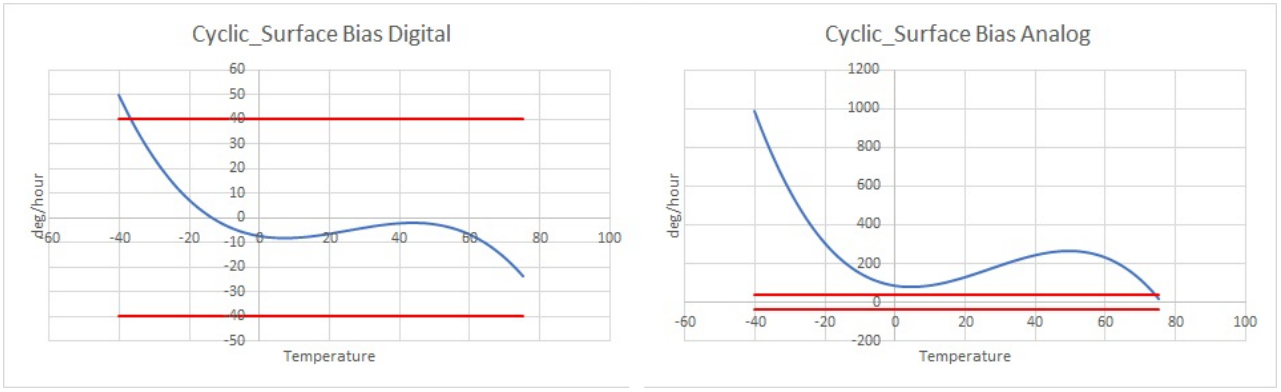


*Figure 4.37: Bias verification (**E**); Analog bias is very wrong and has been worsified, a clue of what might be the cause is that the shape and order of the digital and analog values are similar but the values are different by a order of* $\approx 100$. *This leads to the suspicion that the analog bias errors extreme values are caused by an analog conversion error within the program. Another possibility is that the inaccuracies in both bias compensation values is caused by polynomial overfitting and since the analog is noisier than the digital this results in higher inaccuracies*

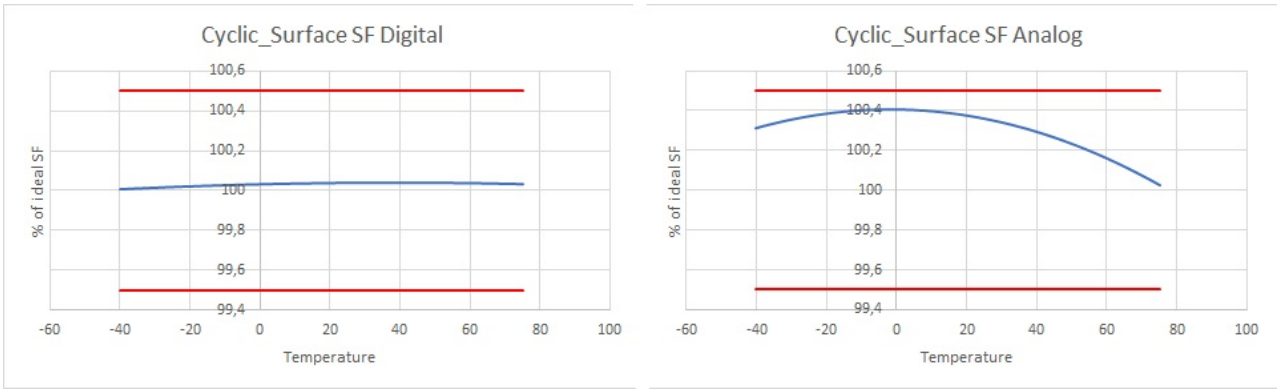


*Figure 4.38: SF verification (**E**); The digital SF looks very good and the analog the opposite of that, the analog SF errors shift could be caused by the same thing as the analog bias.*

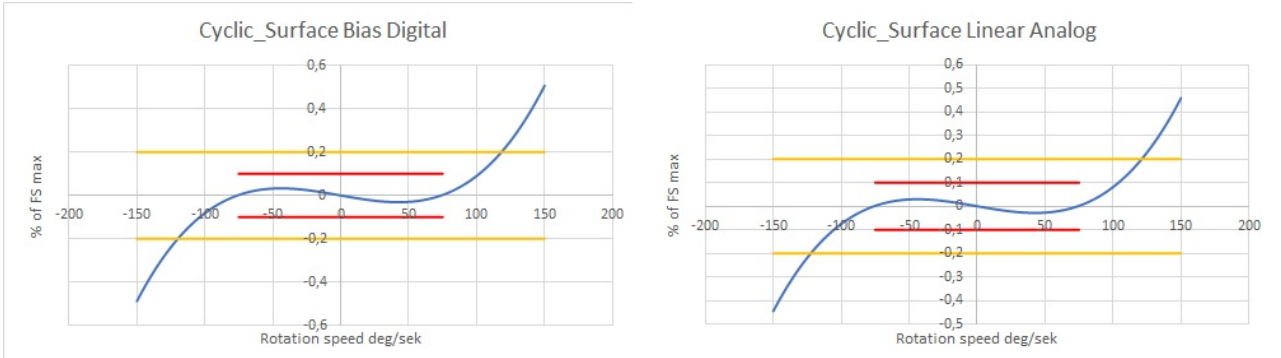


*Figure 4.39: Linear verification (**E**) poor result from linearisation, does not meet requirements in the 0-150 range.*

| Name | Digital | Analog | Unit |
|---|---|---|---|
| Bias | 9,77821368 | 347,9737416 | deg/hour |
| SF | 0,032675989 | 0,310100133 | % of SF ideal error |
| Linear | 0,103758385 | 0,094082378 | % of FS max |

*Table 4.8: Listing of the averages of the compensated data*

| Name | Digital | Analog | Unit |
|---|---|---|---|
| Bias | 73,99 | -45 | % reduced error |
| SF | 99,88 | 98,75 | % reduced error |
| Linear | 45,92 | 74,9 | % reduced error |

*Table 4.9: Listing of the percentage reduction of the error*

## 4.8 Summary of tests

Here the results of the tests are put in the same tables for easier viewing.

| Name | Test 0 | Test 1 | Test 2 | Test 3 |
|---|---|---|---|---|
| Digital Bias | 1,661255986 | 3,267433204 | 1,690415552 | 9,77821368 |
| Analog Bias | 3,378396673 | 2,474239047 | 6,733095445 | 347,9737416 |
| Digital SF | 0,036743828 | 0,1351731 | 0,1679937 | 0,0322029 |
| Analog SF | 0,035844137 | 0,1880049 | 0,289961776 | 0,3101803 |
| Digital Linear | 0,026890181 | 0,09435305 | 0,094985477 | 0,103758385 |
| Analog Linear | 0,04638709 | 0,12013718 | 0,181164728 | 0,094082378 |

*Table 4.10: Listing of the averages of the results*

| Name | Test 0 | Test 1 | Test 2 | Test 3 |
|---|---|---|---|---|
| Digital Bias | 89,28 | 91,47 | 95,09 | 73,99 |
| Analog Bias | 84,14 | 93,9 | 81 | -45 |
| Digital SF | 99,90 | 99,49 | 99,4 | 99,88 |
| Analog SF | 99,90 | 99,24 | 98,83 | 98,75 |
| Digital Linear | 85,72 | 69,9 | 60 | 45,92 |
| Analog Linear | 74,64 | 59,5 | 36,1 | 74,9 |
| Average | 88,93 | 85,58 | 78,40 | 58,073 |

*Table 4.11: Listing of the error reduction factors of the results and a average of them*

# 5 Conclusions & Discussion

The investigation resulted in several ways to improve the calibration process. The thermal modeling of the process itself is something which could potentially remove some uncertainties and optimize several parameters. From the thermal simulation that was done, significant time could be saved in the calibration process if the temperature stabilization time could be optimized. Even though the time derived from this calculation was significantly less than the currently used there are several parameters which influence the result of this such as the stabilisation trigger value and the thermal properties of the materials. Other ways to improve the process is to give more options when creating the profiles that control the hardware. For example the usage of linear rotation compensation optimizes the time that the profile stays on a level, which previously was a constant. Primarily The investigation found that a switch to an automated calibrations system opens up new possibilities for calibration methods, here some alternatives to the current method were formulated and evaluated but this could be drawn even furthur by for example machine learning and similar processes. In conclusion more investigation on the different major parts could be done and a surface level evaluation has been done on some but not fully verified.

Since all but one of the requirements, necessities and desirables of CaTV were implemented (see table 5.1) the program is a potentially a very large success. This is though dependent upon if the functions function as predicted, which will most likely not be the case during the firsts few tests of those. The program itself has many functionalities implemented that are important for the advanced data management and calibration process, however since the program has not been successfully tested multiple times on real world examples it is hard to conclude how well those functionalities perform. The program does at the moment have a few bugs which amongst all can cause a crash such as multitasking priorities causing lockups of the interface. The program does not have many safeguard for the user as misuse of parameters and functions can cause the program to crash. The product and profile functionalities gives smooth and easy creating and visualization of the profiles. The implementation of the product/ profile system is most likely the part of CaTV that will improve the calibration handling overall as it gives a faster and more effective way to handle the management of different gyros.

The average values of the error correction factor in table and 4.11 indicate that the best calibration process based on error reduction is the current (Test 0), Acyclic independent polynomial (Test 1), cyclic independant gauss (Test 2) and then the cyclic surface (Test 3) in that order. However due to many uncertainties such as the test did not use the same gyro. The current method has a previous history of optimized parameters and methodology in which most of the parameters in the new processes are clearly unideal and the methodology has not been tested enough. The software used to collect the data has not been sufficiently verified to conclude it is reliable. It is for these reasons it is hard to draw any broad definitive conclusions from the collected data results. However they can serve as proof of concept for the various new calibration processes as they manage to calibrate the gyros at all and in some cases do so quite well. For example the independent gaussian giving good results on the bias, which since the digital bias noise is gaussian by nature is an indication that there might be a reason for further investigation. Another being the surface function resulting in good digital SF calibration or the acyclic independent polynomial implemented in CaTV getting similar error reduction values as the current process.

To summarize, more work needs to be done in order to get the new profiles and CaTV working at optimal performance. However the values achieved in their first real world calibration test on a gyro gives promising results that this can be done and can be done automatically, better and more efficiently than the currently used profile and software.

| Number | Description | Is implemented? |
|---|---|---|
| Requirements: | | |
| 1 | Read data from gyro | yes |
| 2 | Calculate SF, bias and linearity for analog and digital compensation values | yes |
| 3 | Upload calibrated compensation values automatically | yes |
| 4 | Control test machine | yes |
| Necessities: | | |
| 5 | Implement auto-baudrate scanning | yes |
| 6 | Choose calibration process | yes |
| 7 | Manually set SF for the first calibration | yes |
| 8 | Read the type and serial number of the gyro | no |
| Desirables: | | |
| 9 | Automatically tests the scale factor at the first calibration run and changes depending on the result | yes |
| 10 | Different calibration routines | yes |
| 11 | Calibrating more than one gyro att the time | yes |
| 12 | Automatic COM port searching for the gyro | yes |
| 13 | Better average forming of data | yes |

*Table 5.1: Table of the of the Requirements, Necessities and Desirables of CaTV*

## 5.1 Error factors and Improvements

The largest error factor in impacting the results is the fact that the same calibration process is used to verify the result of the previous calibration. Since the processes have not been tested and verified to work yet this could lead to cascade errors in the calibration and verification process resulting in that it would be hard assessing how much the error of the process in itself was since the verification process was used to verify it. The process verifying itself was chosen because it is how the errors are verified in the currently implemented program and profile and due to time restrictions. An improvement on this may be a verification profile that is specifically used for verifying the gyro calibration accuracy without time any time restriction, this could then be used to verify other faster processes such as the independent, partial derivative, surface or any other future process.

The thermal conduction capacity of the material A is $\alpha_A$ and material B is $\alpha_B$ are in reality dependent upon the temperature and pressure of the material. Since these are constants at the moment in order to improve the thermal simulation the values could be set to be more realistic. Another way to increase the thermal simulation is to attempt to make the simulation more accurate by adding more elements such as more parts (such as the rotation table the air outside the gyro in the space of the temperature chamber) or adding a way to calculate the convection effects as a result of thermal flows.

The SF and linear errors of the independent process in figures 4.10, 4.11, 4.21, 4.22 shows large noise peaks which should not be possible. This could be one cause of the inaccuracies of the SF and bias calibration. This error is most likely caused by the rate tolerance being too small which causes in between values of the rate getting included in the calibration when they shouldn't. Optimizing these tolerances could fix this issue.

Since the analog signal has had issues with reliability and seems to be somewhat inconsistent there may be some errors in the analysis that result because of this or it may be the cause of some functions failing to perform their functions. Some experiments using different parameters and methods for collecting the analog data may resolve the issue.

The linearity of all of the calibrated results(figures 4.18,4.29 and 4.39 ) shows a similar error after the calibration. This error is also out of spec and therefore the calibration is not a success. Since the error is similar for all of the different calibration processes this may be caused by a systematic programming error in the software which would then need to be investigated further to locate the issue.

The CaTV program can be improved in many ways, for example streamlining and improving the performance and by many small quality of life stuff such as:

- More help documentation
- Better plotting functionality
- Printing certifications
- Backwards compatibility with previously implemented programs
- More and better code comments
- Adding ability to import products and profiles
- Adding more settings

## 5.2 Ethics and environment

The possibility of saved resources (primarily time) which can be used on other endeavors. The saved time may not seem significant but during significantly long time spans the time requirements of the current system may add up and an improved methodology is therefore justified. Another aspect is then also the ergonomics of the software used, this is referring to how the interaction between software and user occurs. When an unergonomic system is used, such as the current where editing and controlling the software is done using settings in a text file, this could lead to errors and a difficulty in spotting them. Aswell not to mention it is a system that is unintuitive to learn.

# References


[1] D.M.Shupe. Thermally induced nonreciprocity in the fiber-optic interferometer. *Optical Society of America* (1980).

[2] A. N. D. I.-H. H. T. M. P. Mintchev. New technique for reducing the angle random walk at the output of fiber optic gyroscopes during alignment processes of inertial navigation systems. *Optical Engineering* (2001).

[3] C. N. J. Österman. *Physics handbook for science and enginnering eight edition*. Ed. by Studentlitteratur. Studentlitteratur, 2019.

[4] G. Pascoli. The Sagnac effect and its interpretation by Paul Langevin. *www.sciencedirect.com* (2017). Université de Picardie Jules-Verne,Faculté des sciences, Département de physique.

[5] J.-N. J. R. Radharamanan. EVALUATION OF RING LASER AND FIBER OPTIC GYROSCOPE TECHNOLOGY. *https://www.semanticscholar.org* (2009). School of Engineering, Mercer University.

[6] X. C. Shen. Study on error calibration of fiber optic gyroscope under intense ambient temperature variation. *Applied Optics* (2012).

[7] D. A. J. C. Tannehill; and R. H. Pletcher. *Computational Fluid Mechanics and Heat Transfer*. Ed. by T. bibinitperiod F. G. CRC Press. Boca Raton : CRC Press, Taylor & Francis Group, 2013.

[8] L. R. B. Westgren. *BETA: Mathematics Handbook for science and enginnering fifth edition*. Ed. by Studentlitteratur. Studentlitteratur, 2015.

# A Filter

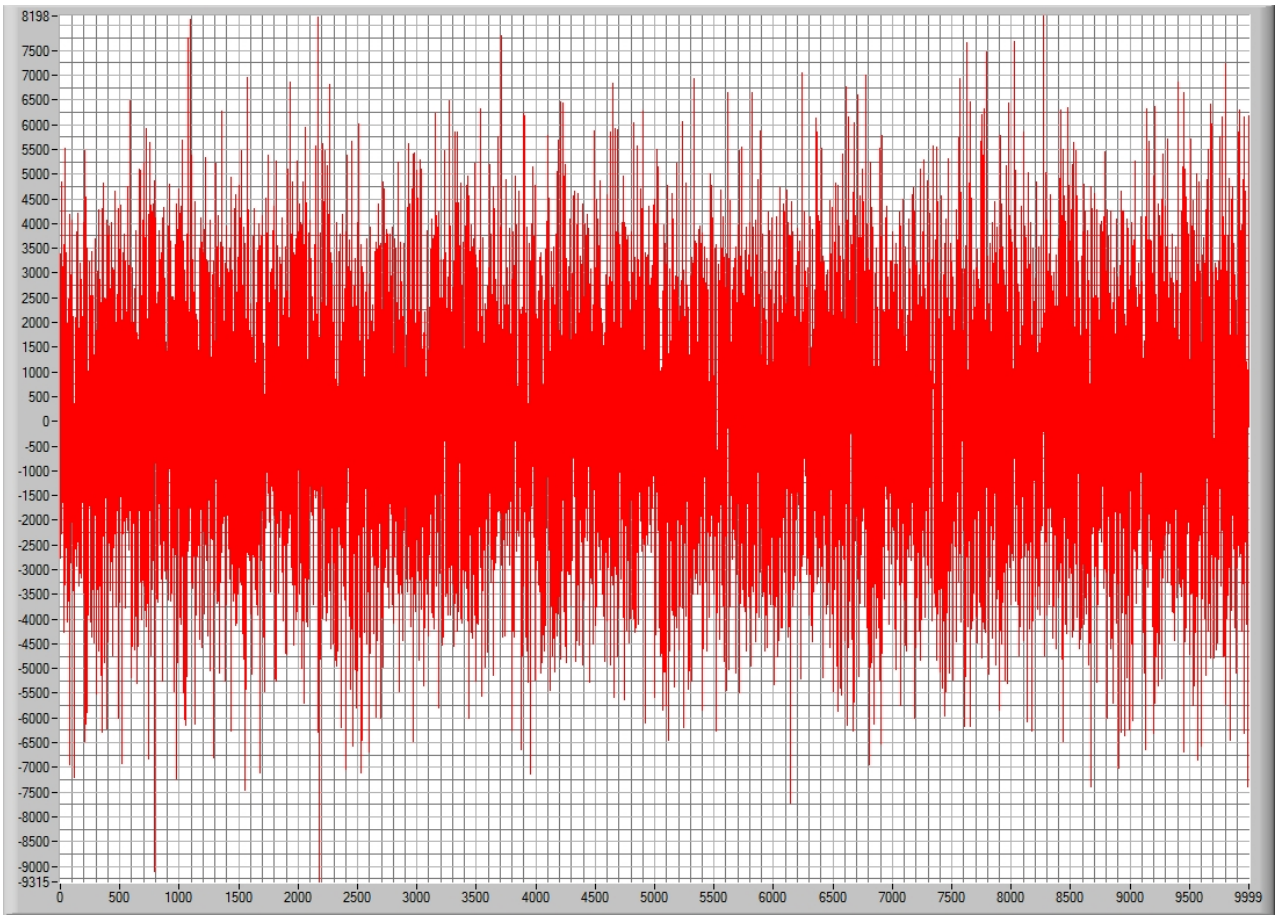


*Figure A.1: The image of the digital data used for the filter tests (**L**)*

## A.1 Weighted average filter

The weighted average filter uses a weighted average equation

$$\bar{y}_{weight} = \frac{\sum_{i=1}^{n} w_i y_i}{\sum_{i=1}^{n} w_i} \tag{A.1}$$

The currently collected value is $y_1$, the other values $y_{i>1}$ are the previously collected values. $w_1$ is set to 1 and the weights of the other values determine what type of filter. Three types have been implemented:

$$Constant: \quad w_{i>1} = C \tag{A.2}$$

$$proportional\ to\ mean: \quad w_{i>1} = \frac{C}{|y_i - \bar{y}|} \tag{A.3}$$

$$proportional\ to\ median: \quad w_{i>1} = \frac{C}{|y_i - \tilde{y}|} \tag{A.4}$$

The parameters C and n determine the filter strength. With the previous established equations the filter becomes:

$$y_{filteredval} = \frac{y_{currentval} + \sum_{i=2}^{n} w_i y_{previousval}[i]}{1 + \sum_{i=2}^{n} w_i} \tag{A.5}$$

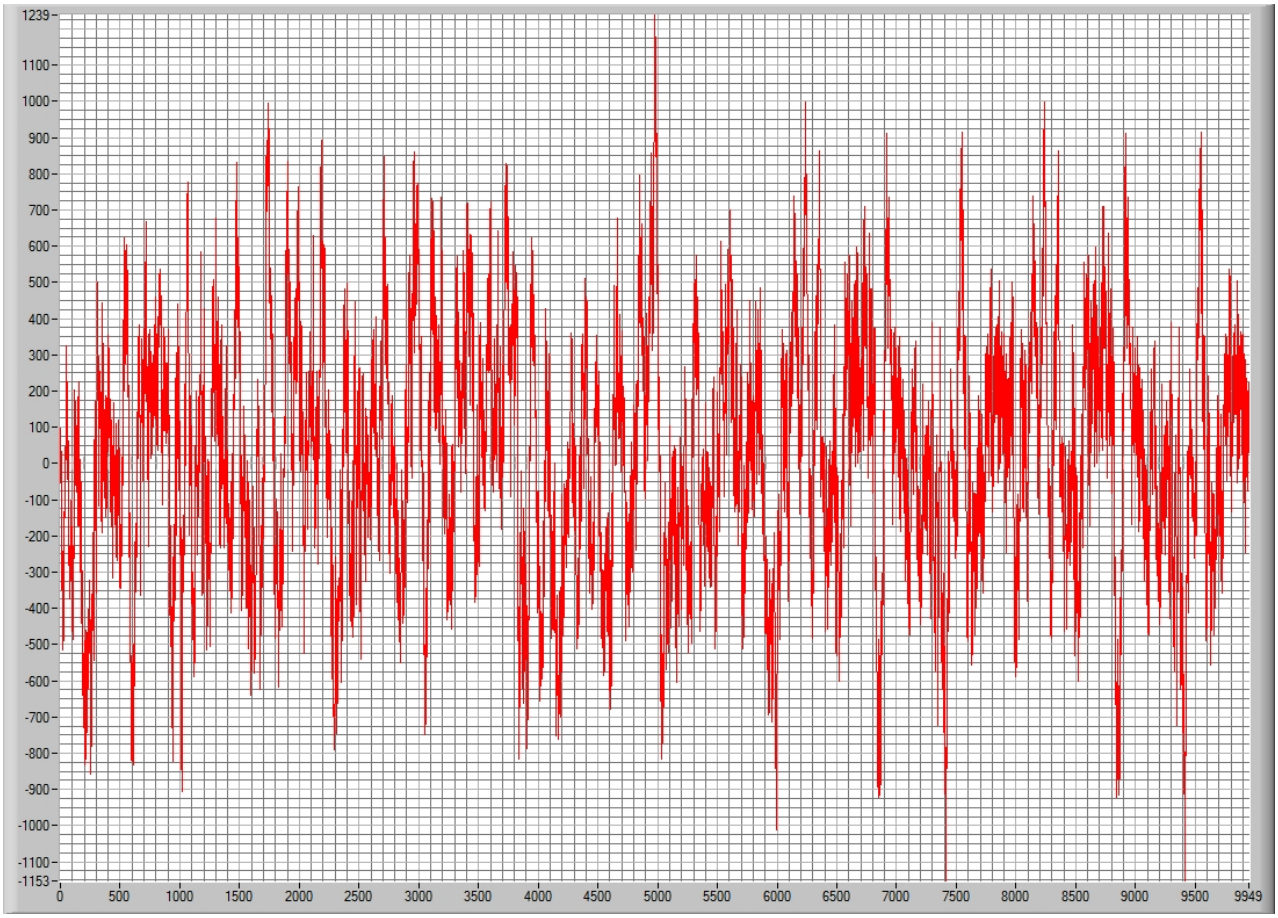


*Figure A.2: The signal filtered with weighted average using constant with $C = 0.5$ and $n = 50$ (**L**)*

## A.2 Butterworth IIR freq

Uses the LabWindows builtin functions AllocIIRFilterPtr and IIRCascadeFiltering to construct a butterworth with specified lower cutoff frequency and upper cutoff frequency.

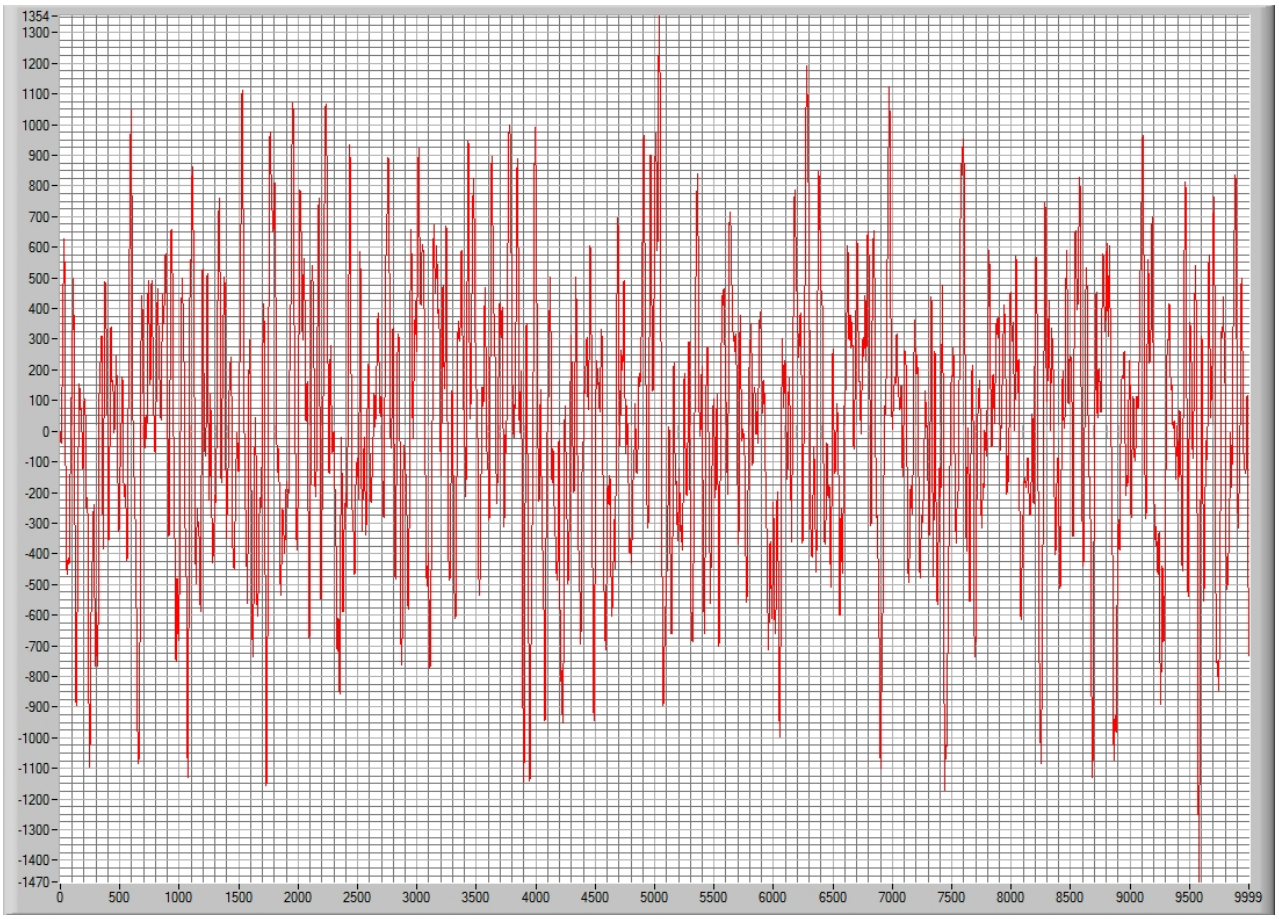


*Figure A.3: The signal filtered with butterworth IIR with lower cutoff frequency of 40 and upper of 450 (**L**)*

## A.3 Gaussian filter

Filters the data through the following equation:

$$y_{gauss} = Probability \times y + (1 - Probability) \times \bar{y}_N \tag{A.6}$$

The probability is calculated using the gaussian fit with the GaussFit function of a histogram of the N:th previous data. This generated a probability distribution over the axis, this is then normalised and interpolated to get the probability. $\bar{y}_N$ is the center of the fitted distribution generated by GaussFit.

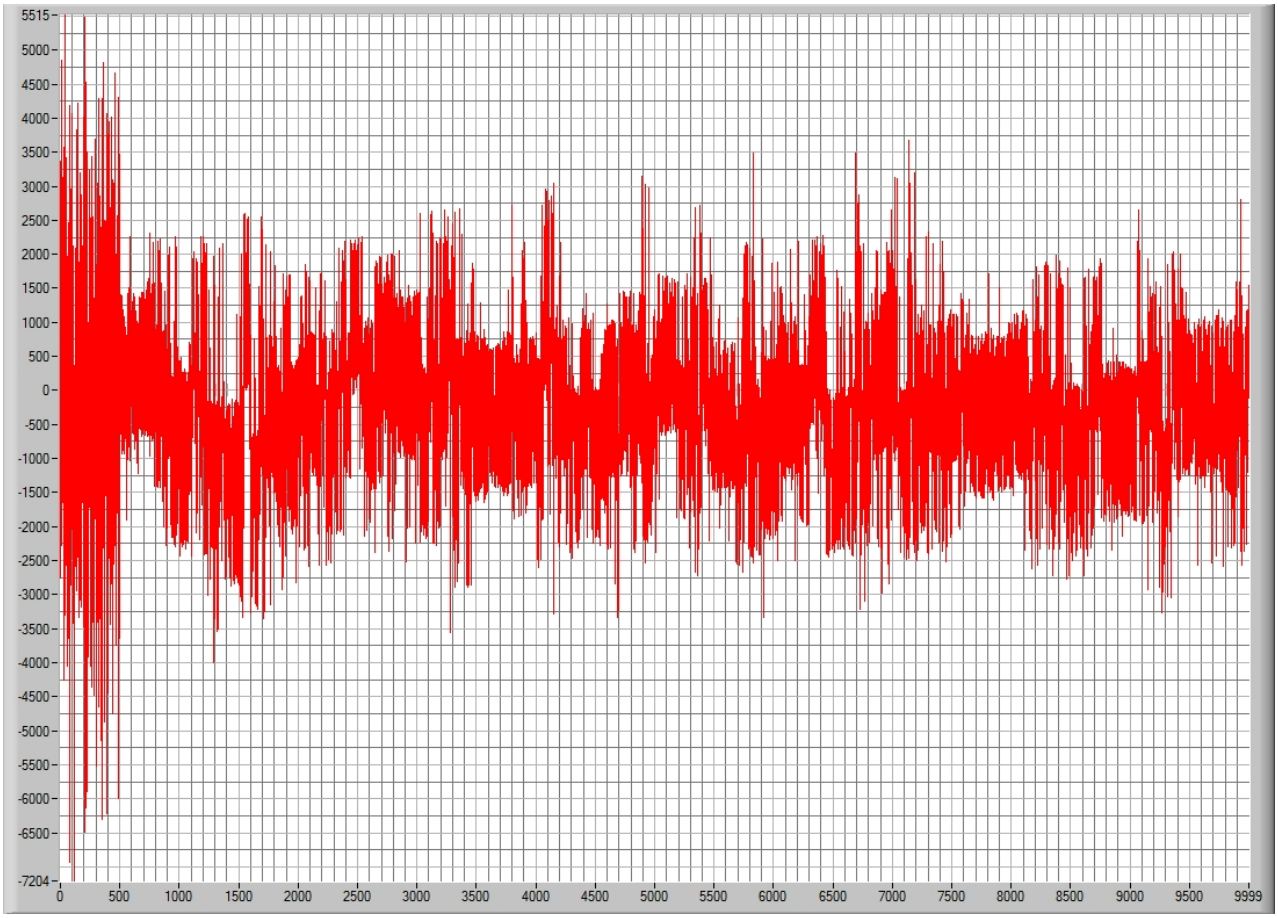


*Figure A.4: The signal filtered with gaussian with $N = 500$, the leftmost 500 values are unchanged due to the filter being initiated (**L**)*

## A.4 Fast fourier transform

Uses the LabWindows builtin functions FFTEx to perform a Fast fourier transform of the signal.

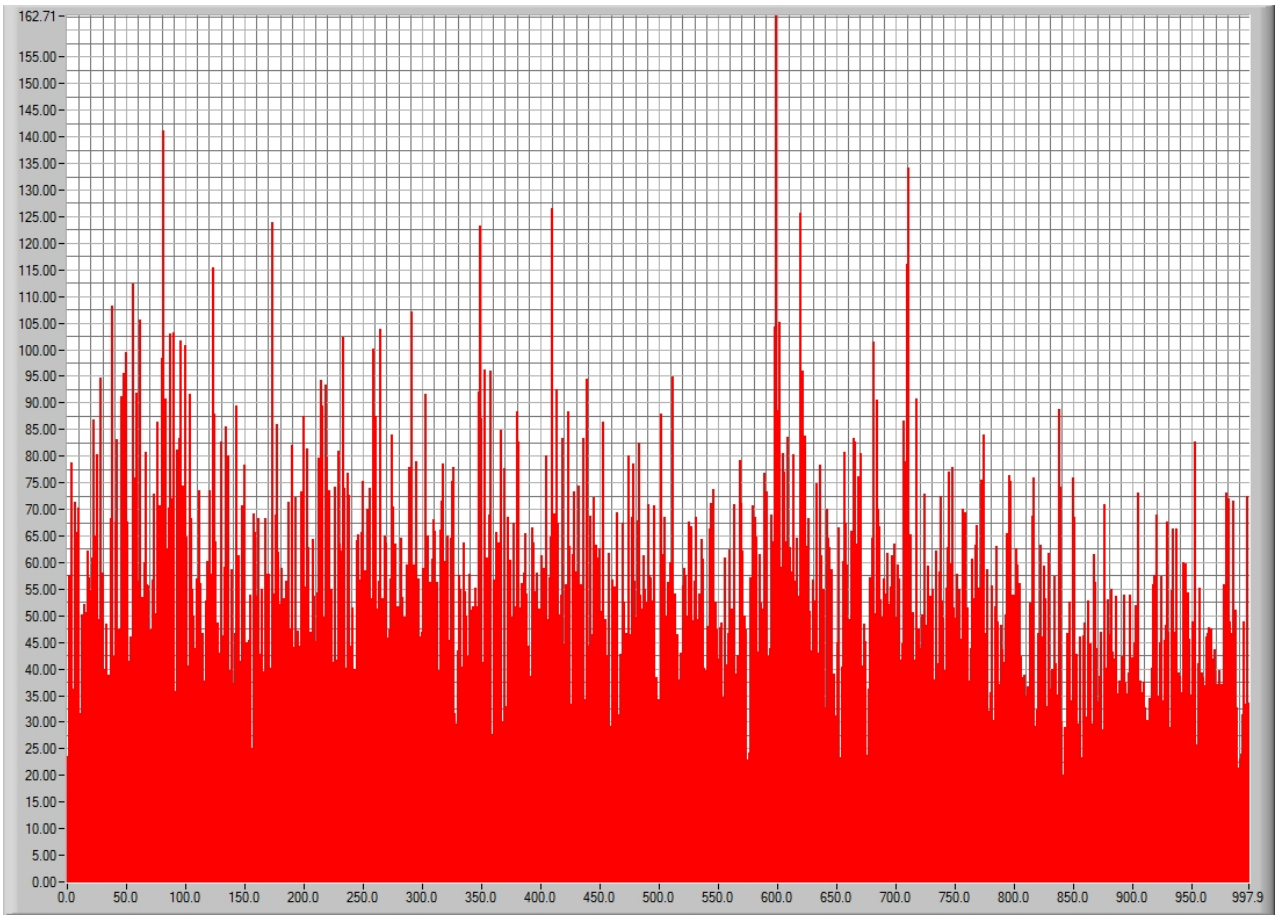


*Figure A.5: a fast fourier transform of the signal (**L**)*

# B Fiber optic gyro specification 8808 000-4xx

SAAB


## FIBER OPTIC GYRO
8088 000-4xx DIGITAL/ANALOG

The new generation of Saab's high performance Fiber Optic Gyro with both analog and digital output. Backed up by over 50-years' experience in inertial sensors.

This new generation Fiber Optic Gyro is specifically designed for stabilization applications where there is a need for high performance single-axis rate sensing. The units are equipped with both analog and digital interface in parallel giving the flexibility to be used as a standard configuration in various systems.

**Operation:**
A Fiber Optic Gyro is based on the Sagnac effect. The time for light to travel in a coil is dependent of the rotation of the coil. In a ring fiber optic gyro light is divided into two beams entering a fiber coil in opposite directions. After exiting the coil the two beams are combined in a coupler and a phase difference proportional to the rate of rotation is measured

*Fiber Optic Gyro (FOG).*

**Applications:**
- Gun stabilization
- Missile stabilization
- Inertial measurement units
- Sight stabilization
- Camera stabilization
- Antenna stabilization
- Autonomous vehicles

**Features:**
- Solid state
- Low drift
- High shock usability
- No delay on analog interface
- High internal sampling rate
- Low delay on digital interface
- Single +5VDC Supply
- Small size
- Available with EMI protection

**Company Background:**
Saab has been a producer of gyros of various designs for over 50 years. Production was initially intended for Saab designed aircraft sight and missile requirements.

Since the end of 70's, the gyro production have expanded into a product line of its own including design and production of gyro products for worldwide customers. Up to the present time, we have produced more than 50.000 sensors. Gyros based on FOG technology has been the main product since the end of 90's.

*Mechanical Gyros.*

SAAB

## DIMENSIONAL DRAWING 8088 000-4xx

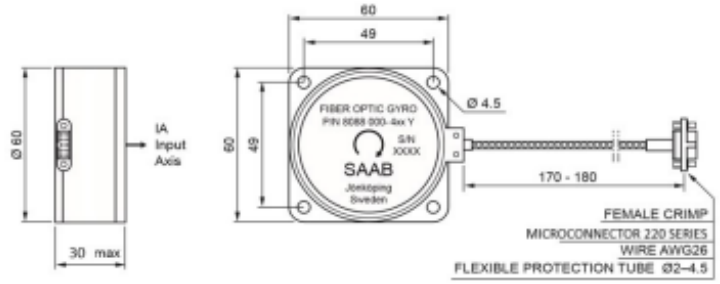


## SPECIFICATION VERSION 8088 000-4xx

| CHARACTERISTICS | UNIT | VALUE |
|---|---|---|
| Range | °/s | 50 -350 |
| Bias at 20°C (initial cond.) | °/h | 20 |
| Bias variation peak to peak over temperature range | °/h | 40 |
| Bias stability | °/h rms | 1 |
| SF error in Room Temperature | % | 0.1 |
| SF variation Over Temperature Range | % | 0.3 |
| Linearity error 0-150 °/s | % of Full Scale | 0.2 |
| Bandwidth | Hz | <1000 |
| Start up time | msec | 100 |
| Weight | grams max | 100 |
| Temperature Sensor Output | | |
| Built In Test Output | | |
| **POWER REQUIREMENTS** | | |
| Supply Voltage | VDC | +5 (4.90 to 5.25) |
| Input Power | W | 1.5 |
| **ENVIRONMENTS** | | |
| Shock | g : msec | 90 : 6 |
| Vibration, sine | g : Hz | 10 : 20-2000 |
| Vibration, random | g²/Hz : Hz | 0.09 : 20-2000 |
| Operating temperature range (OTR) | °C | -40 to +70 |
| Storage temperature range | °C | -46 to +75 |
| **DIGITAL OUTPUT FORMAT RS422** | | |
| Resolution | Bits | 20-24 |
| Transmission Rate | kBaud | 115.2 - 2000 |
| Output Update Rate | kHz | 1-4 |
| **ANALOG OUTPUT FORMAT** | | |
| Differential Output | VDC | ±2 |
| Output Load | kΩ | 10 |



Specifications subject to change without notice March 2018

www.saabgroup.com

Saab AB, Avionics Systems
SE-561 84 Huskvarna
Sweden

Phone: +46 36 19 41 50

NAVAL LAND

# C FlowChart of Independent process implemented in CaTV program

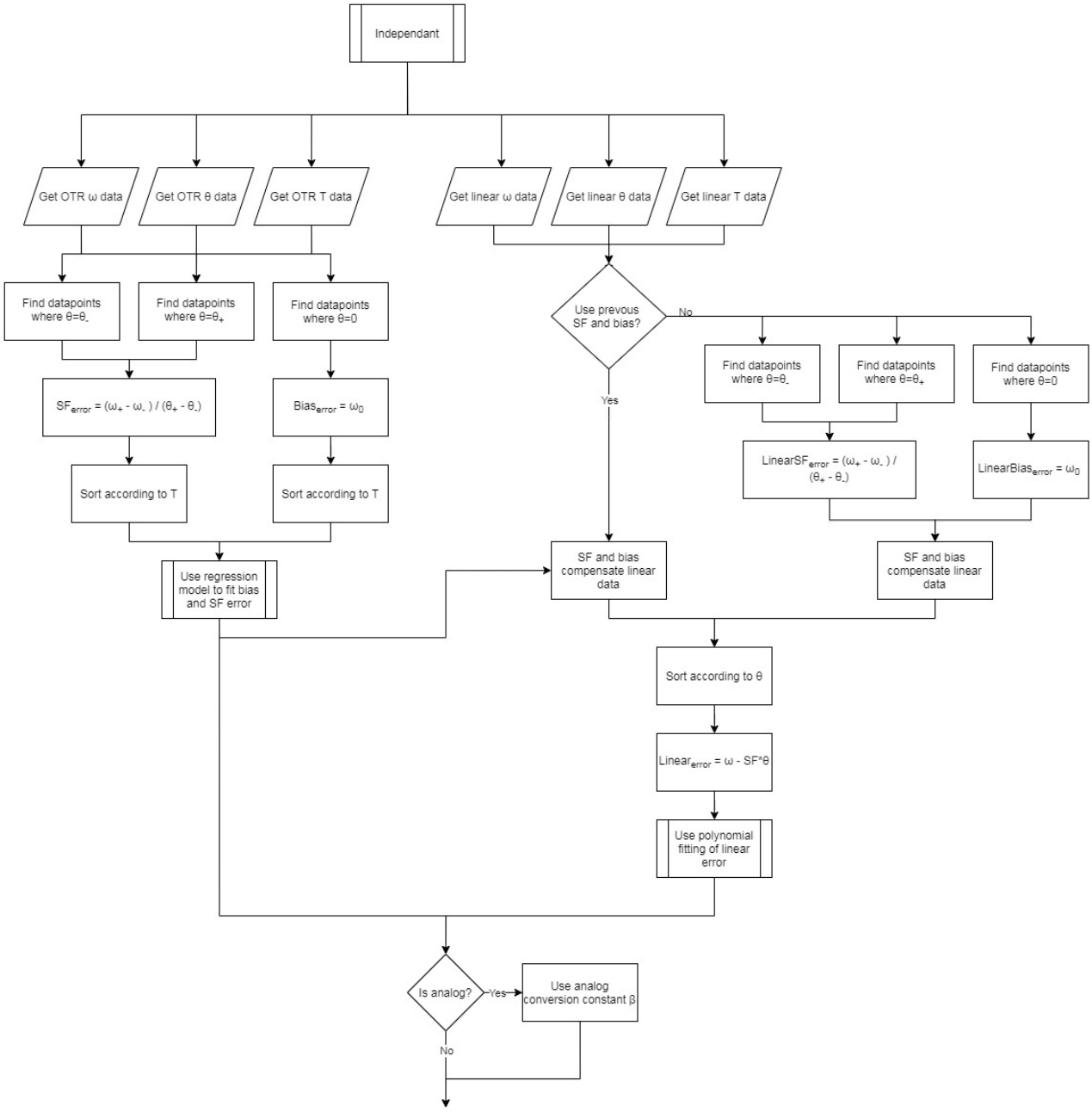


*Figure C.1: Flowchart of the independent compensation calibration process that is implemented in the end program*

# D Initial flow chart of the program

Contains the initial flow chart of the program

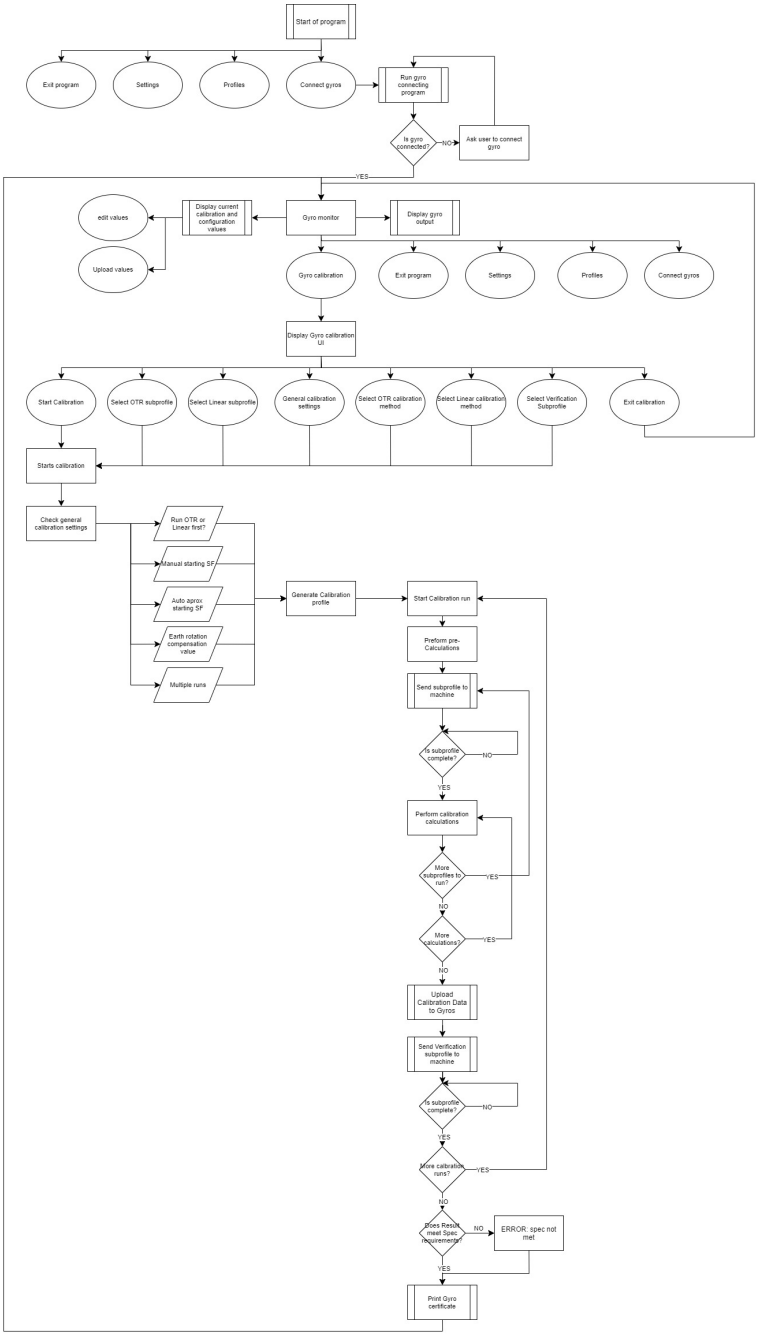


*Figure D.1: Initial flow chart of program*

# E CaTV program flow chart

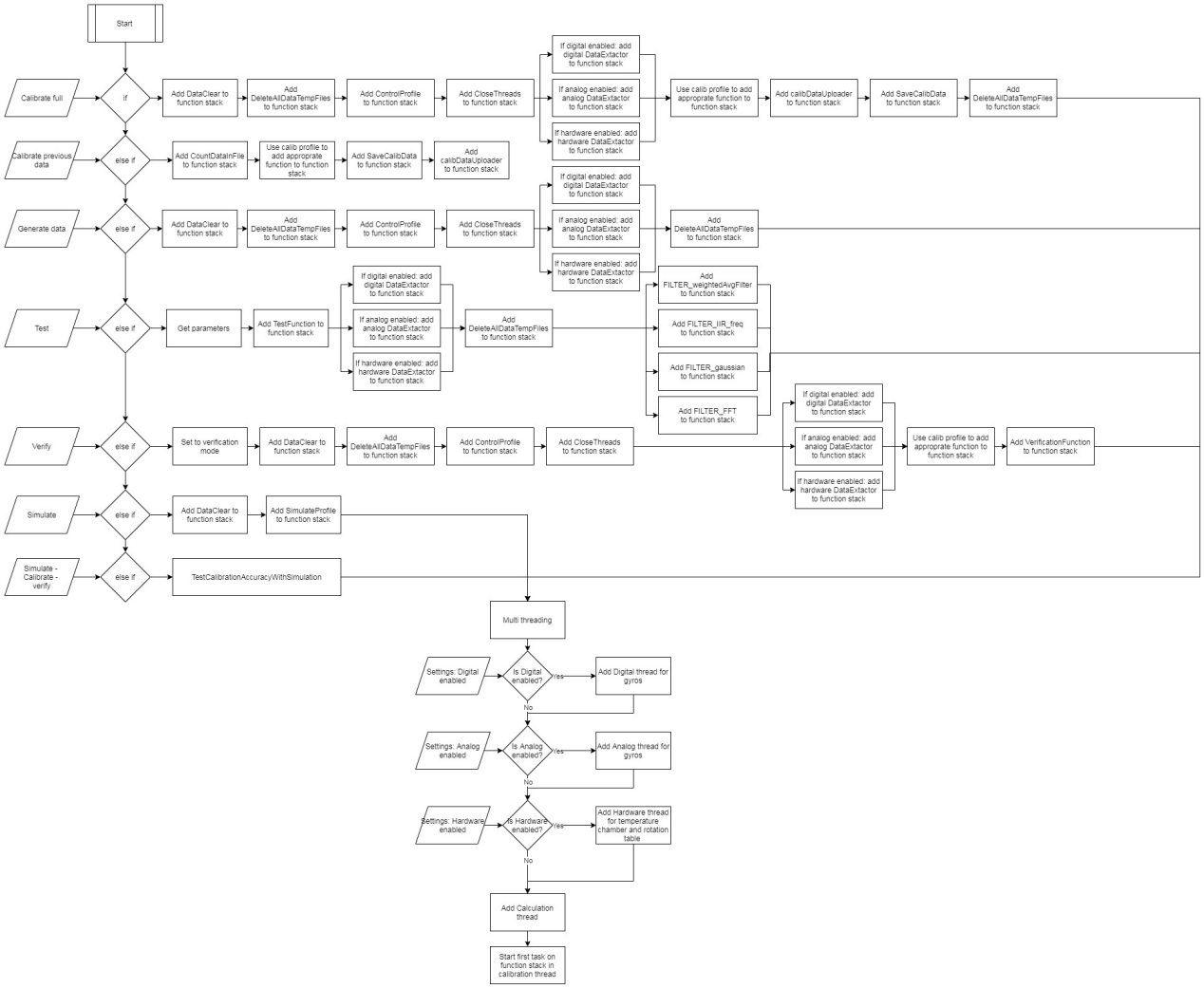


*Figure E.1: Flowchart for the function of start, displays wich functions are added to the function stack and then the starting of the multi threading functionalities*

# F CaTV program images

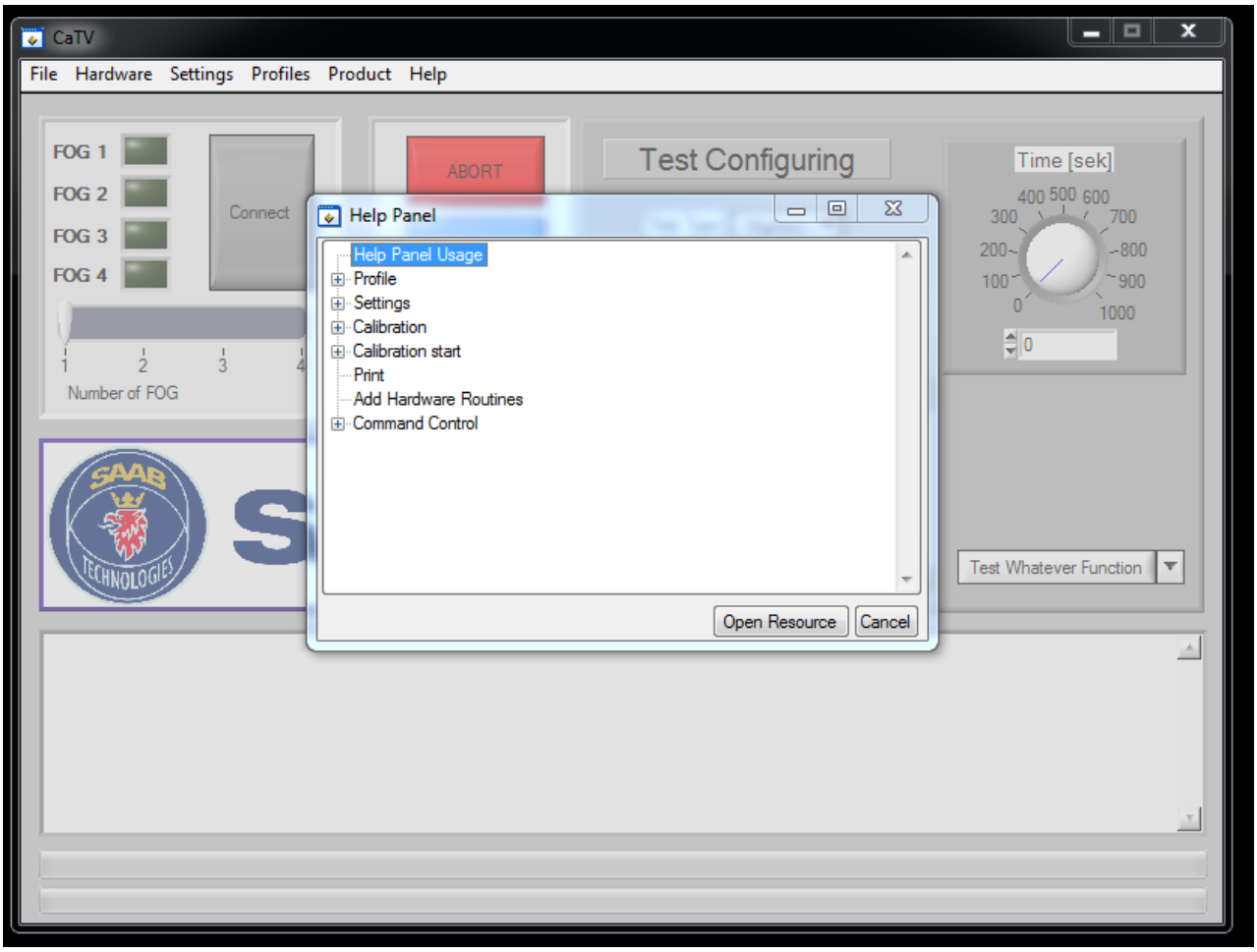


*Figure F.1: Help panel used for help resources*

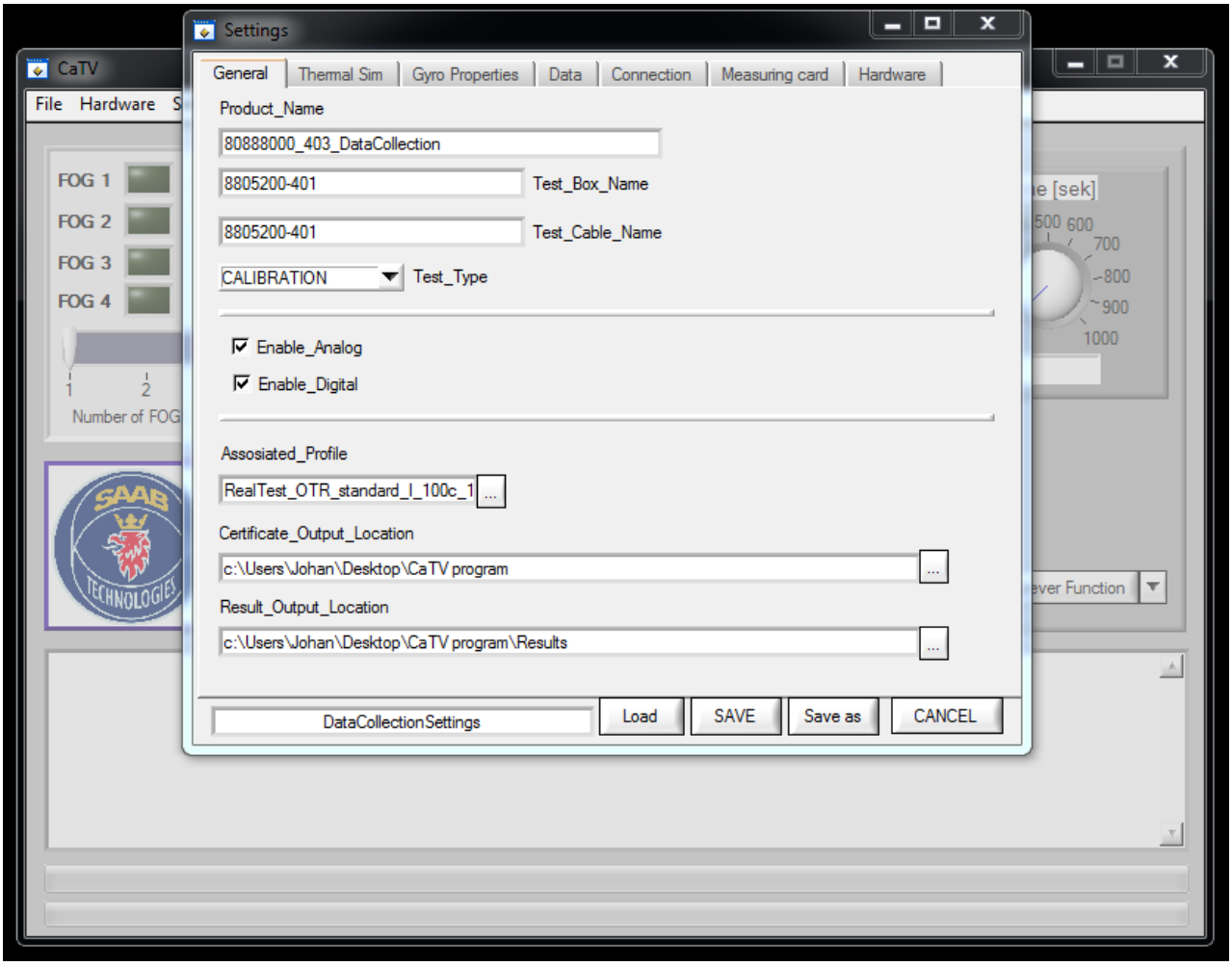


*Figure F.2: General settings panel used for name, locations and enabling outputs*

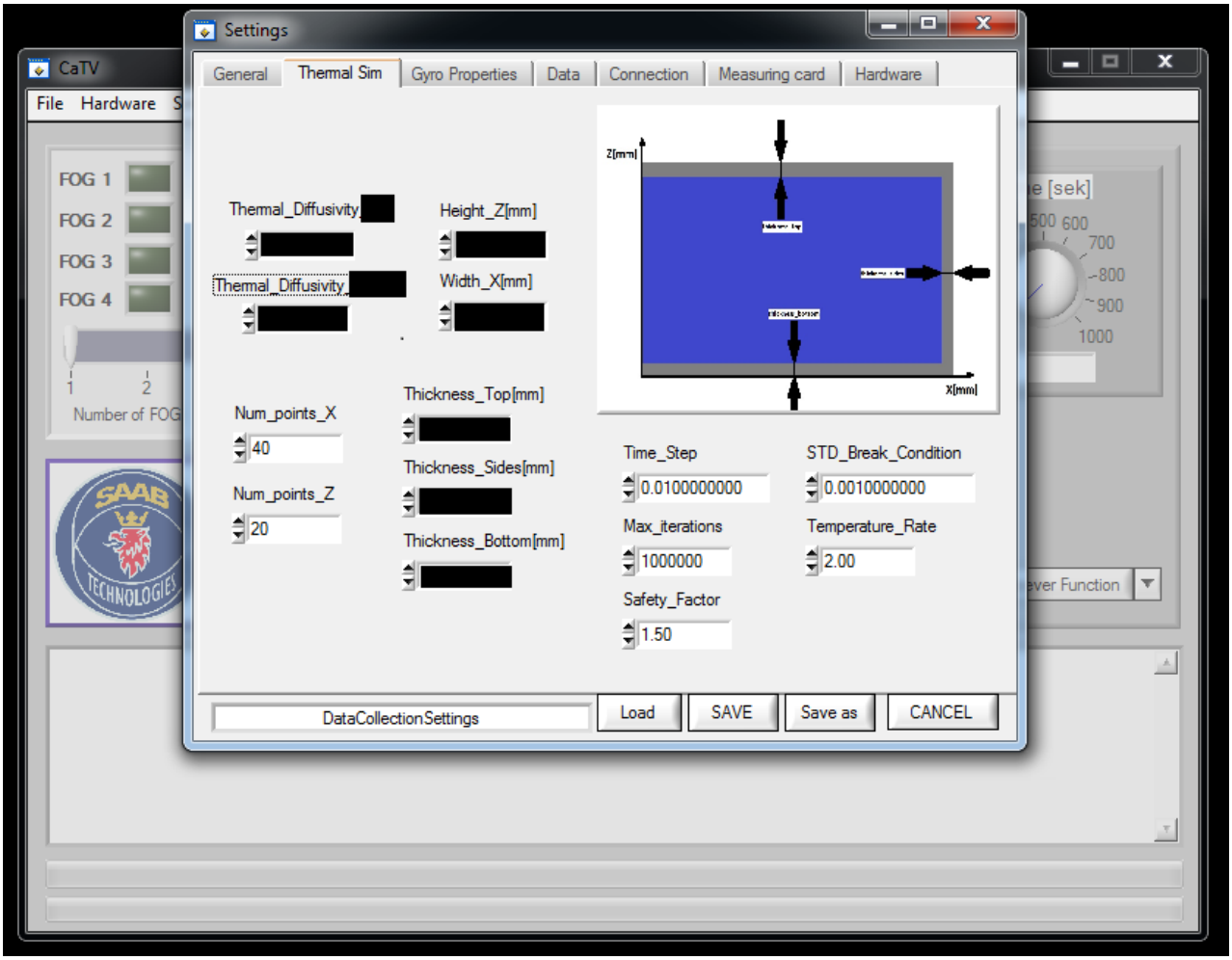


*Figure F.3: Thermal Sim settings panel used for setting thermal simulation parameters*

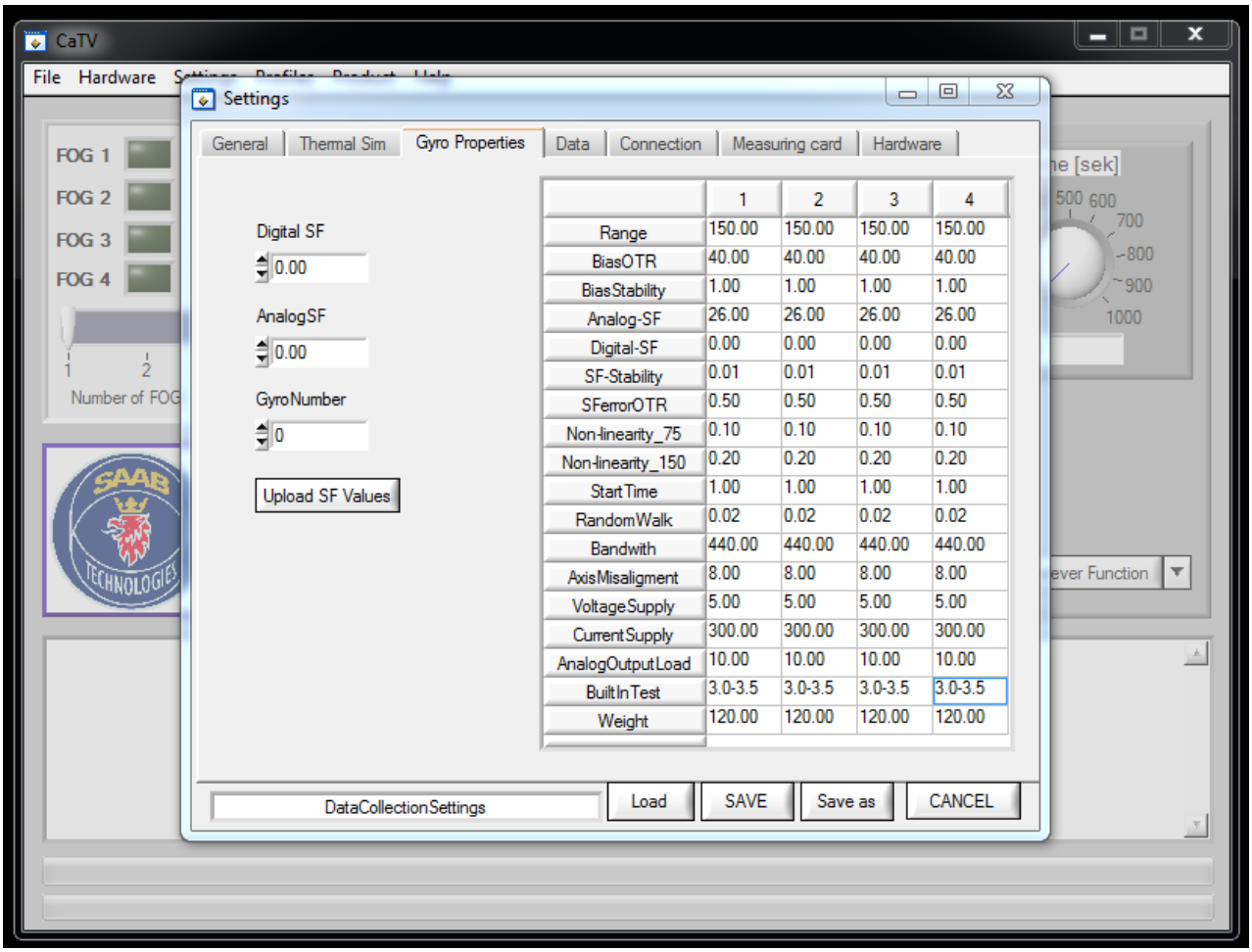


| | 1 | 2 | 3 | 4 |
|---|---|---|---|---|
| Range | 150.00 | 150.00 | 150.00 | 150.00 |
| BiasOTR | 40.00 | 40.00 | 40.00 | 40.00 |
| Bias Stability | 1.00 | 1.00 | 1.00 | 1.00 |
| Analog-SF | 26.00 | 26.00 | 26.00 | 26.00 |
| Digital-SF | 0.00 | 0.00 | 0.00 | 0.00 |
| SF-Stability | 0.01 | 0.01 | 0.01 | 0.01 |
| SFerrorOTR | 0.50 | 0.50 | 0.50 | 0.50 |
| Non-linearity_75 | 0.10 | 0.10 | 0.10 | 0.10 |
| Non-linearity_150 | 0.20 | 0.20 | 0.20 | 0.20 |
| Start Time | 1.00 | 1.00 | 1.00 | 1.00 |
| Random Walk | 0.02 | 0.02 | 0.02 | 0.02 |
| Bandwith | 440.00 | 440.00 | 440.00 | 440.00 |
| Axis Misaligment | 8.00 | 8.00 | 8.00 | 8.00 |
| Voltage Supply | 5.00 | 5.00 | 5.00 | 5.00 |
| Current Supply | 300.00 | 300.00 | 300.00 | 300.00 |
| Analog Output Load | 10.00 | 10.00 | 10.00 | 10.00 |
| Built In Test | 3.0-3.5 | 3.0-3.5 | 3.0-3.5 | 3.0-3.5 |
| Weight | 120.00 | 120.00 | 120.00 | 120.00 |

*Figure F.4: Contains the characteristics of the gyros*

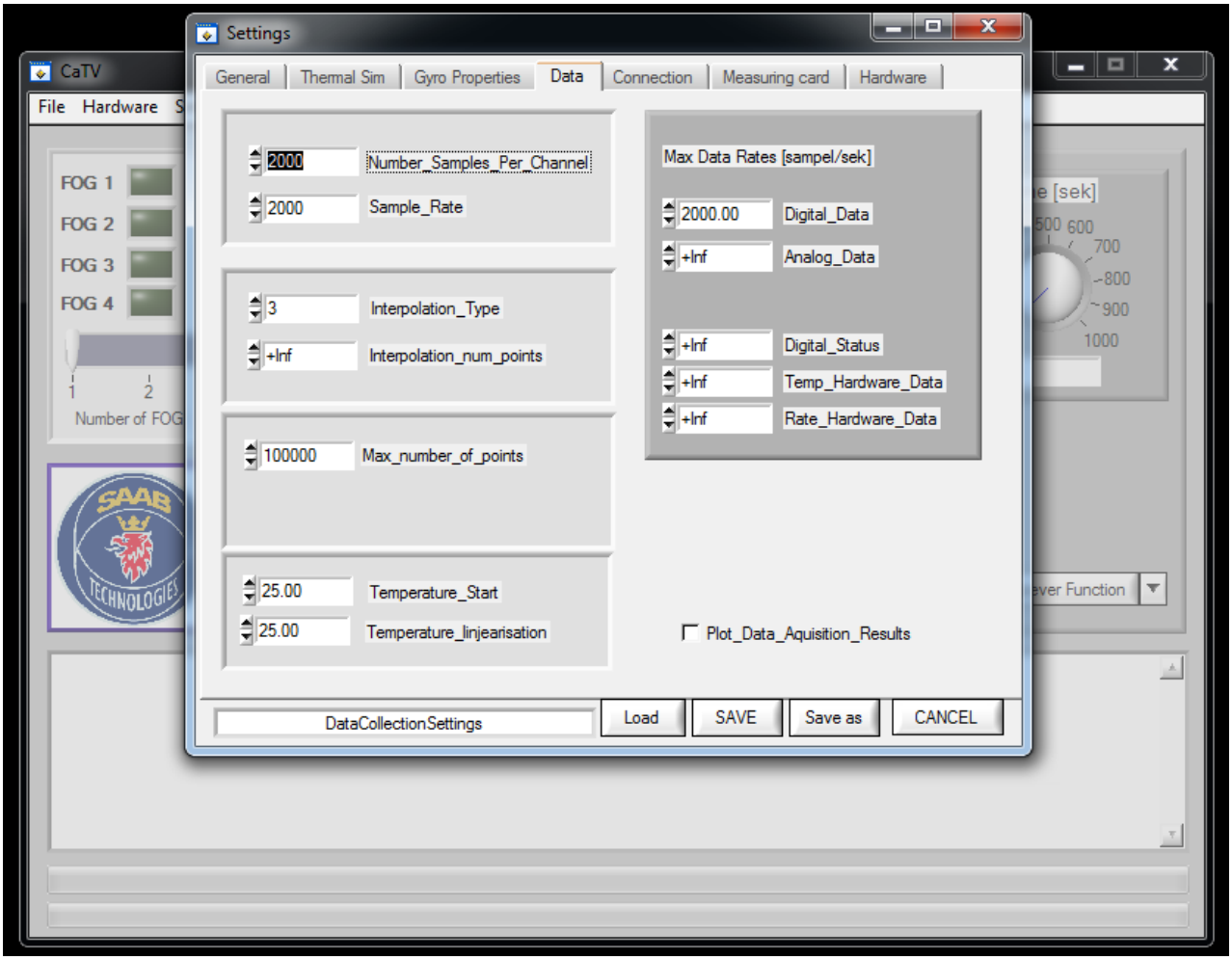


*Figure F.5: Settings for data management*

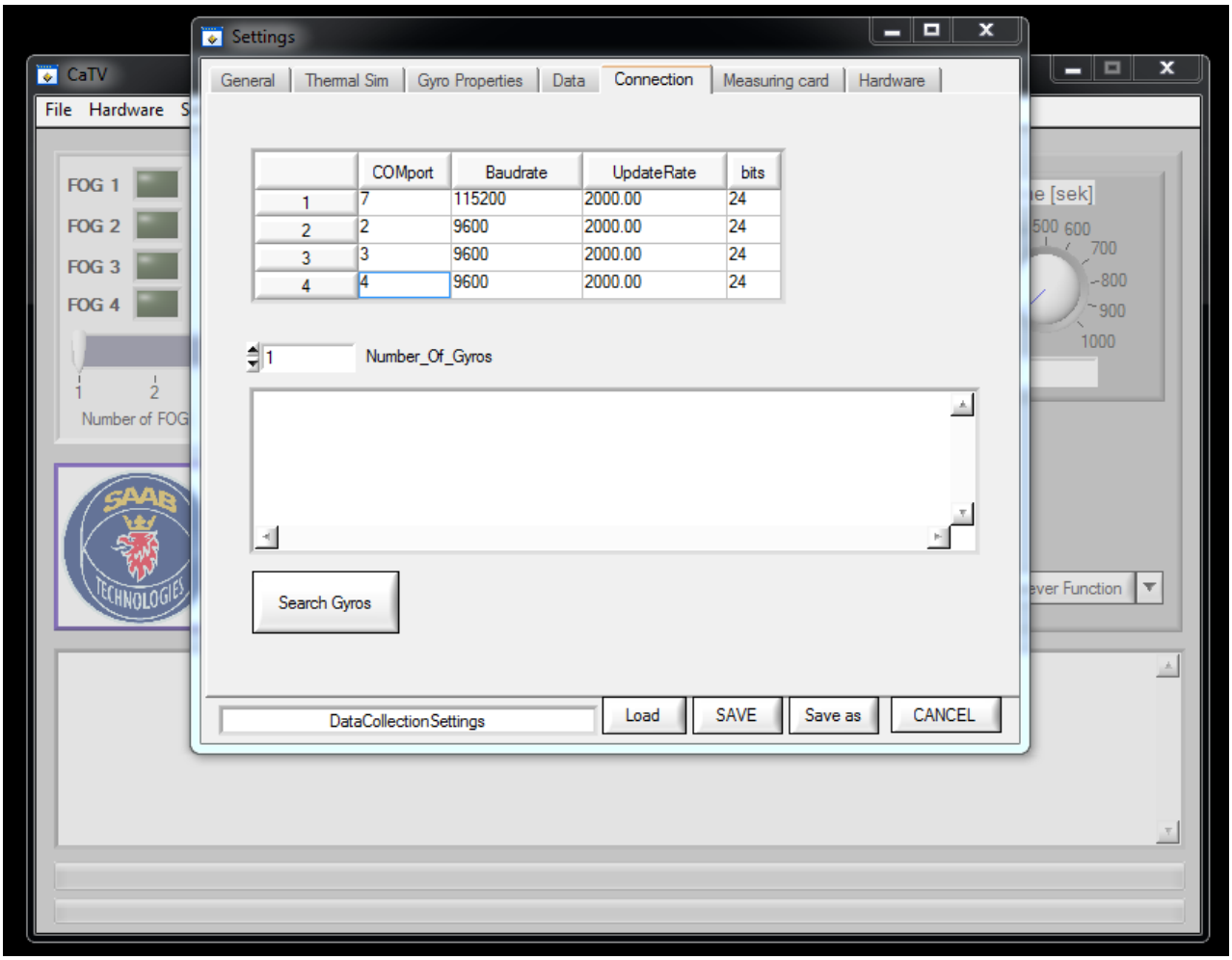


*Figure F.6: Settings for digital connection of gyros with gyro search function*

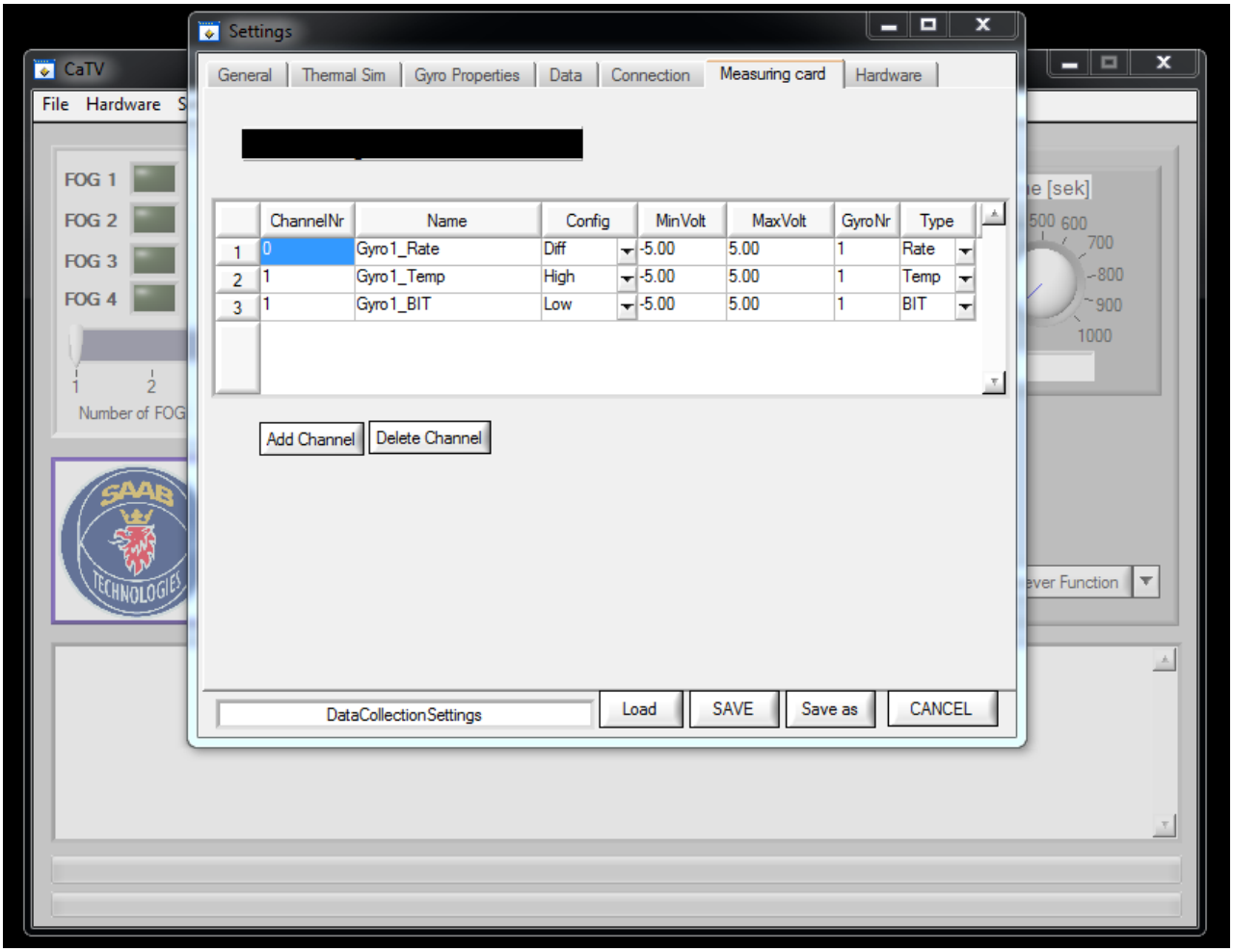


*Figure F.7: Settings for measuring card channels*

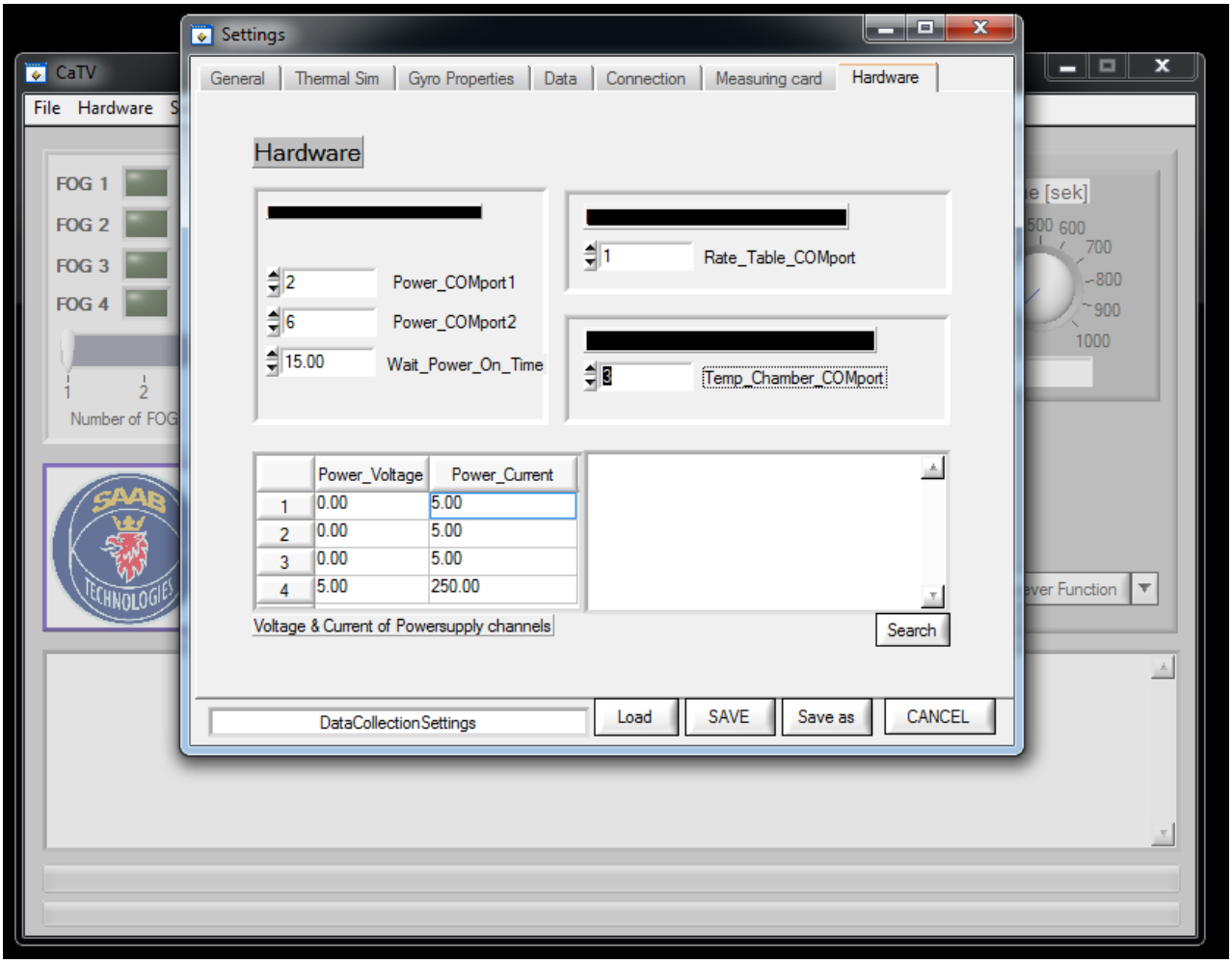


*Figure F.8: Settings for the temperature chamber, power and rotation table*

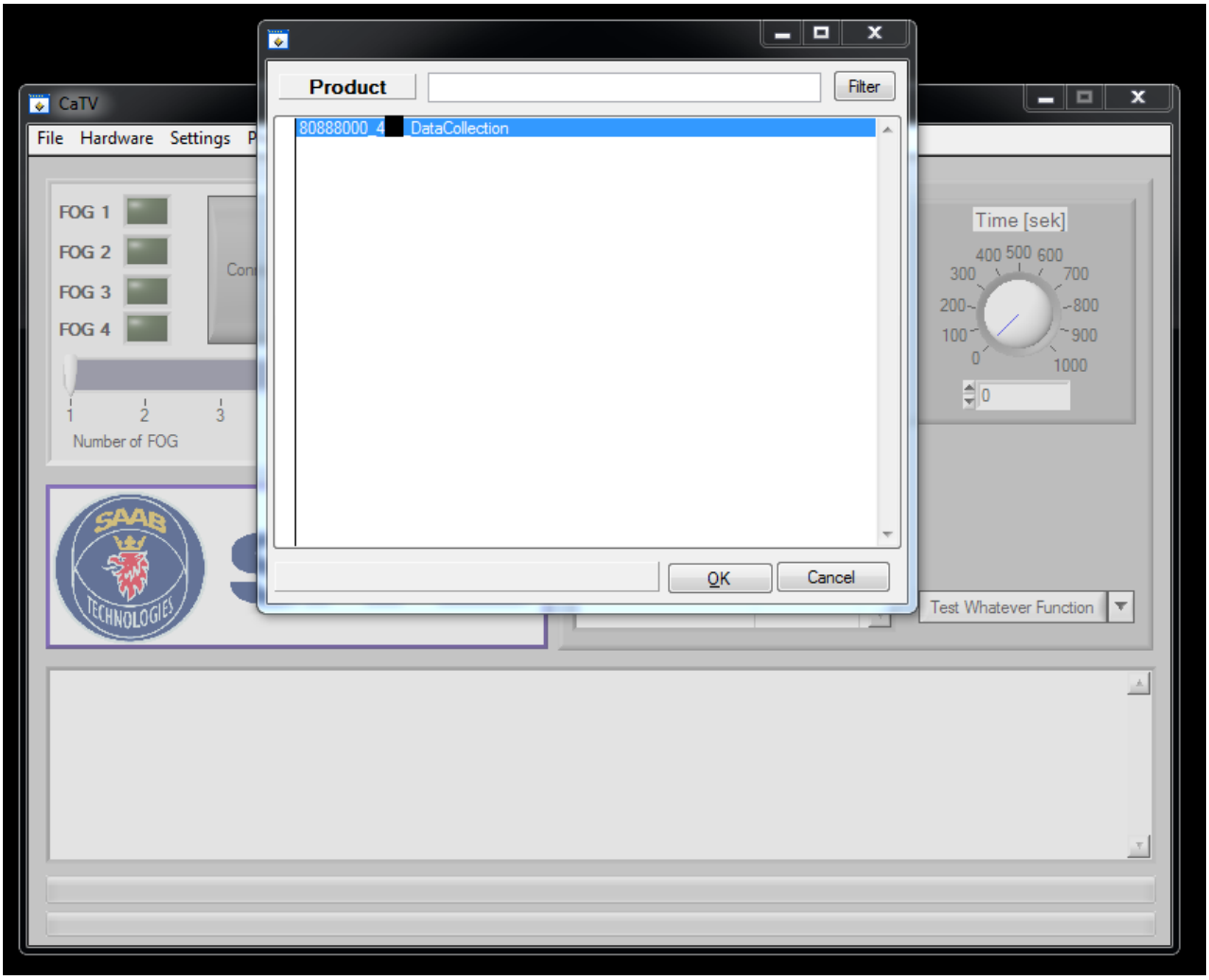


*Figure F.9: Product selection panel where available products are shown*

# G Simulation test results

Simulation 0

| | TotAccuracy | linjAccuracy_D | linjAccuracy_A | SFAccuracy_D | SFAccuracy_A | biasAccuracy_D | biasAccuracy_A |
|---|---|---|---|---|---|---|---|
| 1 | 146429,5525 | 59082,54977 | 59074,23514 | 7541,283648 | 7549,540374 | 6570,202821 | 6611,740775 |
| 2 | 76584,49361 | 1954,865631 | 1954,409837 | 19254,57962 | 19259,88317 | 17082,15884 | 17078,59653 |
| 3 | 72042,47586 | 13963,76284 | 13964,55482 | 7015,327542 | 7015,77713 | 14944,29321 | 15138,76032 |
| 4 | 114372,7437 | 34451,33149 | 34443,24125 | 9051,485553 | 9045,615979 | 13530,09521 | 13850,97418 |
| 5 | 101787,7059 | 52,04138 | 51,880355 | 39096,76212 | 39083,38294 | 11717,4055 | 11786,23361 |
| 6 | 87132,38183 | 24776,38622 | 24769,96434 | 11127,87428 | 11122,08681 | 7787,834175 | 7548,236003 |
| 7 | 65765,60996 | 18546,24234 | 18536,21175 | 6081,114683 | 6082,294667 | 8180,958021 | 8338,788493 |
| 8 | 104695,849 | 17130,29624 | 17126,92152 | 17239,25535 | 17234,53645 | 18253,02678 | 17711,8127 |
| 9 | 66743,65325 | 8690,013481 | 8689,10843 | 16909,78192 | 16914,51411 | 7685,778016 | 7854,457288 |
| 10 | 129373,9026 | 27469,11258 | 27468,55399 | 28597,30207 | 28579,91357 | 8514,110132 | 8744,910301 |

Simulation 1

| | TotAccuracy | linjAccuracy_D | linjAccuracy_A | SFAccuracy_D | SFAccuracy_A | biasAccuracy_D | biasAccuracy_A |
|---|---|---|---|---|---|---|---|
| 1 | 85847,77327 | 368,799352 | 368,80389 | 30304,73126 | 30302,29165 | 12347,56835 | 12155,57877 |
| 2 | 111442,1384 | 18,856533 | 18,99251 | 46320,6311 | 46325,21535 | 9381,968042 | 9376,474886 |
| 3 | 50176,17496 | 4372,031262 | 4372,07905 | 12271,26887 | 12278,92087 | 8424,24232 | 8457,63258 |
| 4 | 41469,71947 | 6014,148302 | 6020,422657 | 2327,992208 | 2324,311332 | 12309,94669 | 12472,89828 |
| 5 | 155820,3976 | 51213,31562 | 51205,49999 | 15879,80107 | 15908,3439 | 10750,52759 | 10862,90941 |
| 6 | 113493,9652 | 14198,43954 | 14196,18233 | 37181,37734 | 37170,7259 | 5311,479246 | 5435,760845 |
| 7 | 70964,7342 | 91,836909 | 91,984966 | 17582,03416 | 17599,77253 | 17911,28179 | 17687,82385 |
| 8 | 68137,87365 | 2109,032814 | 2106,402975 | 24223,89099 | 24205,58739 | 7732,687735 | 7760,271748 |
| 9 | 168834,2559 | 6815,468172 | 6811,103535 | 68743,29165 | 68728,29822 | 8874,538982 | 8861,555352 |
| 10 | 42972,22089 | 2108,987312 | 2107,117891 | 6151,854706 | 6141,864779 | 13262,80858 | 13199,58763 |

Simulation 2

| | TotAccuracy | linjAccuracy_D | linjAccuracy_A | SFAccuracy_D | SFAccuracy_A | biasAccuracy_D | biasAccuracy_A |
|---|---|---|---|---|---|---|---|
| 1 | 18133,65159 | 8975,169742 | 8980,053585 | 51,043552 | 51,049738 | 38,117634 | 38,217338 |
| 2 | 355,156278 | 102,593097 | 101,831379 | 46,590006 | 46,578262 | 28,7861 | 28,777434 |
| 3 | 5221,207186 | 2539,301415 | 2540,990645 | 37,856935 | 37,835445 | 32,626953 | 32,595793 |
| 4 | 416,815248 | 102,264397 | 101,986159 | 37,332837 | 37,327535 | 68,967327 | 68,936992 |
| 5 | 1771,612118 | 772,455667 | 772,227349 | 41,71164 | 41,705241 | 71,744441 | 71,767781 |
| 6 | 121945,3121 | 60809,98285 | 60790,59086 | 36,931689 | 36,933461 | 135,403257 | 135,470036 |
| 7 | 82180,43451 | 40983,58583 | 40984,25016 | 53,089155 | 53,089565 | 53,191134 | 53,228666 |
| 8 | 5271,74418 | 2523,382546 | 2521,455516 | 37,987896 | 37,963127 | 75,493458 | 75,461638 |
| 9 | 60406,45525 | 30081,64526 | 30077,45267 | 57,238961 | 57,239281 | 66,423838 | 66,45525 |
| 10 | 16014,12757 | 7908,307746 | 7913,103324 | 37,042057 | 37,037052 | 59,349312 | 59,288076 |

Simulation 3

| | TotAccuracy | linjAccuracy_D | linjAccuracy_A | SFAccuracy_D | SFAccuracy_A | biasAccuracy_D | biasAccuracy_A |
|---|---|---|---|---|---|---|---|
| 1 | 5175,85024 | 2473,589697 | 2475,939265 | 42,296887 | 42,311955 | 70,868431 | 70,844005 |
| 2 | 66336,07833 | 33087,0341 | 33089,57867 | 35,992249 | 36,004852 | 43,723714 | 43,744736 |
| 3 | 1121,083865 | 502,778667 | 504,573366 | 30,518396 | 30,512331 | 26,354929 | 26,346176 |
| 4 | 22247,65399 | 11032,88744 | 11025,96386 | 42,725394 | 42,749679 | 51,675718 | 51,651898 |
| 5 | 36408,09341 | 18124,55311 | 18131,88199 | 34,558324 | 34,558681 | 41,255353 | 41,285955 |
| 6 | 221,660658 | 30,147669 | 30,161519 | 41,014779 | 41,009092 | 39,641963 | 39,685635 |
| 7 | 21996,64992 | 10941,0565 | 10933,64739 | 31,704494 | 31,705385 | 29,252579 | 29,28357 |
| 8 | 4872,600603 | 2357,561797 | 2358,718355 | 39,089412 | 39,103235 | 39,050483 | 39,077321 |
| 9 | 13098,72893 | 6405,297313 | 6412,516475 | 35,226077 | 35,22245 | 105,279071 | 105,187547 |
| 10 | 52314,16988 | 26070,04605 | 26082,97388 | 41,898101 | 41,886397 | 38,675654 | 38,689792 |

Simulation 4

| | TotAccuracy | linjAccuracy_D | linjAccuracy_A | SFAccuracy_D | SFAccuracy_A | biasAccuracy_D | biasAccuracy_A |
|---|---|---|---|---|---|---|---|
| 1 | 45461,62141 | 22587,7289 | 22583,30302 | 131,912621 | 131,86346 | 13,396684 | 13,416722 |
| 2 | 71986,1359 | 35796,41587 | 35788,80384 | 189,056663 | 189,09872 | 11,364652 | 11,396141 |
| 3 | 8279,131677 | 3916,320119 | 3918,654803 | 215,757162 | 215,752506 | 6,316297 | 6,33079 |
| 4 | 4674,187902 | 2204,24598 | 2204,733327 | 124,01958 | 124,054643 | 8,619025 | 8,515347 |
| 5 | 32516,49948 | 16041,11294 | 16038,64216 | 212,277476 | 212,284135 | 6,088151 | 6,09462 |
| 6 | 1693,476638 | 653,908359 | 653,839549 | 185,121493 | 185,020654 | 7,815378 | 7,771205 |
| 7 | 3563,837789 | 1532,403318 | 1530,974982 | 243,365013 | 243,398495 | 6,854321 | 6,84166 |
| 8 | 126742,7754 | 63221,04097 | 63226,40796 | 143,119434 | 143,105553 | 4,538487 | 4,562991 |
| 9 | 3715,424198 | 1717,929165 | 1718,964229 | 130,624014 | 130,586473 | 8,688757 | 8,63156 |
| 10 | 4898,0003 | 2312,793784 | 2313,22737 | 126,842037 | 126,83651 | 9,154797 | 9,145801 |

Simulation 5

| | TotAccuracy | linjAccuracy_D | linjAccuracy_A | SFAccuracy_D | SFAccuracy_A | biasAccuracy_D | biasAccuracy_A |
|---|---|---|---|---|---|---|---|
| 1 | 6197,970709 | 2539,428677 | 2538,0829 | 145,828533 | 145,853295 | 414,494045 | 414,283258 |
| 2 | 34721,54805 | 12841,05404 | 12836,58761 | 190,283477 | 190,25927 | 4327,709486 | 4335,654175 |
| 3 | 54192,46101 | 25294,54833 | 25296,91947 | 187,382627 | 187,417663 | 1612,827904 | 1613,365021 |
| 4 | 10221,14272 | 3426,508378 | 3418,079708 | 125,59626 | 125,564483 | 1562,70799 | 1562,685901 |
| 5 | 58312,99781 | 25169,5162 | 25158,86822 | 214,490496 | 214,448643 | 3780,933618 | 3774,740636 |
| 6 | 9470,329437 | 3544,516169 | 3543,238949 | 188,791712 | 188,776668 | 1001,75774 | 1003,2482 |
| 7 | 25687,49478 | 8093,427065 | 8088,078078 | 197,133328 | 197,109183 | 4544,593317 | 4567,153811 |
| 8 | 59140,48624 | 27772,01481 | 27774,32633 | 142,178484 | 142,205063 | 1655,049765 | 1654,711788 |
| 9 | 11386,26293 | 5353,682266 | 5359,644531 | 133,260457 | 133,211539 | 203,34785 | 203,116288 |
| 10 | 18507,89569 | 8824,674708 | 8818,468741 | 153,132775 | 153,169899 | 279,253947 | 279,195621 |

Simulation 6

| | TotAccuracy | linjAccuracy_D | linjAccuracy_A | SFAccuracy_D | SFAccuracy_A | biasAccuracy_D | biasAccuracy_A |
|---|---|---|---|---|---|---|---|
| 1 | 10559,27864 | 5013,972871 | 5021,255308 | 147,901629 | 147,928245 | 114,226565 | 113,994021 |
| 2 | 16190,59242 | 7909,845406 | 7903,041065 | 124,102939 | 124,171778 | 64,764506 | 64,666729 |
| 3 | 6416,593674 | 2922,002423 | 2926,027572 | 161,445195 | 161,35654 | 122,811106 | 122,950839 |
| 4 | 99878,94247 | 49727,95735 | 49736,66505 | 110,898098 | 110,907197 | 96,226541 | 96,288235 |
| 5 | 7242,324252 | 3355,200043 | 3351,111598 | 128,889846 | 128,899689 | 139,14573 | 139,077347 |
| 6 | 5728,922098 | 2617,171243 | 2612,799382 | 114,281729 | 114,311565 | 135,2265 | 135,131679 |
| 7 | 9001,427319 | 4272,233601 | 4284,97269 | 151,801821 | 151,796843 | 70,30135 | 70,321014 |
| 8 | 3029,299012 | 1252,12366 | 1250,374014 | 117,816832 | 117,794034 | 145,669164 | 145,521307 |
| 9 | 14184,275 | 6842,052851 | 6843,79457 | 108,820419 | 108,794247 | 140,510837 | 140,302074 |
| 10 | 2913,495596 | 1204,516444 | 1201,402386 | 121,394525 | 121,338327 | 132,480469 | 132,363445 |

Simulation 7

| | TotAccuracy | linjAccuracy_D | linjAccuracy_A | SFAccuracy_D | SFAccuracy_A | biasAccuracy_D | biasAccuracy_A |
|---|---|---|---|---|---|---|---|
| 1 | 17628,32227 | 8623,562159 | 8624,283623 | 93,113843 | 93,137654 | 97,107581 | 97,117411 |
| 2 | 51138,26044 | 25319,49867 | 25321,81933 | 120,995683 | 121,005378 | 127,559097 | 127,382274 |
| 3 | 66383,32149 | 32934,88306 | 32974,57136 | 93,733379 | 93,719595 | 143,291186 | 143,122903 |
| 4 | 64409,04161 | 31988,08656 | 31952,91073 | 100,010569 | 99,956904 | 133,96732 | 134,109519 |
| 5 | 46208,19314 | 22886,50756 | 22853,53633 | 96,36192 | 96,382102 | 137,700394 | 137,704834 |
| 6 | 3417,758656 | 1528,000747 | 1529,791864 | 100,692084 | 100,672813 | 79,337625 | 79,263523 |
| 7 | 31929,15392 | 15770,34367 | 15768,10868 | 95,97444 | 95,974129 | 99,440726 | 99,31227 |
| 8 | 32757,7355 | 16154,82671 | 16162,4154 | 91,051178 | 91,055261 | 129,207093 | 129,179862 |
| 9 | 18492,75863 | 9030,571893 | 9026,133601 | 97,301821 | 97,300619 | 120,62399 | 120,826707 |
| 10 | 4819,621932 | 2191,047626 | 2188,934965 | 89,678417 | 89,684425 | 130,162462 | 130,114037 |

Simulation 8

| | TotAccuracy | linjAccuracy_D | linjAccuracy_A | SFAccuracy_D | SFAccuracy_A | biasAccuracy_D | biasAccuracy_A |
|---|---|---|---|---|---|---|---|
| 1 | 406,275055 | 202,334955 | 202,490566 | 0,721754 | 0,721647 | 0,003489 | 0,002645 |
| 2 | 10856,83482 | 5428,727535 | 5425,828551 | 1,137414 | 1,136783 | 0,00247 | 0,002072 |
| 3 | 1601,9221 | 800,482157 | 800,664166 | 0,384531 | 0,384745 | 0,003484 | 0,003017 |
| 4 | 23711,07942 | 11852,91415 | 11855,10955 | 1,523981 | 1,524355 | 0,004078 | 0,003313 |
| 5 | 81,14011 | 38,906709 | 38,876953 | 1,67234 | 1,671949 | 0,006723 | 0,005437 |
| 6 | 2501,07805 | 1249,52749 | 1250,446505 | 0,549015 | 0,548631 | 0,003424 | 0,002985 |
| 7 | 41856,00447 | 20927,57573 | 20925,75802 | 1,330027 | 1,331759 | 0,004941 | 0,003994 |
| 8 | 20099,94372 | 10049,31751 | 10048,85912 | 0,880489 | 0,879776 | 0,00367 | 0,00315 |
| 9 | 180225,8776 | 90112,14157 | 90111,31857 | 1,205034 | 1,204486 | 0,004326 | 0,003647 |
| 10 | 1718,296241 | 858,74846 | 858,977193 | 0,279133 | 0,278742 | 0,006978 | 0,005734 |

Simulation 9

| | TotAccuracy | linjAccuracy_D | linjAccuracy_A | SFAccuracy_D | SFAccuracy_A | biasAccuracy_D | biasAccuracy_A |
|---|---|---|---|---|---|---|---|
| 1 | 15267,71611 | 7630,014655 | 7632,798489 | 1,500145 | 1,500072 | 0,95517 | 0,947575 |
| 2 | 5487,706112 | 2739,741385 | 2738,073182 | 4,115539 | 4,116134 | 0,832772 | 0,8271 |
| 3 | 20254,03958 | 10125,13205 | 10123,28584 | 1,986002 | 1,987423 | 0,827109 | 0,821159 |
| 4 | 1554,730635 | 774,760819 | 775,400594 | 1,164993 | 1,165107 | 1,126338 | 1,112783 |
| 5 | 42535,36258 | 21261,96773 | 21263,72485 | 3,846686 | 3,848098 | 0,99 | 0,985214 |
| 6 | 3633,787746 | 1812,376463 | 1812,943837 | 3,329511 | 3,330395 | 0,906014 | 0,901526 |
| 7 | 47402,29928 | 23695,72028 | 23689,32457 | 4,279218 | 4,277827 | 4,356245 | 4,341142 |
| 8 | 9982,449881 | 4988,008565 | 4988,393802 | 2,24019 | 2,238441 | 0,785624 | 0,783258 |
| 9 | 2539,20332 | 1264,143469 | 1265,10213 | 4,214485 | 4,212746 | 0,770769 | 0,759721 |
| 10 | 1260,032008 | 621,399451 | 621,494127 | 4,014316 | 4,017238 | 4,576272 | 4,530605 |

Simulation 10

| | TotAccuracy | linjAccuracy_D | linjAccuracy_A | SFAccuracy_D | SFAccuracy_A | biasAccuracy_D | biasAccuracy_A |
|---|---|---|---|---|---|---|---|
| 1 | 6420,867007 | 3142,965139 | 3140,372542 | 28,425536 | 28,414798 | 40,370062 | 40,31893 |
| 2 | 25097,47278 | 12503,05113 | 12494,71429 | 23,288688 | 23,273336 | 26,572209 | 26,573136 |
| 3 | 38396,11507 | 19141,71067 | 19148,51425 | 22,47197 | 22,484062 | 30,505474 | 30,428641 |
| 4 | 108722,4614 | 54315,43647 | 54305,16414 | 26,66607 | 26,649558 | 24,276488 | 24,268682 |
| 5 | 32057,54166 | 15993,44071 | 15996,80751 | 17,62214 | 17,626411 | 16,025135 | 16,019762 |
| 6 | 24255,38868 | 12096,15259 | 12090,6588 | 21,84722 | 21,851374 | 12,435631 | 12,443059 |
| 7 | 37062,81155 | 18496,54732 | 18494,61043 | 20,681728 | 20,681644 | 15,162041 | 15,128395 |
| 8 | 25645,45589 | 12741,38364 | 12741,27975 | 45,585631 | 45,581109 | 35,808485 | 35,81727 |
| 9 | 7457,124272 | 3625,464961 | 3625,915934 | 57,593799 | 57,566377 | 45,299408 | 45,283793 |
| 10 | 31720,32644 | 15809,34152 | 15822,22294 | 21,063431 | 21,062179 | 23,32672 | 23,309644 |

Simulation 11

| | TotAccuracy | linjAccuracy_D | linjAccuracy_A | SFAccuracy_D | SFAccuracy_A | biasAccuracy_D | biasAccuracy_A |
|---|---|---|---|---|---|---|---|
| 1 | 7441,380913 | 3664,978444 | 3660,516535 | 20,483749 | 20,489064 | 37,455921 | 37,457201 |
| 2 | 22741,32997 | 11304,21428 | 11303,80622 | 24,853864 | 24,844617 | 41,815785 | 41,79521 |
| 3 | 3599,587893 | 1638,201774 | 1640,184051 | 22,187526 | 22,188308 | 138,420587 | 138,405646 |
| 4 | 3629,520759 | 1770,2948 | 1769,648092 | 29,564547 | 29,57 | 15,226633 | 15,216688 |
| 5 | 14830,36303 | 7346,24189 | 7351,271306 | 33,256622 | 33,254062 | 33,162145 | 33,177006 |
| 6 | 38714,24027 | 19317,11478 | 19308,09572 | 19,529545 | 19,537045 | 24,987373 | 24,975814 |
| 7 | 4735,472512 | 2274,623574 | 2270,944217 | 22,02305 | 22,034299 | 72,914971 | 72,932401 |
| 8 | 1862,184523 | 833,53795 | 835,31375 | 20,012965 | 20,007465 | 76,676471 | 76,635921 |
| 9 | 14116,8178 | 7020,08733 | 7020,061142 | 24,655736 | 24,651863 | 13,684568 | 13,677162 |
| 10 | 156,918369 | 32,142524 | 32,117828 | 15,727604 | 15,717089 | 30,620129 | 30,593195 |

Simulation 12

| | TotAccuracy | linjAccuracy_D | linjAccuracy_A | SFAccuracy_D | SFAccuracy_A | biasAccuracy_D | biasAccuracy_A |
|---|---|---|---|---|---|---|---|
| 1 | 45294,8636 | 21925,77399 | 21921,91339 | 723,610948 | 723,53869 | 0,014604 | 0,011974 |
| 2 | 30010,76198 | 14243,75783 | 14245,32545 | 760,796893 | 760,863448 | 0,009743 | 0,008617 |
| 3 | 11268,22293 | 4624,875226 | 4625,158192 | 1005,062169 | 1005,047409 | 4,373339 | 3,7066 |
| 4 | 20277,38239 | 9491,899684 | 9496,39736 | 644,4963 | 644,554673 | 0,017975 | 0,016395 |
| 5 | 18699,42985 | 8607,017962 | 8604,697169 | 743,8017 | 743,868274 | 0,02247 | 0,022273 |
| 6 | 130919,7377 | 64702,41492 | 64703,97096 | 756,597377 | 756,620283 | 0,070152 | 0,06401 |
| 7 | 202962,329 | 100773,8641 | 100764,7953 | 711,836598 | 711,785831 | 0,023783 | 0,023378 |
| 8 | 21247,18211 | 9823,755065 | 9826,750501 | 798,30877 | 798,352867 | 0,008019 | 0,006891 |
| 9 | 49339,98584 | 23985,75585 | 23989,64455 | 682,29831 | 682,222832 | 0,034161 | 0,030135 |
| 10 | 22942,27637 | 10664,55965 | 10661,72733 | 807,956808 | 808,006865 | 0,014572 | 0,011152 |

Simulation 13

| | TotAccuracy | linjAccuracy_D | linjAccuracy_A | SFAccuracy_D | SFAccuracy_A | biasAccuracy_D | biasAccuracy_A |
|---|---|---|---|---|---|---|---|
| 1 | 53690,11084 | 26085,21974 | 26081,97619 | 758,803831 | 758,917043 | 2,613526 | 2,580508 |
| 2 | 52383,95704 | 25519,21928 | 25543,90891 | 656,577834 | 656,489856 | 3,901818 | 3,859329 |
| 3 | 153448,3171 | 76090,41635 | 76127,41573 | 612,739885 | 612,880071 | 2,443994 | 2,421046 |
| 4 | 67213,97363 | 32932,67875 | 32938,53547 | 668,097634 | 668,05475 | 3,306972 | 3,300054 |
| 5 | 6844,466638 | 2711,906637 | 2711,860507 | 707,707184 | 707,829263 | 2,590839 | 2,572207 |
| 6 | 8942,726661 | 3627,183072 | 3629,161052 | 840,120013 | 840,243374 | 3,013396 | 3,005753 |
| 7 | 43503,34819 | 20997,7329 | 20991,78172 | 754,333382 | 754,414837 | 2,537087 | 2,548255 |
| 8 | 83357,1936 | 40984,47779 | 40991,42322 | 688,183396 | 688,187469 | 2,481292 | 2,440426 |
| 9 | 68665,31167 | 33567,46854 | 33572,48054 | 758,396709 | 758,414373 | 4,28739 | 4,264111 |
| 10 | 21987,49908 | 10206,11539 | 10205,7463 | 783,012903 | 783,152723 | 4,721249 | 4,750509 |

Simulation 14

| | TotAccuracy | linjAccuracy_D | linjAccuracy_A | SFAccuracy_D | SFAccuracy_A | biasAccuracy_D | biasAccuracy_A |
|---|---|---|---|---|---|---|---|
| 1 | 6498,418905 | 1844,380417 | 1852,337454 | 1307,703838 | 1307,65964 | 93,229738 | 93,107816 |
| 2 | 15572,65251 | 6108,906243 | 6107,741821 | 1637,456707 | 1637,514059 | 40,558563 | 40,475118 |
| 3 | 104895,5964 | 50218,25699 | 50153,13439 | 2188,182845 | 2187,930873 | 74,09626 | 73,995061 |
| 4 | 15475,72754 | 6257,004094 | 6251,71355 | 1446,859684 | 1446,421469 | 36,934987 | 36,793753 |
| 5 | 38095,80958 | 17716,90872 | 17722,2137 | 1262,477763 | 1261,757025 | 66,356372 | 66,095987 |
| 6 | 16561,41748 | 5417,356473 | 5429,581022 | 2826,689899 | 2828,785388 | 29,5454 | 29,459294 |
| 7 | 13891,95102 | 5019,139828 | 5019,157684 | 1780,596335 | 1780,31266 | 146,356434 | 146,388074 |
| 8 | 52153,97348 | 23206,30951 | 23195,62934 | 2788,318221 | 2787,620451 | 87,999736 | 88,096217 |
| 9 | 104906,8783 | 50834,50384 | 50755,41896 | 1609,147577 | 1609,450254 | 49,203017 | 49,154631 |
| 10 | 64946,527 | 31433,01253 | 31344,97691 | 1053,391148 | 1053,336805 | 30,957958 | 30,851646 |

Simulation 15

| | TotAccuracy | linjAccuracy_D | linjAccuracy_A | SFAccuracy_D | SFAccuracy_A | biasAccuracy_D | biasAccuracy_A |
|---|---|---|---|---|---|---|---|
| 1 | 195276,9706 | 96179,44886 | 96195,45616 | 1406,674311 | 1407,40347 | 44,050748 | 43,937076 |
| 2 | 4244382,806 | 6711,19421 | 6716,710358 | 2115389,7 | 2115390,312 | 87,44248 | 87,446937 |
| 3 | 15149,6504 | 6278,064676 | 6282,901637 | 1263,559436 | 1263,667116 | 30,732506 | 30,72503 |
| 4 | 9312,446706 | 3299,258481 | 3299,081675 | 1211,024445 | 1211,015031 | 146,139159 | 145,927914 |
| 5 | 1309946,527 | 12320,76866 | 12317,15421 | 642601,4616 | 642595,9708 | 55,633254 | 55,53881 |
| 6 | 9732,91528 | 2256,653668 | 2253,019789 | 2476,540745 | 2477,684168 | 134,777009 | 134,239902 |
| 7 | 1158220,547 | 2468,5918 | 2469,584291 | 576590,0262 | 576590,7612 | 50,81836 | 50,765594 |
| 8 | 1830114,054 | 14549,97387 | 14538,1397 | 900450,1297 | 900450,3243 | 62,937187 | 62,54892 |
| 9 | 394456,9767 | 58246,07728 | 58261,74772 | 138938,3999 | 138937,8574 | 36,501906 | 36,392496 |
| 10 | 357923,8075 | 56739,21262 | 56779,16315 | 122173,004 | 122171,946 | 30,335158 | 30,146474 |

Simulation 16

| | TotAccuracy | linjAccuracy_D | linjAccuracy_A | SFAccuracy_D | SFAccuracy_A | biasAccuracy_D | biasAccuracy_A |
|---|---|---|---|---|---|---|---|
| 1 | 2666884,355 | 67772,40332 | 67866,67949 | 186489,5267 | 186480,2095 | 1079164,93 | 1079110,606 |
| 2 | 967690,1032 | 319846,4851 | 320075,7794 | 163513,6683 | 163518,028 | 367,493769 | 368,648585 |
| 3 | 916073,6898 | 297825,3404 | 297983,6366 | 159975,2089 | 159971,8904 | 158,685579 | 158,927906 |
| 4 | 653868,0837 | 155668,9342 | 155849,6551 | 170865,5819 | 170873,0617 | 305,385385 | 305,465517 |
| 5 | 2174939,847 | 918152,1168 | 917853,9128 | 169205,4734 | 169206,2316 | 260,947592 | 261,164945 |
| 6 | 822985,5849 | 205181,9515 | 205270,9752 | 205430,5252 | 205451,0364 | 825,793743 | 825,302874 |
| 7 | 770455,7331 | 198586,2845 | 198616,4791 | 186566,3281 | 186530,8608 | 77,786886 | 77,993641 |
| 8 | 808628,9257 | 239104,5783 | 239048,7339 | 164651,5528 | 164670,9638 | 576,358101 | 576,738803 |
| 9 | 897423,5547 | 281603,0347 | 281402,0343 | 166594,8935 | 166610,7184 | 606,479683 | 606,39403 |
| 10 | 2181081,852 | 948888,8845 | 948587,4175 | 141717,7205 | 141727,819 | 80,055666 | 79,955305 |

Simulation 17

| | TotAccuracy | linjAccuracy_D | linjAccuracy_A | SFAccuracy_D | SFAccuracy_A | biasAccuracy_D | biasAccuracy_A |
|---|---|---|---|---|---|---|---|
| 1 | 752749,8131 | 198854,9991 | 198605,5199 | 177132,3169 | 177136,482 | 509,852458 | 510,642779 |
| 2 | 3092993,524 | 366321,6525 | 366393,6039 | 154840,0088 | 154835,8912 | 1025298,708 | 1025303,66 |
| 3 | 3123892,022 | 362820,642 | 362523,1773 | 182087,6999 | 182086,1163 | 1017188,611 | 1017185,775 |
| 4 | 3462766,683 | 558637,0351 | 558435,1707 | 203050,5182 | 203041,262 | 969822,8372 | 969779,8602 |
| 5 | 1056424,049 | 360934,2221 | 361169,5805 | 166192,6838 | 166200,9643 | 963,680502 | 962,917416 |
| 6 | 745272,6309 | 196238,3302 | 196420,9889 | 174640,7046 | 174650,9667 | 1660,99189 | 1660,648592 |
| 7 | 1018928,233 | 308824,4987 | 308615,3831 | 200033,9827 | 200018,7151 | 717,956113 | 717,696979 |
| 8 | 3235525,877 | 282153,6865 | 282270,3162 | 195119,04 | 195117,9973 | 1140422,691 | 1140442,146 |
| 9 | 1616213,561 | 46805,70904 | 46763,575 | 222352,6979 | 222366,3863 | 538959,8882 | 538965,3044 |
| 10 | 514028,5023 | 87541,08666 | 87359,94879 | 168842,6539 | 168850,8281 | 716,707678 | 717,277154 |

Simulation 18

| | TotAccuracy | linjAccuracy_D | linjAccuracy_A | SFAccuracy_D | SFAccuracy_A | biasAccuracy_D | biasAccuracy_A |
|---|---|---|---|---|---|---|---|
| 1 | 3198398,48 | 423343,9153 | 423674,0436 | 225308,5874 | 225308,2574 | 950417,0846 | 950346,5915 |
| 2 | 1128048,646 | 360691,0283 | 361150,6914 | 181341,618 | 181324,2342 | 21767,63796 | 21773,43594 |
| 3 | 751118,8053 | 168564,4592 | 168767,7909 | 196053,7375 | 196060,562 | 10835,80346 | 10836,45221 |
| 4 | 1004167,252 | 302729,1168 | 302892,2616 | 184926,1063 | 184914,4077 | 14351,59241 | 14353,76689 |
| 5 | 1761719,334 | 692110,3592 | 692417,2166 | 177474,2607 | 177470,5955 | 11124,74716 | 11122,15455 |
| 6 | 1443585,503 | 506625,4912 | 506709,4463 | 204819,0171 | 204816,4501 | 10306,23466 | 10308,86348 |
| 7 | 3571353,66 | 269274,4248 | 268991,8714 | 197274,3682 | 197269,513 | 1319277,717 | 1319265,766 |
| 8 | 1954557,96 | 781001,9895 | 781296,6787 | 170362,934 | 170366,3847 | 25762,11999 | 25767,85272 |
| 9 | 1588312,336 | 565972,1227 | 565755,6583 | 219990,5897 | 219983,1808 | 8303,457601 | 8307,326695 |
| 10 | 1434657,477 | 515828,6631 | 515713,4908 | 185285,3269 | 185268,2371 | 16280,50729 | 16281,25189 |

Simulation 19

| | TotAccuracy | linjAccuracy_D | linjAccuracy_A | SFAccuracy_D | SFAccuracy_A | biasAccuracy_D | biasAccuracy_A |
|---|---|---|---|---|---|---|---|
| 1 | 978371,4865 | 387544,7155 | 387224,3082 | 101291,2769 | 101299,9849 | 505,559133 | 505,641812 |
| 2 | 1646929,471 | 725789,0077 | 725852,365 | 97220,56247 | 97220,17103 | 423,387277 | 423,977178 |
| 3 | 495032,6293 | 142522,8563 | 142585,345 | 104722,8355 | 104707,6836 | 246,75462 | 247,154281 |
| 4 | 1985726,787 | 885114,1244 | 885149,4913 | 104359,8039 | 104366,5079 | 3368,19132 | 3368,668625 |
| 5 | 860002,7553 | 327164,0108 | 326909,683 | 102099,6546 | 102095,6405 | 866,768245 | 866,998306 |
| 6 | 947626,9362 | 349840,7107 | 349704,9982 | 123671,268 | 123661,4712 | 374,201223 | 374,286839 |
| 7 | 987419,1386 | 394778,0907 | 395031,4899 | 97822,25563 | 97819,19168 | 983,680913 | 984,429832 |
| 8 | 512223,9144 | 143820,3657 | 143701,3559 | 112033,4524 | 112026,0807 | 321,041874 | 321,617865 |
| 9 | 1172375,298 | 493617,2471 | 493494,3956 | 91386,57912 | 91382,72147 | 1247,548371 | 1246,806189 |
| 10 | 2069987,749 | 935047,0691 | 934790,034 | 97186,39029 | 97182,71919 | 2891,63999 | 2889,896722 |

Simulation 20

| | TotAccuracy | linjAccuracy_D | linjAccuracy_A | SFAccuracy_D | SFAccuracy_A | biasAccuracy_D | biasAccuracy_A |
|---|---|---|---|---|---|---|---|
| 1 | 4268462,766 | 316773,916 | 316674,3353 | 138575,5613 | 138575,9073 | 1678936,435 | 1678926,611 |
| 2 | 1849501,758 | 826016,6702 | 825970,1983 | 96140,25209 | 96129,04052 | 2623,450344 | 2622,146632 |
| 3 | 533686,833 | 161808,5957 | 161880,0424 | 102041,5264 | 102036,9708 | 2959,574059 | 2960,123655 |
| 4 | 1305196,233 | 533043,5415 | 533138,6761 | 114420,2317 | 114419,9878 | 5086,978717 | 5086,817352 |
| 5 | 962618,5686 | 374627,8698 | 374212,6103 | 101173,5427 | 101179,2668 | 5712,762236 | 5712,516752 |
| 6 | 1375207,504 | 585001,2462 | 585103,9029 | 100795,3992 | 100799,471 | 1753,690826 | 1753,79389 |
| 7 | 565184,327 | 180179,522 | 180332,4792 | 100441,8655 | 100450,9142 | 1889,223039 | 1890,323098 |
| 8 | 1547674,784 | 674352,8317 | 674603,2697 | 96959,7717 | 96956,13339 | 2401,784978 | 2400,992264 |
| 9 | 737459,0634 | 260165,152 | 260243,5599 | 106050,7513 | 106044,9154 | 2477,255603 | 2477,429282 |
| 10 | 1270502,691 | 527549,1079 | 527499,5892 | 106148,9343 | 106150,7845 | 1577,403288 | 1576,872293 |

Simulation 21

| | TotAccuracy | linjAccuracy_D | linjAccuracy_A | SFAccuracy_D | SFAccuracy_A | biasAccuracy_D | biasAccuracy_A |
|---|---|---|---|---|---|---|---|
| 1 | 5501120,63 | 405465,0453 | 405826,6161 | 178718,539 | 178719,7629 | 2166201,553 | 2166189,114 |
| 2 | 917280,1567 | 303912,0038 | 303804,0006 | 136723,2658 | 136719,9222 | 18065,70099 | 18055,26342 |
| 3 | 1041345,624 | 377484,158 | 377577,7739 | 118499,92 | 118500,0976 | 24640,55531 | 24643,11956 |
| 4 | 1326773,515 | 520925,8026 | 520568,905 | 129211,3848 | 129209,7663 | 13429,42358 | 13428,23306 |
| 5 | 1958132,989 | 825267,9558 | 825185,8495 | 109859,1171 | 109855,8347 | 43981,80654 | 43982,42527 |
| 6 | 2397699,973 | 1017237,679 | 1017120,73 | 128874,5447 | 128871,5492 | 52797,10272 | 52798,36801 |
| 7 | 7635473,68 | 593332,7824 | 593216,8864 | 178498,2144 | 178488,251 | 3045950,998 | 3045986,548 |
| 8 | 1122255,023 | 422360,3156 | 422597,6321 | 124634,7378 | 124630,8685 | 14014,3099 | 14017,15894 |
| 9 | 634471,5889 | 189120,8239 | 189347,8632 | 116402,0963 | 116400,7344 | 11599,01505 | 11601,05597 |
| 10 | 2103366,63 | 904506,3344 | 904490,0487 | 124188,5477 | 124184,2223 | 22997,28096 | 23000,19604 |

Simulation 22

| | TotAccuracy | linjAccuracy_D | linjAccuracy_A | SFAccuracy_D | SFAccuracy_A | biasAccuracy_D | biasAccuracy_A |
|---|---|---|---|---|---|---|---|
| 1 | 3223191,985 | 419247,8697 | 419429,5135 | 226962,0921 | 226953,3318 | 965287,392 | 965311,786 |
| 2 | 3073693,77 | 1167103,779 | 1167055,03 | 364565,6786 | 364569,3662 | 5198,988311 | 5200,928121 |
| 3 | 2906414,056 | 275899,2296 | 275857,1237 | 256469,6704 | 256470,2538 | 920859,7707 | 920858,0077 |
| 4 | 462958,1139 | 85358,6263 | 85460,99927 | 142255,8191 | 142256,6657 | 3813,482839 | 3812,520655 |
| 5 | 3606278,973 | 488134,0818 | 488143,2856 | 235074,4787 | 235072,5767 | 1079926,36 | 1079928,19 |
| 6 | 3018334,661 | 344989,5076 | 344762,2645 | 223901,3105 | 223904,0398 | 940386,1149 | 940391,4236 |
| 7 | 1154832,451 | 432174,4809 | 432064,8725 | 141332,085 | 141328,2113 | 3966,494728 | 3966,306641 |
| 8 | 1067302,916 | 394199,9483 | 394333,612 | 134437,916 | 134435,8605 | 4947,822697 | 4947,756219 |
| 9 | 2163275,623 | 677975,3562 | 678098,22 | 397914,2487 | 397908,8128 | 5690,292839 | 5688,69254 |
| 10 | 1987056,861 | 846927,4108 | 846883,5703 | 143205,846 | 143198,8822 | 3420,09203 | 3421,059876 |

Simulation 23

| | TotAccuracy | linjAccuracy_D | linjAccuracy_A | SFAccuracy_D | SFAccuracy_A | biasAccuracy_D | biasAccuracy_A |
|---|---|---|---|---|---|---|---|
| 1 | 3414720,939 | 152336,6116 | 152348,2052 | 306345,5491 | 306342,5775 | 1248669,851 | 1248678,145 |
| 2 | 3041343,02 | 253788,3083 | 253800,6736 | 305339,3954 | 305334,5425 | 961536,2966 | 961543,8035 |
| 3 | 2739474,259 | 115956,1509 | 115961,3584 | 294945,9797 | 294945,9827 | 958828,8386 | 958835,9487 |
| 4 | 3870744,675 | 388448,479 | 388351,7547 | 282002,79 | 282000,2307 | 1264973,091 | 1264968,33 |
| 5 | 2648976,785 | 126925,3265 | 126896,4427 | 275614,7626 | 275604,6764 | 921971,159 | 921964,4175 |
| 6 | 2585747,683 | 141139,1146 | 141100,7078 | 273557,6294 | 273554,0375 | 878212,5168 | 878183,6775 |
| 7 | 2740463,347 | 108187,6202 | 108253,1053 | 324034,8053 | 324037,8746 | 937978,121 | 937971,8208 |
| 8 | 3307027,833 | 1509488,901 | 1509712,82 | 140090,1022 | 140086,5332 | 3824,848631 | 3824,627782 |
| 9 | 3158314,975 | 155158,0316 | 155187,6642 | 280020,6466 | 280017,5046 | 1143965,424 | 1143965,704 |
| 10 | 2059737,612 | 130643,2128 | 130625,49 | 332859,0782 | 332867,5219 | 566378,0125 | 566364,2967 |

Simulation 24

| | TotAccuracy | linjAccuracy_D | linjAccuracy_A | SFAccuracy_D | SFAccuracy_A | biasAccuracy_D | biasAccuracy_A |
|---|---|---|---|---|---|---|---|
| 1 | 2582445,432 | 245843,1336 | 245712,4302 | 340440,9895 | 340439,1606 | 705005,1371 | 705004,5808 |
| 2 | 3839117,554 | 333462,523 | 333367,0384 | 288856,8573 | 288851,7011 | 1297304,94 | 1297274,494 |
| 3 | 3042962,81 | 257025,7041 | 257063,9723 | 307590,7656 | 307589,4625 | 956862,0304 | 956830,8748 |
| 4 | 2593484,895 | 75247,03485 | 75251,46209 | 274765,5172 | 274762,9119 | 946731,2914 | 946726,678 |
| 5 | 3198917,625 | 189504,8799 | 189494,5206 | 293859,9078 | 293860,1557 | 1116098,65 | 1116099,511 |
| 6 | 3399244,054 | 302115,9654 | 302112,3418 | 297710,0685 | 297714,5364 | 1099794,793 | 1099796,35 |
| 7 | 3459014,948 | 202410,2907 | 202398,9151 | 277923,6357 | 277922,3858 | 1249184,974 | 1249174,747 |
| 8 | 3487837,433 | 463470,3432 | 463424,2488 | 291693,7048 | 291694,9642 | 988775,187 | 988778,9845 |
| 9 | 4425280,833 | 719055,7233 | 718918,3712 | 314996,878 | 315001,1374 | 1178642,102 | 1178666,621 |
| 10 | 2736042,793 | 162241,6661 | 162206,6326 | 298059,8134 | 298059,153 | 907741,3432 | 907734,1845 |

Simulation 25

| | TotAccuracy | linjAccuracy_D | linjAccuracy_A | SFAccuracy_D | SFAccuracy_A | biasAccuracy_D | biasAccuracy_A |
|---|---|---|---|---|---|---|---|
| 1 | 18475008,97 | 1798827,968 | 1798963,673 | 85298,1572 | 85294,01918 | 7353328,76 | 7353296,393 |
| 2 | 2062866,391 | 971498,0124 | 971694,4903 | 55146,87836 | 55147,76806 | 4689,477968 | 4689,764145 |
| 3 | 1322165,939 | 568134,7456 | 568283,6237 | 78311,72832 | 78314,06433 | 14560,89014 | 14560,88668 |
| 4 | 4118610,317 | 1901252,987 | 1901290,734 | 130342,1471 | 130344,1467 | 27688,47832 | 27691,82371 |
| 5 | 4066168,858 | 1938255,68 | 1938419,701 | 64648,27402 | 64647,36498 | 30098,03728 | 30099,8006 |
| 6 | 23840867,57 | 623592,958 | 623652,8823 | 212255,3955 | 212254,2993 | 11084597,76 | 11084514,28 |
| 7 | 4222358,942 | 2031994,982 | 2032268,064 | 59455,63136 | 59456,65186 | 19589,54676 | 19594,06638 |
| 8 | 10023919,33 | 971767,1788 | 971773,4394 | 108322,4805 | 108322,6539 | 3931883,52 | 3931850,06 |
| 9 | 15119814,12 | 986147,438 | 986306,9517 | 102534,6451 | 102533,2577 | 6471117,213 | 6471174,617 |
| 10 | 1268689,757 | 479375,6792 | 479709,7189 | 138510,612 | 138508,1442 | 16293,78796 | 16291,81432 |

Simulation 26

| | TotAccuracy | linjAccuracy_D | linjAccuracy_A | SFAccuracy_D | SFAccuracy_A | biasAccuracy_D | biasAccuracy_A |
|---|---|---|---|---|---|---|---|
| 1 | 653813,6869 | 174724,7351 | 174690,582 | 135262,7446 | 135263,9958 | 16936,31185 | 16935,31755 |
| 2 | 8845812,158 | 893910,2015 | 894096,9032 | 97238,34856 | 97235,66026 | 3431654,423 | 3431676,621 |
| 3 | 12067214,73 | 476584,1612 | 476660,317 | 199045,7916 | 199046,1889 | 5357922,14 | 5357956,128 |
| 4 | 2862675,308 | 1261276,767 | 1261093,914 | 152328,5134 | 152326,1583 | 17824,2666 | 17825,68876 |
| 5 | 2314242,44 | 1078880,043 | 1078882,269 | 61722,02367 | 61722,40769 | 16518,9546 | 16516,74234 |
| 6 | 2853692,59 | 1277666,317 | 1277780,738 | 123753,8924 | 123753,198 | 25369,66649 | 25368,77745 |
| 7 | 2113481,745 | 888192,5181 | 888599,6717 | 137573,0704 | 137568,8097 | 30772,9828 | 30774,69192 |
| 8 | 13666469,22 | 1063519,828 | 1063608,836 | 170055,551 | 170053,035 | 5599589,427 | 5599642,545 |
| 9 | 8734317,602 | 256133,6922 | 256254,3539 | 119469,9614 | 119468,6194 | 3991495,418 | 3991495,558 |
| 10 | 2029672,39 | 856738,3248 | 857075,5034 | 126371,0166 | 126368,6477 | 31557,07164 | 31561,82584 |

Simulation 27

| | TotAccuracy | linjAccuracy_D | linjAccuracy_A | SFAccuracy_D | SFAccuracy_A | biasAccuracy_D | biasAccuracy_A |
|---|---|---|---|---|---|---|---|
| 1 | 1614929,905 | 571551,1165 | 571685,4724 | 162628,0096 | 162635,0278 | 73220,1726 | 73210,10616 |
| 2 | 11735672,56 | 1493878,766 | 1493265,492 | 105822,9728 | 105823,0259 | 4268428,071 | 4268454,229 |
| 3 | 9238740,641 | 339241,8075 | 339233,5306 | 214589,87 | 214594,2081 | 4065552,413 | 4065528,812 |
| 4 | 12630611,26 | 1261177,682 | 1261536,652 | 190408,3426 | 190403,4026 | 4863500,726 | 4863584,455 |
| 5 | 14415233,15 | 1006110,43 | 1006328,111 | 190925,2204 | 190926,5441 | 6010504,453 | 6010438,389 |
| 6 | 25632642,23 | 540991,3255 | 541205,4113 | 239407,9034 | 239408,0316 | 12035806,69 | 12035822,87 |
| 7 | 708506,8597 | 134589,9773 | 134653,6831 | 167311,6612 | 167308,6511 | 52323,12583 | 52319,7611 |
| 8 | 13530759,31 | 1721340,08 | 1721131,879 | 108901,637 | 108898,2772 | 4935242,174 | 4935245,266 |
| 9 | 11876518,64 | 877632,5078 | 877563,9444 | 175199,7342 | 175204,699 | 4885425,474 | 4885492,281 |
| 10 | 9406429,532 | 819015,0142 | 818361,5175 | 112547,1915 | 112547,3457 | 3771984,056 | 3771974,407 |

Simulation 28

| | TotAccuracy | linjAccuracy_D | linjAccuracy_A | SFAccuracy_D | SFAccuracy_A | biasAccuracy_D | biasAccuracy_A |
|---|---|---|---|---|---|---|---|
| 1 | 516,508444 | 135,9136 | 135,91348 | 121,702841 | 121,717703 | 0,628102 | 0,632718 |
| 2 | 1422,505016 | 564,117203 | 564,073405 | 146,288555 | 146,309496 | 0,855795 | 0,860562 |
| 3 | 4405,573521 | 2050,240707 | 2050,383448 | 151,625732 | 151,626791 | 0,84438 | 0,852463 |
| 4 | 8495,548431 | 4063,9758 | 4063,842527 | 183,111732 | 183,080951 | 0,770748 | 0,766672 |
| 5 | 3117,244511 | 1396,800052 | 1396,003703 | 161,394717 | 161,365694 | 0,837344 | 0,843001 |
| 6 | 86426,94347 | 43107,17845 | 43107,11345 | 106,07813 | 106,066514 | 0,251224 | 0,255708 |
| 7 | 30551,85021 | 15137,4394 | 15137,02655 | 138,276454 | 138,252801 | 0,427968 | 0,427045 |
| 8 | 21190,0245 | 10495,93496 | 10496,71381 | 98,178804 | 98,171132 | 0,51181 | 0,513987 |
| 9 | 1559,920964 | 652,376824 | 652,260879 | 126,931448 | 126,922339 | 0,719024 | 0,710452 |
| 10 | 2786,911469 | 1283,038305 | 1283,297634 | 109,748361 | 109,732497 | 0,55117 | 0,543502 |

Simulation 29

| | TotAccuracy | linjAccuracy_D | linjAccuracy_A | SFAccuracy_D | SFAccuracy_A | biasAccuracy_D | biasAccuracy_A |
|---|---|---|---|---|---|---|---|
| 1 | 10290,57765 | 5119,823427 | 5118,27227 | 26,226572 | 26,232317 | 0,012736 | 0,01033 |
| 2 | 43160,80417 | 21545,79051 | 21548,41038 | 33,293812 | 33,272919 | 0,019624 | 0,016934 |
| 3 | 110740,7613 | 55341,01312 | 55339,84196 | 29,942085 | 29,957133 | 0,003586 | 0,0034 |
| 4 | 18639,84674 | 9292,036096 | 9294,044587 | 26,878605 | 26,859361 | 0,015123 | 0,012968 |
| 5 | 21941,05578 | 10944,65366 | 10942,92432 | 26,714649 | 26,723066 | 0,020406 | 0,019672 |
| 6 | 2536,976732 | 1242,583283 | 1241,375107 | 26,492029 | 26,500637 | 0,013554 | 0,012122 |
| 7 | 1772,107921 | 856,593513 | 855,637521 | 29,935385 | 29,901302 | 0,021954 | 0,018246 |
| 8 | 19742,85658 | 9841,350319 | 9838,069708 | 31,718601 | 31,702537 | 0,008034 | 0,007379 |
| 9 | 9351,326841 | 4649,651147 | 4647,493309 | 27,084407 | 27,092064 | 0,003257 | 0,002656 |
| 10 | 18557,77237 | 9245,703583 | 9250,875391 | 30,597152 | 30,582092 | 0,007418 | 0,006739 |

Simulation 30

| | TotAccuracy | linjAccuracy_D | linjAccuracy_A | SFAccuracy_D | SFAccuracy_A | biasAccuracy_D | biasAccuracy_A |
|---|---|---|---|---|---|---|---|
| 1 | 22668,36984 | 11242,35409 | 11241,81148 | 90,838757 | 90,848069 | 1,259959 | 1,257494 |
| 2 | 6778,777507 | 3262,474668 | 3262,588142 | 124,789738 | 124,804587 | 2,058157 | 2,062216 |
| 3 | 5893,827522 | 2870,471925 | 2870,17799 | 75,602933 | 75,610695 | 0,983216 | 0,980763 |
| 4 | 4702,00672 | 2195,016715 | 2194,776799 | 153,596341 | 153,560508 | 2,524266 | 2,532091 |
| 5 | 36502,91831 | 18111,89464 | 18112,26212 | 137,525883 | 137,50335 | 1,866931 | 1,865384 |
| 6 | 7635,280985 | 3700,046525 | 3699,868461 | 115,992223 | 115,966434 | 1,699654 | 1,707688 |
| 7 | 609,163794 | 167,413955 | 167,389166 | 134,243839 | 134,254959 | 2,93435 | 2,927525 |
| 8 | 12711,4787 | 6214,923008 | 6215,68129 | 138,141539 | 138,166252 | 2,286335 | 2,280279 |
| 9 | 30985,13482 | 15372,1886 | 15372,36088 | 117,39745 | 117,408082 | 2,892044 | 2,887761 |
| 10 | 817,548311 | 266,711661 | 266,757365 | 139,532246 | 139,522426 | 2,508085 | 2,516527 |

Simulation 31

| | TotAccuracy | linjAccuracy_D | linjAccuracy_A | SFAccuracy_D | SFAccuracy_A | biasAccuracy_D | biasAccuracy_A |
|---|---|---|---|---|---|---|---|
| 1 | 5819,435841 | 2794,441075 | 2793,727658 | 115,632661 | 115,609125 | 0,013123 | 0,012199 |
| 2 | 16556,75753 | 8171,589811 | 8173,116889 | 106,022875 | 106,018211 | 0,004586 | 0,005161 |
| 3 | 15286,67104 | 7519,375772 | 7519,089412 | 124,109942 | 124,078527 | 0,008642 | 0,008742 |
| 4 | 25870,23905 | 12779,90401 | 12778,25585 | 156,032079 | 156,027686 | 0,00946 | 0,009968 |
| 5 | 11166,44709 | 5478,817384 | 5478,900001 | 104,370005 | 104,351628 | 0,003918 | 0,004153 |
| 6 | 13669,88544 | 6696,872196 | 6696,485949 | 138,245737 | 138,268114 | 0,006834 | 0,006607 |
| 7 | 585,36366 | 146,362777 | 146,426128 | 146,265605 | 146,27831 | 0,016043 | 0,014798 |
| 8 | 104449,553 | 52105,19072 | 52104,69333 | 119,833058 | 119,819251 | 0,008717 | 0,007904 |
| 9 | 3675,458653 | 1663,379206 | 1663,28136 | 174,359963 | 174,379706 | 0,029187 | 0,029231 |
| 10 | 10935,74565 | 5372,441103 | 5371,920529 | 95,686587 | 95,680428 | 0,008498 | 0,008506 |